REPORT NO.
UCD/CGMDR-05/04

CENTER FOR GEOTECHNICAL MODELING

COLLABORATIVE RESEARCH: DYNAMIC BEHAVIOR OF SLICKENSIDED SURFACES - CENTRIFUGE DATA REPORT FOR CLM02

BY

C. L. MEEHAN
J. M. DUNCAN
R. W. BOULANGER

Collaborative research supported by the National Science Foundation through award CMS-0321789 to Virginia Tech and award CMS-0324499 to UC Davis.
The intention of this report is to make the data available to interested researchers. While great effort has been made to accurately report the results, the results herein are subject to revision. Please see the conditions and limitations within.

DEPARTMENT OF CIVIL & ENVIRONMENTAL ENGINEERING
COLLEGE OF ENGINEERING
UNIVERSITY OF CALIFORNIA AT DAVIS

SEPTEMBER 2005

COLLABORATIVE RESEARCH:
DYNAMIC BEHAVIOR OF SLICKENSIDED SURFACES
Centrifuge Data Report for Test Series CLM02

Report written by: Christopher Meehan

Date:	September, 2005
Date of testing:	July 21, 2005
Project:	Collaborative Research: Dynamic Behavior of Slickensided Surfaces
NSF Contract number:	CMS-0321789 (Duncan) & CMS-0324499 (Boulanger)
Sponsor(s):	National Science Foundation
Previous reports in this test series:	Centrifuge Data Report for Test Series CLM01

ACKNOWLEDGMENTS

This model test was funded by the National Science Foundation under the direction of J. M. Duncan and R. W. Boulanger. The contents of this report do not necessarily represent a policy of that agency or an endorsement by the federal government. The author would like to acknowledge the suggestions and assistance of Mike Duncan, Ross Boulanger, Chad Justice, Dan Wilson, Tom Kohnke, Tom Coker, Victor Ray, Roger Claremont, Lars Pedersen, and Cypress Winters.

The model tests were performed using the large geotechnical centrifuge at UC Davis. Development of this centrifuge was supported primarily by the National Science Foundation (NSF), NASA, and the University of California. Recent upgrades have been funded by NSF award #CMS 0086566 through the George E. Brown, Jr. Network for Earthquake Engineering Simulation (NEES).

CONDITIONS AND LIMITATIONS

TABLE OF CONTENTS

LIST OF FIGURES

LIST OF TABLES

PURPOSE AND GENERAL CONFIGURATION OF THE TEST

This document describes a centrifuge test that was performed using the UC Davis geotechnical centrifuge. The purpose of this test was to measure the amount of displacement that occurs during earthquake shaking along a preformed slickensided clay surface. The recorded data can be used to evaluate the effectiveness of Newmark's method for predicting earthquake-induced displacements in clays.

The data recorded in this centrifuge test will be used in conjunction with traditional geotechnical laboratory test data measured at Virginia Tech on soil from the same field site. Evaluation of the entire data set will allow for the development of a clear approach for evaluating the dynamic undrained shear resistance of slickensided rupture surfaces.

The soil that was used to construct the model is Rancho Solano Clay, which was obtained from the Rancho Solano residential development located in Fairfield, California. General configuration parameters for the test are as follows:

Centrifuge:	9 m-radius centrifuge at UC Davis
Model Container:	Rigid Container 1 (RC 1)
Soil Tested:	Rancho Solano Clay
Centrifugal Acceleration:	45 g
Pore Fluid:	Deionized Water

OVERALL CONCEPT OF THE CENTRIFUGE MODEL TEST

A conceptual sketch that captures the most important elements of the centrifuge model is shown in Figure 1. In the model, a heavily overconsolidated clay layer was confined between two rigid steel plates, which were fixed securely to the clay. At the center of the clay layer, a preformed slickensided clay surface was created, along which shear displacement can occur during static and seismic loading. The entire clay/steel plate system was inclined to encourage sliding by attaching it to an inclined rigid base constructed out of concrete. This system was constructed to simulate the "sliding block" analogy that is commonly used by engineers in practice to predict the displacement of a landslide during an earthquake.

The system was instrumented to measure the accelerations and resulting displacements that occur during seismic loading, as well as any pore pressures that are generated within the model. Accelerometers were placed along the upper and lower steel plates, parallel and perpendicular to the direction of sliding. Relative displacements between the upper and the lower steel plates were measured using Linear Variable Differential Transformers (LVDTs) and Linear Potentiometers (LPs). Pore pressures were measured by placing pore pressure transducers (PPTs) within the clay at locations that did not interfere with the shearing that occurred along the slickensided plane.

Once the model was constructed and instrumented, it was spun-up in the centrifuge. The model was then saturated and allowed to come to pore pressure equilibrium. Once pore pressure equilibrium had been achieved, both fast and slow displacement-controlled loading were applied to the specimen to measure the fast shear resistance and the drained shear resistance that can be mobilized along the preformed slickensided surface. The hydraulic actuator and pulley system shown in Figure 1 was used to apply the displacement-controlled loading. The static load on the specimen was then removed, and the specimen was subjected to a series of seismic loading events using the horizontal shaking table located on the UC Davis centrifuge. Accelerations, pore pressures, and displacements were measured during both the static and seismic loading events for use in evaluating the effectiveness of Newmark's method for predicting earthquake-induced displacements in clays.

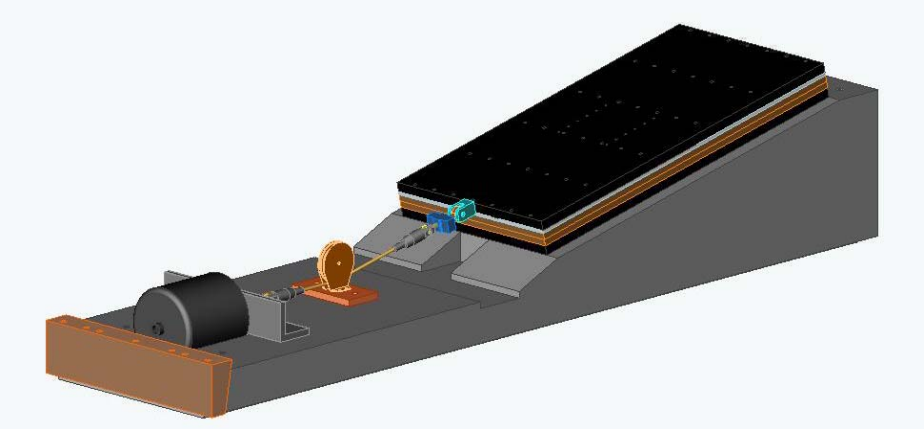

Figure 1: Centrifuge test specimen representing an element of soil on a slickensided rupture surface within the slope.

CONFIGURATION OF THE CENTRIFUGE MODEL TEST (CLM02)

The centrifuge test that is described in this report was performed in RC1, a rigid box container, and consisted of two side-by-side "sliding block" clay models. The models were set at different slope inclinations, the flatter slope at an angle of 10.5 degrees and the steeper slope at an angle of 12 degrees, in order to produce two different sliding responses for each loading event. The side-by-side model layout that was used for centrifuge test CLM02 is shown in Figure 2. Detailed centrifuge model drawings can be found in Appendix A.

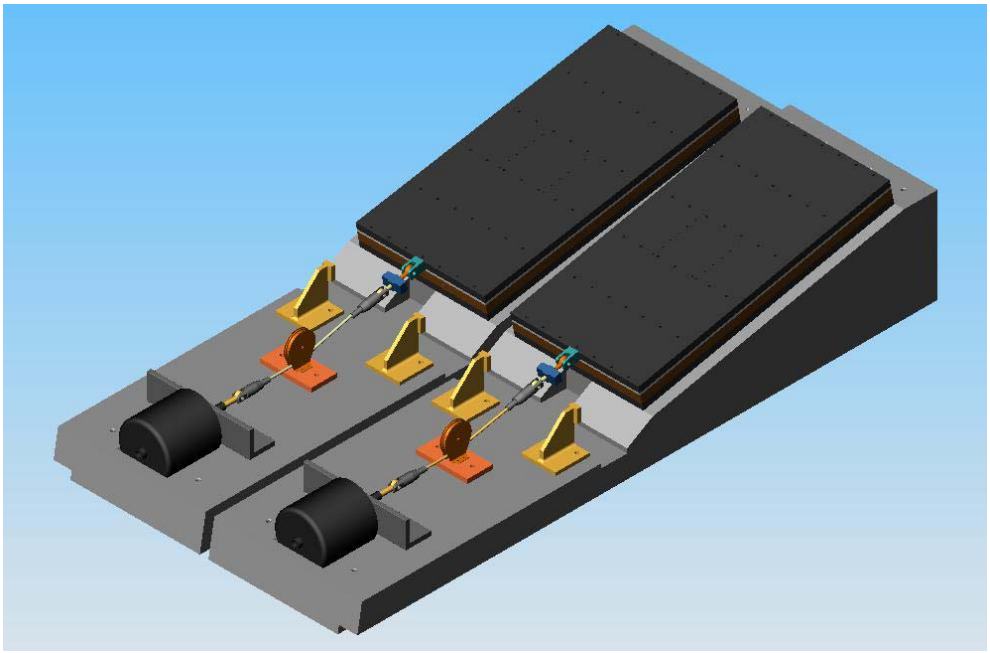

Figure 2: Model layout for centrifuge test CLM02.

As discussed in the previous section, each "sliding block" model consisted of a 1 inch thick clay layer that was confined between two 3/4-inch thick steel plates. The preformed slickensided surface was located at the center of the clay layer. The clay layer was singly-drained, with pore pressures being allowed to dissipate through a porous plastic layer that was fixed securely between the upper steel plate and the clay. The overall model layout that was used for this centrifuge test is shown in Figures A1 and A2. A detailed cross section that shows the clay "sliding block" system is shown in Figure A3.

MODEL PREPARATION

The first step in the model preparation process was to create the two reinforced concrete bases that were necessary for transmitting the shaking energy from the base of the rigid container up to the base of the soil model. These concrete bases served as the foundation for the lower steel plates, providing both a bearing surface and a reaction force for the steel plates and the actuator during the slow, static pull and during the seismic shaking events. Figure 3 shows the two concrete bases prior to their installation in the rigid container.

Figure 3: Concrete base used to support Rancho Solano Clay test specimens.

The base of the rigid container was lined with a thin layer of coarse sand (Monterey #3 sand), which was used to transmit energy during seismic shaking from the base of the rigid container to the base of the concrete. The two concrete bases were then placed side-by-side in the rigid container, and all open spaces were back-filled with Monterey #3 sand, which was vibrated firmly into place. Figure 4 shows the two reinforced concrete slopes side-by-side in the rigid container prior to back-filling with the Monterey sand.

Figure 4: Two concrete bases side-by-side in the rigid container.

In order to measure the shear resistance along the preformed slickensided surface, a hydraulic actuator system was developed to apply a downslope "static load" to each test specimen. Each actuator in the hydraulic system was able to apply 2000 pounds of force at two different displacement rates: a fast rate of approximately 0.05 in/min and a slow rate of approximately 0.0005 in/min. Using the remotely-operated hydraulic system, the actuators could be independently advanced or retracted at either displacement rate from the centrifuge control room. Prior to their installation in the rigid container, calibration and proof-testing of the hydraulic actuators was performed by lifting 400 pound dead weights, using both the "slow"

and the "fast" displacement rate capabilities for each actuator. Figure 5 shows the two hydraulic actuators and their control systems mounted on top of the concrete base in the rigid container.

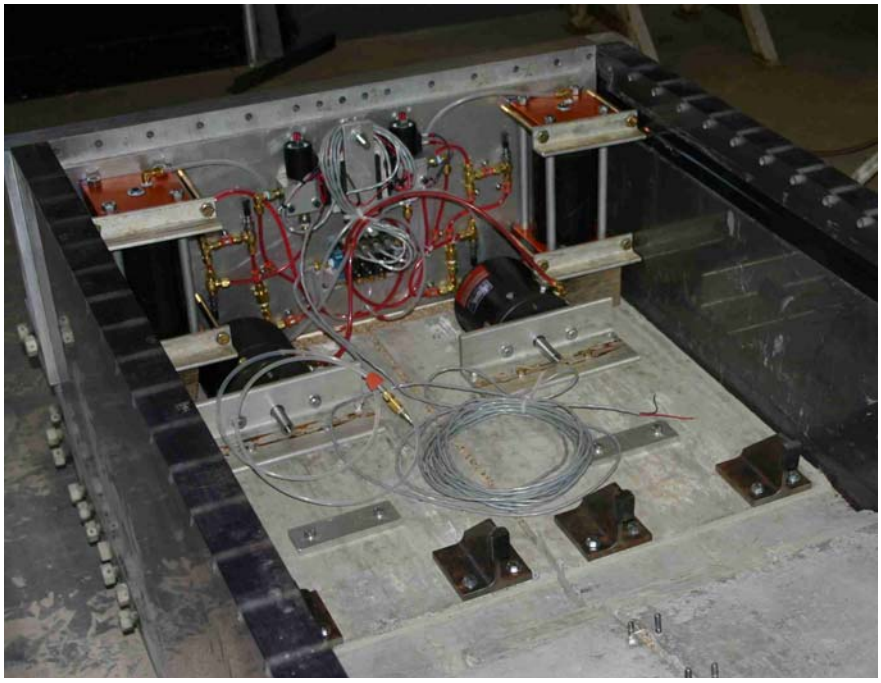

Figure 5: The hydraulic actuators and their flow-control systems.

At this point in the model construction process, the model container was ready for each of the "sliding block" soil models. Each sliding block model that was placed in the rigid container consisted of a 1 inch thick clay layer that was confined between two 3/4-inch thick steel plates. Detailed shop drawings and design specifications for the upper and lower steel plates are shown in Figures A4 and A5.

To ensure that sliding would occur within the clay layer, it was necessary to roughen the interface between the lower steel plate and the clay and the interface between the upper porous plastic and the clay. The lower steel surface was roughened by gluing sand grains to the steel plate using a multi-purpose glue coating (Gator Guard II, manufactured by Dominion Sure Seal Ltd.). The porous plastic interface was roughened by machining a series of saw teeth into the plastic to allow adequate binding with the clay particles at both the micro-scale and the macro-scale level. Slip between the porous plastic and the upper steel plate was prevented by bonding the plastic to the steel using an acrylic epoxy (Acrylic Structural Plastic Adhesive DP-8010, manufactured by 3M Scotch-Weld) and mechanical connection points. A close-up view of the roughened surfaces of the upper steel plate and the lower steel plate is shown in Figure 6.

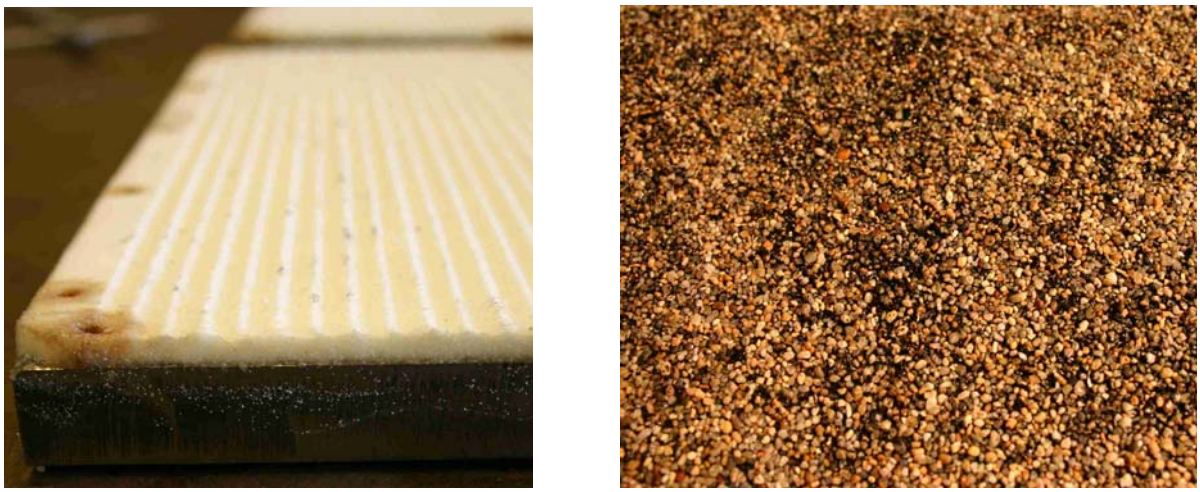

Figure 6: The roughened surfaces of the upper steel plate and the lower steel plate.

SOIL PREPARATION & INCLUSION IN THE MODEL

As the more mechanical components of the model were being constructed and tested, the soil that was used in the testing program was being prepared. The soil that was used in this centrifuge test was Rancho Solano Clay, which was obtained from Rancho Solano residential development located in Fairfield, California. A more detailed description of Rancho Solano Clay can be found in the following section, entitled SOIL PROPERTIES.

The first step in the soil preparation process was to batch-mix the soil to ensure uniformity of the test specimens. This was accomplished by thoroughly mixing and remolding the soil at approximately 1.5 times its Liquid Limit in a large mixer. This mixing process yielded a homogenous clay slurry that had no appreciable stress history. All of the clay slurry that was used in the testing program was then passed through a #40 soil sieve, to remove larger soil particles that could interfere with the preparation of the preformed slickensided failure plane. The soil was passed through the #40 sieve by hand-trowelling the soil on top of the sieve while applying vacuum pressure to the bottom of the sieve, as shown in Figure 7.

Figure 7: Pushing the soil through the #40 sieve.

Upon completion of the batch mixing and soil preparation process, pore pressure transducers were placed along each of the steel plates, and the clay slurry was consolidated against the steel plates to create a stiff clay that could be polished to form slickensides. The installation and location of the PPTs is discussed in more detail in the INSTRUMENTATION AND MEASUREMENTS section. Figures A6 and A7 show the overall design concept for the consolidation molds that were used to consolidate the clay. Two consolidation molds were built, one for each of the slopes that were tested in the model. The layered system shown in Figure A8 was used in each consolidation mold, to speed up the consolidation time and to make it easier to prepare the specimens for testing. Figure 8 shows each of the clay models being consolidated side-by-side in the consolidation press located at the UC Davis Center for Geotechnical Modeling.

Figure 8: Two centrifuge test specimens being consolidated in the consolidation press.

During consolidation, a load increment ratio of 1 was used for each load step, and each load was maintained until the soil was strong enough to handle the next consolidation load step without significant soil extrusion. The progress of the clay consolidation was tracked using dial gauge readings; two dial gauges were used for each consolidation mold, as shown in Figure 8. Pore pressure transducers embedded in the consolidating clay slurry were used to track pore pressure dissipation during consolidation. Refer to the INSTRUMENTATION AND MEASUREMENTS section for a more in-depth discussion about the location and method of installation of the PPTs. Appendix B summarizes the data gathered during consolidation for each of the consolidation molds.

The final consolidation pressure for each of the soil specimens was 100 pounds per square inch (14,400 psf). This consolidation pressure was maintained until the completion of primary consolidation, as determined from the dial gauge and pore pressure transducer readings. Upon completion of consolidation, the specimens were unloaded in stages over an

approximately 15 minute period. The consolidation molds were disassembled, and the upper and lower plates were removed from each mold. Excess clay was trimmed from the edges of the steel plate using a wire-cutter, and the specimen was manually cut to the appropriate height using a Starrett straight-edge.

Once each half of a test specimen had been cut to the appropriate thickness, the clay was polished in order to form a slickensided failure surface. The soil was polished using a smooth teflon polishing wheel that had been mounted on a horizontal milling machine. During polishing, the 1.5-inch diameter teflon wheel was rotated at 15 revolutions-per-minute, while the specimen was fed under it at an approximate feed rate of 3 inches per minute. Figure 9 shows the smooth teflon wheel that was used to polish each half of the two test specimens for each sliding block model. Typically, two to four passes with a change-in-height setting of 0.005 inches for each pass were needed to fully polish the entire surface of a clay plate.

Figure 9: The soil polishing wheel.

Once the upper and lower halves of each sliding block system had been polished, each half was weighed separately, and the two halves were sandwiched together to form the sliding block test specimens. A series of vertical kaolinite markers were then installed into the soil at each of the 5/32 inch diameter hole locations shown in Figure A4. The kaolinite markers were installed by first excavating a hole in the stiff clay soil using a drill bit advanced vertically downwards through the 5/32 inch diameter holes in the steel plate. The excavated hole was then injected with a kaolinite slurry from the bottom up, using a "tremie-like" approach, as shown in Figure 10. The purpose of these vertical kaolinite markers was to show shear localization in the Rancho Solano Clay after the test. Excavated pictures of these kaolinite markers can be found in the section entitled SLIDING BLOCK MODEL DISSECTION.

Figure 10: Installing a kaolinite marker in a sliding block test specimen.

After the kaolinite markers had been installed, accelerometers and displacement transducers were then mounted on each sliding block system. For more details on accelerometer and displacement transducer locations, see the INSTRUMENTATION AND MEASUREMENTS section.

The next step in the model construction process was to install the weir system that was used to prevent drying of the clay model throughout the centrifuge test. This weir system consisted of a series of aluminum rails that were bonded to the upper steel plate using a quick-set epoxy and a series of holes that were drilled behind each of the aluminum rails, as shown in Figure A4. During the centrifuge test, water was applied to the upper boundary of the clay specimen by adding deionized water to the upper end of each steel plate. Any excess water that was applied to the top weir cascaded sequentially down the system of weirs to the end of the steel plate. It then flowed off the end of the steel plate into a channel in the concrete base, where it was guided to an open drain at the bottom of the rigid box container. The series of holes drilled behind each weir allowed water to flow through the steel plate into the porous plastic layer, which allowed for a relatively uniform application of water to the upper face of the clay specimen. Leakage of water along the boundary of the porous plastic was prevented by sealing the edges of the porous plastic with an acrylic epoxy.

Once the instrumentation, kaolinite markers, and weir system for each sliding block model had been installed, the models were placed into the rigid container and bolted firmly into place. The cables for the accelerometers, displacement transducers, and pore pressure transducers were then routed in the rigid container and zip-tied firmly into place, in order to prevent cable tangling or breakage during the test. Figure 11 shows the side-by-side sliding block models in place in the rigid container prior to spin-up in the centrifuge.

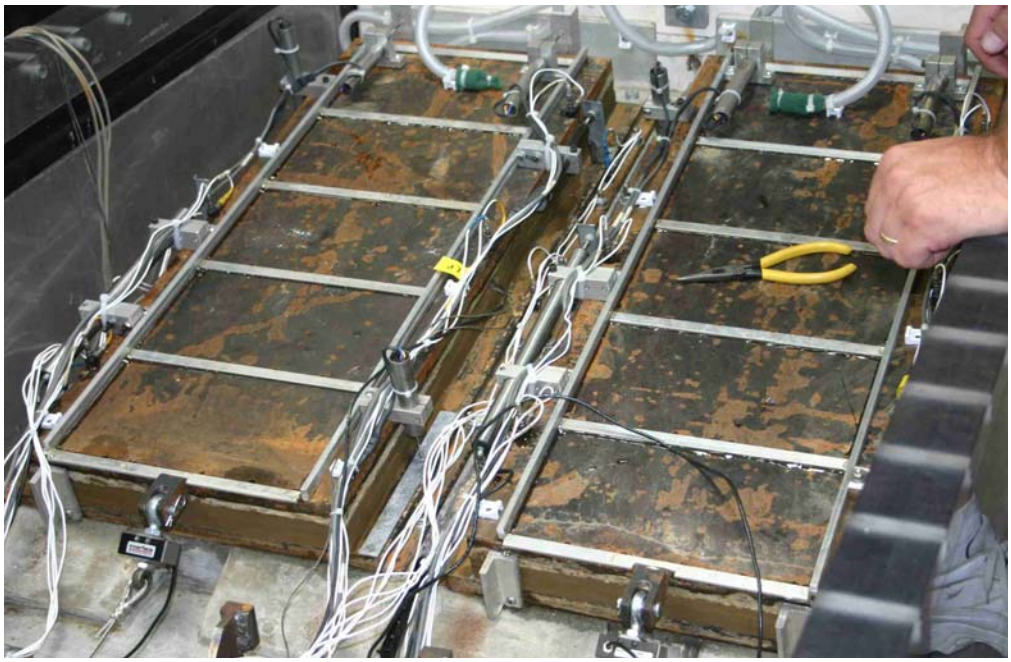

Figure 11: Side-by-side sliding block models in the rigid container.

SOIL PROPERTIES

Various soil properties for the Rancho Solano Clay are summarized in Table 1. These soil property values are based on laboratory classification tests that were performed at Virginia Tech, using bulk soil samples that had been shipped to Virginia Tech from UC Davis. Soil homogenization and preparation prior to the soil classification tests was identical to the process that was followed when preparing specimens for centrifuge testing at UC Davis.

Table 1: Soil Properties for Rancho Solano Clay*

Soil Property	Value	Units
ASTM Classification	Brown Lean Clay (CL)	N/A
Specific Gravity	2.79	none
LL	41	%
PL	19	%
PI	22	%
Clay Fraction	27	%
Preconsolidation Pressure	14,400	psf
Effective Overburden During Test (Approximate)	1,400	psf
Overconsolidation Ratio (Approximate)	10	none

*Note: The clay was not oven-dried at any point during the preparation process.

Additionally, the water content of the Rancho Solano Clay was measured at UC Davis at various points during the model construction and model dissection stages of the centrifuge test. This water content data is presented in Table 2.

Table 2: Measured Water Contents for the Rancho Solano Clay

Description	Date	Specimen Type	Measured Water Contents, (%)			
			10.5 bottom	10.5 top	12 bottom	12 top
Before Consolidation	7/8	Slurry	59.5	67.9	57.6	60.9
After Consolidation	7/14	Trimmings	25.3	26.6	24.5	25.2
Immediately after Spin-Down (Inside edge of slope)	7/21	Trimmings	22.6		22.9	
Model Dissection (3 specimen locations)	7/27	Bulk Sample	23.9, 23.7, 23.4		22.8, 23.0, 22.4	

Upon completion of the soil polishing process, prior to the assembly of each sliding block system, the weights of each half of the sliding block system were recorded. For each lower plate, this weight consisted of the lower steel plate, the Epoxy-bonded Monterey Sand, and all of the clay that was located below the preformed shearing plane in the fully assembled sliding block system. For each upper plate, this weight consisted of the upper steel plate, the porous plastic layer, and all of the clay that was located above the preformed shearing plane in the fully assembled sliding block system. The weights for each of the halves of the respective sliding block systems used in this centrifuge test are given in Table 3.

Table 3: Measured Weights for the Sliding Block Systems

Steel Plate Description	Weight (lbs)
10.5 degree slope, base plate	127.4
10.5 degree slope, top plate	102.6
12 degree slope, base plate	127.9
12 degree slope, top plate	102.9

INSTRUMENTATION AND MEASUREMENTS

The centrifuge facilities and instrumentation system are described at the NEES Site Specifications website: http://www.nacse.org/neesSiteSpecs/do/siteSelection. Instrumentation and facilities that will be used in this test that are not described on the website are described below.

For centrifuge test CLM02, each of the sliding block models was instrumented with accelerometers, displacement transducers, pore pressure transducers, and load cells to measure the behavior of each of the slopes during the static and seismic loading events. The instrumentation channel list that was used during centrifuge test CLM02 is given in Table 4. The approximate instrument sizes and dimensions for the accelerometers, displacement transducers and pore pressure transducers are shown in Figure A9. The instrument layout

that was used for each sliding block model is shown in Figure A10. The instrument numbering scheme that corresponds to the instrumentation channel list given in Table 4 is shown in Figure A11.

As shown in Figure A10, accelerometers were placed at multiple locations along either side of each steel plate in order to measure the acceleration applied parallel to and perpendicular to the direction of sliding. Parallel and perpendicular accelerations were measured at the base of the system (along the edge of the lower steel plate) and at the top of the system (along the edge of the upper steel plate). Two additional horizontal accelerometers were placed on the outside of the model container to measure the shaker response during dynamic loading and to evaluate the acceleration that was applied at the base of the model.

Displacement transducers were placed at multiple locations along the upper steel plate to measure the relative slope displacement between the upper sliding mass and the fixed lower mass. The displacement transducers moved along with the upper plate, measuring displacements relative to flags that were fixed securely to the lower steel plate. Displacement transducers were also placed perpendicular to the upper steel plate to measure displacement perpendicular to the slickensided shearing plane. It should be noted that two different types of displacement transducers were used to measure displacement parallel to the direction of sliding: Linear Variable Differential Transformers (LVDTs) and Linear Potentiometers (LPs).

Saturated pore pressure transducers were placed at the locations shown in Figure A10 prior to the placement of the clay slurry. Modeling clay was used to hold the PPTs and their electronic cables in place while the clay slurry was gently trowelled into place around the head of the instrument. The clay was then consolidated to the desired stiffness around the PPT. One additional pressure transducer (P17) was also mounted outside of the clay to measure the ambient air pressure in the sample container during the test.

Load cells were used to measure the force that was applied by the hydraulic actuator and pulley system during the static loading phases of the test. For each slope, one load cell was placed in-line with the hydraulic actuator and pulley system at the point of connection of the cable to the upper steel plate.

In order to evaluate the recorded instrumentation data during the centrifuge test, the calibration factors shown in Table 4 were applied to convert from voltage to the appropriate model units. Instrument calibrations were performed before the centrifuge test and verified by comparison to the manufacturer's calibrations. The calibration factors were also adjusted so that the data would obey the desired sign conventions established for measuring model units. The sign conventions are as follows:

- Acceleration is positive when applied in a downslope direction (from the upslope edge of the steel plate to the downslope edge of the steel plate).
- Acceleration is positive when applied perpendicularly away from the concrete base (from the lower steel plate to the upper steel plate).

- Downslope sliding of the upper steel plate relative to the lower steel plate, in a direction parallel to the preformed slickensided plane, corresponds to a positive relative displacement (parallel).
- Movement of the upper steel plate away from the lower steel plate, in a direction perpendicular to the preformed slickensided plane, corresponds to a positive relative displacement (perpendicular).
- Positive pore pressures are positive.
- Applied static loads in the downslope direction are positive.

The offset factors shown in Table 4 were also applied to the measured data, in order to adjust the measured voltages to reflect the desired "zero" values. As shown in Table 4, no direct offsets were applied to the measured accelerometer values. The offsets for the displacement transducers (LVDTs and LPs) were applied such that the initial voltage reading for each transducer corresponded to an initial relative displacement of zero prior to spin-up. The offsets for the pore pressure transducers (PPTs) were applied so that a reading of zero voltage for each of the pore pressure transducers would correspond to zero applied pressure. The offsets for the load cells (LCs) were applied so that a reading of zero voltage for each load cell would correspond to zero applied load.

In addition to the quantitative instrumentation discussed previously, the model was fixed with a series of six different cameras that could be used to qualitatively evaluate the behavior of the centrifuge model during the test. The six camera feeds that were observed during the test are as follows:

- Camera 1: View looking upslope between the two sliding block models.
- Camera 2: View looking downslope at the lower half of the steel plates and the pulley portion of the static loading system.
- Camera 3: View looking upslope at each of the sliding block models.
- Camera 4: View of the manometer at the North end of the specimen container.
- Camera 5: View of the manometer at the South end of the specimen container.
- Camera 6: View of the entire model being spun on the centrifuge inside of the rotunda.

Table 4: Instrumentation Channel List

Inst #	Inst Name	Inst Type	Serial #	Model	Inst Range	Amplifier Channel #	Amplifier Gain	Calibration - Model		Offset	
1	A19	ACC	21067	12	100 g	DC48	1	-18.4843	g/V	0	V
2	A10	ACC	3202	10.5	50 g	DC49	1	9.7087	g/V	0	V
3	A11	ACC	21048	10.5	100 g	DC50	1	-19.4932	g/V	0	V
4	A22	ACC	3963	12	50 g	DC51	1	9.5785	g/V	0	V
5	A23	ACC	21318	12	100 g	DC52	1	-21.5517	g/V	0	V
6	A24	ACC	3964	12	50 g	DC53	1	9.5238	g/V	0	V
7	A25	ACC	21319	12	100 g	DC54	1	-19.1571	g/V	0	V
8	A26	ACC	4523	12	50 g	DC55	1	9.5329	g/V	0	V
9	A27	ACC	21320	12	100 g	DC56	1	-20.0803	g/V	0	V
10	A28	ACC	4596	12	50 g	DC57	1	9.4967	g/V	0	V
11	A29	ACC	21321	12	100 g	DC58	1	-19.6464	g/V	0	V
12	A30	ACC	5267	12	50 g	DC59	1	9.6339	g/V	0	V
13	A31	ACC	21322	12	100 g	DC60	1	-19.9601	g/V	0	V
14	A32	ACC	5269	12	50 g	DC61	1	9.6432	g/V	0	V
15	A33	ACC	21323	12	100 g	DC62	1	-21.2766	g/V	0	V
16	A34	ACC	5276	12	50 g	DC63	1	9.5602	g/V	0	V
17	P1	PPT	7985-100	10.5	100 psi	XDCR0	250	-4.6593	psi/V	0.007	V
18	P2	PPT	11146-100	10.5	100 psi	XDCR1	100	5.9380	psi/V	-0.008	V
19	P3	PPT	7811-100	10.5	100 psi	XDCR2	250	4.5360	psi/V	-0.012	V
20	P4	PPT	11151-100	10.5	100 psi	XDCR4	100	6.1059	psi/V	0.081	V
21	P5	PPT	7722-100	10.5	100 psi	XDCR5	250	4.6839	psi/V	0.502	V
22	P6	PPT	11152-100	10.5	100 psi	XDCR6	100	6.0122	psi/V	0.132	V
23	P7	PPT	11149-100	10.5	100 psi	XDCR7	100	6.2719	psi/V	-0.175	V
24	P8	PPT	10315-100	10.5	100 psi	XDCR8	250	4.9444	psi/V	0.136	V
25	P9	PPT	11150-100	12	100 psi	XDCR9	100	6.0772	psi/V	0.073	V
26	P10	PPT	10323-50	12	50 psi	XDCR10	100	5.2278	psi/V	-0.023	V
27	P11	PPT	10041-100	12	100 psi	XDCR11	250	4.7105	psi/V	-0.115	V
28	P12	PPT	11148-100	12	100 psi	XDCR12	100	6.0378	psi/V	-0.021	V
29	P13	PPT	10321-50	12	50 psi	XDCR15	100	5.3916	psi/V	0.021	V
30	P14	PPT	11147-100	12	100 psi	XDCR16	100	6.2419	psi/V	-0.03	V
31	P15	PPT	11143-50	12	50 psi	XDCR17	50	5.5427	psi/V	0.022	V
32	P16	PPT	11141-50	12	50 psi	XDCR18	50	5.4212	psi/V	-0.085	V
33	P17	PPT	11154-200	-	200 psi	XDCR19	250	4.9935	psi/V	-0.054	V
34	L1	LC	181325	10.5	2000 lb	XDCR20	250	200.8	lbf/V	0.055	V
35	L2	LC	181363	12	2000 lb	XDCR21	250	202.4	lbf/V	0.059	V
36	A13	ACC	21043	10.5	100 g	DC32	1	-18.2482	g/V	0	V
37	A14	ACC	3948	10.5	50 g	DC33	1	9.4518	g/V	0	V
38	A5	ACC	5604	10.5	100 g	DC34	1	-18.7266	g/V	0	V
39	A6	ACC	3164	10.5	50 g	DC35	1	9.3809	g/V	0	V
40	A7	ACC	21059	10.5	100 g	DC36	1	-18.3150	g/V	0	V
41	A8	ACC	3166	10.5	50 g	DC37	1	9.3897	g/V	0	V
42	A9	ACC	21046	10.5	100 g	DC38	1	-18.7266	g/V	0	V
43	A20	ACC	3962	12	50 g	DC39	1	9.3897	g/V	0	V
44	A21	ACC	21070	12	100 g	DC40	1	-21.6450	g/V	0	V
45	A12	ACC	3204	10.5	50 g	DC41	1	9.2851	g/V	0	V
46	A3	ACC	5602	10.5	100 g	DC42	1	-18.5874	g/V	0	V
47	A4	ACC	3157	10.5	50 g	DC43	1	9.1075	g/V	0	V
48	A15	ACC	21060	10.5	100 g	DC44	1	-19.0840	g/V	0	V
49	A16	ACC	3949	10.5	50 g	DC45	1	9.4162	g/V	0	V
50	A17	ACC	21061	10.5	100 g	DC46	1	-20.2020	g/V	0	V
51	A18	ACC	3955	10.5	50 g	DC47	1	9.3809	g/V	0	V
52	D1	LVDT	A017-01	10.5	4"	PBP64	N/A (1)	0.5668	in/V	-3.678	V
53	D2	LP	416	10.5	4"	PBP65	N/A (1)	0.3997	in/V	-4.888	V
54	D3	LVDT	469053	10.5	2"	PBP66	N/A (1)	0.2280	in/V	-4.027	V
55	D4	LVDT	455851	10.5	2"	PBP67	N/A (1)	0.2369	in/V	-4.093	V
56	D5	LVDT	469051	10.5	2"	PBP68	N/A (1)	-0.2342	in/V	-0.186	V
57	D6	LVDT	418434	10.5	1.5"	PBP69	N/A (1)	-0.1673	in/V	0.022	V
58	D7	LVDT	A017-02	12	4"	PBP70	N/A (1)	0.5706	in/V	-3.411	V
59	D8	LP	423	12	4"	PBP71	N/A (1)	0.4002	in/V	-4.795	V
60	D9	LVDT	455850	12	2"	PBP72	N/A (1)	0.2365	in/V	-3.555	V
61	D10	LVDT	419741	12	2"	PBP73	N/A (1)	0.2292	in/V	-3.689	V
62	D11	LVDT	434653	12	1"	PBP74	N/A (1)	-0.1385	in/V	0.078	V
63	D12	LVDT	434655	12	1"	PBP75	N/A (1)	-0.1397	in/V	-0.010	V
64	A1	ACC	5598	-	100 g	PBP76	1	18.7266	g/V	0	V
65	A2	ACC	5599	-	100 g	PBP77	1	19.0476	g/V	0	V

TESTING THE MODEL IN THE CENTRIFUGE

Upon completion of model construction, the cover was placed on the rigid container, and the centrifuge model was placed on the centrifuge arm. The balance of both the centrifuge bucket and the centrifuge arm was then checked to ensure that the model would experience balanced loading during the test.

The centrifuge test was started by gradually increasing the rotation rate of the centrifuge arm in order to apply increasing centrifugal acceleration to the centrifuge model. The centrifuge rotation rate was held constant for a period of time at 34.4 RPMs and 45.0 RPMs, to allow consolidation-induced pore pressures to dissipate prior to the final arrival at a rotation rate of 68.2 RPMs. These centrifuge rotation rates correspond to centrifugal accelerations of 11.5 g's, 19.6 g's, and 45.0 g's, respectively. The centrifuge rotation rate was then held constant at 68.2 RPMs in order to maintain a centrifugal acceleration of 45 g's throughout the remainder of the centrifuge test.

Once the target centrifugal acceleration had been reached, water was applied to each of the slopes, and time was allowed for the model to come to equilibrium. The centrifuge model was then subjected to a series of "static loading" and "seismic loading" events, which were intended to move the upper steel plates downslope relative to the lower steel plates by inducing shearing in each of the clay layers. The sequence of static loading and seismic loading events is shown in Table 5.

Table 5: Centrifuge Test Loading Events

Event ID	Name of Motion	Time	Freq. (Hz)	# Cycles	Amp. Factor	Peak to Peak Base Accel. (g)	Cent. Accel. (g)	Ratio H/V Accel.
Spin-Up		10:33 AM						
CLM02_S1	Static Pull #1	1:59 PM						
CLM02_01	Shake #1	5:20 PM	55	5	.24	4.2	45.3	.05
CLM02_02	Shake #2	5:43 PM	55	5	.97	28.5	45.0	.32
CLM02_03	Shake #3	6:25 PM	55	20	3.00	45.6	45.0	.51
CLM02_04	Shake #4 (Dummy Shake)	7:56 PM	N/A	N/A	N/A	N/A	N/A	N/A
CLM02_S2	Static Pull #2	8:20 PM						
Spin-Down		10:35 PM						

During the static loading events, each upper steel plate was moved downslope relative to its lower steel plate by applying a displacement controlled load in the downslope direction at the front face of the upper steel plate. For Static Pull #1, the load was applied in two stages: a fast loading stage followed by a slow loading stage. During the fast loading stage, stress was mobilized in the system by advancing the actuator at a rate of approximately 0.05 in/min.

The fast loading stage was maintained until the peak shearing resistance had been reached. At that point, a transition was made to the slow loading stage, by slowing the rate of advance of the actuator to approximately 0.0005 in/min. The slow loading stage was maintained until a constant residual shearing resistance had been measured. For Static Pull #2, the load was applied in three stages: a fast loading stage, a slow loading stage, and another fast loading stage. During the first fast loading stage, stress was mobilized in the system by advancing the actuator at a rate of approximately 0.05 in/min. The fast loading stage was maintained until the peak shearing resistance had been reached. At that point, a transition was made to the slow loading stage, by slowing the rate of advance of the actuator to approximately 0.0005 in/min. The slow loading stage was maintained until a constant residual shearing resistance had been measured. The actuators were then switched back to the fast loading stage (0.05 in/min), in order to explore the effect of loading rate on the strength of the clay.

Each of the seismic loading events consisted of a series of either five or twenty sinusoidal pulses of approximately the same amplitude with a frequency of 55 Hz. The shaking was applied lengthwise in the rigid model container (horizontally, looking at a side view of the model slopes), which allowed for downslope sliding of the upper steel plate relative to the lower steel plate.

Throughout the test, data acquisition was performed on all of the instrumentation channels listed in Table 4. "Slow Data" was acquired by sampling all instrument channels at a frequency that varied from 1/2 to 1 Hz throughout the entire centrifuge test. The data presented for both Static Pull #1 and Static Pull #2 came from the acquired "Slow Data". For each of the shaking events (Shake #1 through Shake #4), "Fast Data" was acquired by sampling at a frequency of 4096 Hz. Data plots for each of the centrifuge test loading events are given in Appendix C. See the section entitled ORGANIZATION OF DATA FILES AND PLOTS for a more in-depth discussion about how the data in Appendix C is organized.

During the centrifuge test, a manometer mounted on the outside of the rigid container was used to evaluate the orientation of the g-field relative to the model slopes. This manometer consisted of a closed tube on the outside of the rigid container that was filled with automatic transmission fluid (ATF), as shown in Figure 12. The horizontal distance between the vertical riser tubes on the North end and the South end of the model container was 71.5 inches. Two rulers were mounted on either side of the vertical manometer tubes to provide reference points for the fluid levels on either side of the manometer. Two cameras (Camera 4 and Camera 5) were mounted such that the ATF levels in the manometer could be read during the test. Table 6 lists the ATF levels that were recorded during the centrifuge test and the calculated values of perceived slope angle change that will occur as a result of the change in relative g-field orientation.

Figure 12: Manometer used to evaluate the orientation of the g-field.

Table 6: ATF Levels and G-Field Orientation During the Centrifuge Test

Description	Time	ATF Height (N side – in.)	ATF Height (S side – in.)	Slope Angle Change (degrees)*
Initial Reading, prior to spin-up	10:21 AM	5.725	5.8	-0.0036**
During first slow pull	2:46 PM	5.98	5.62	0.349
During first slow pull	4:27 PM	5.99	5.64	0.341
Prior to Shake 1	5:19 PM	6.0	5.65	0.341
Prior to Shake 2	5:43 PM	6.0	5.65	0.341
Prior to Shake 3	6:22 PM	6.0	5.65	0.341
Prior to Shake 4	7:53 PM	6.08	5.6	0.445

*Note: A positive reading corresponds to Bucket South End High, which means that the slope is steeper.
** Note: This was the baseline value for the manometer calculations, since the actual slope angle change for this point was measured directly at 1-g using a machinist's level.

To prevent drying of the model during the centrifuge test, water was applied to the clay through the upper porous plastic layer using the weir system described in the section entitled SOIL PREPARATION AND INCLUSION IN THE MODEL. During the centrifuge test, a brief pulse of water (typically applied for around 10 to 20 seconds or so) was applied at the following times: 11:43 AM, 1:23 PM, 2:56 PM, 3:17 PM, 5:12 PM, 6:36 PM, 6:41 PM, 6:45 PM, 6:51 PM, 6:58 PM, 7:00 PM, 7:07 PM, 7:13 PM, 7:21 PM, 7:27 PM, 7:37 PM, and 7:48 PM. For this test, wind-current induced drying of the clay was also reduced using a custom-built Plexiglas cover that was mounted over the opening in the top of the rigid container.

SCALE FACTORS

All data presented in this report is given in the form of model-scale units. The converted data files posted on the NEES central website (http://central.nees.org) are also posted in the form of model-scale units. No scale factor has been applied because it is felt that the test results can be best interpreted and analyzed in terms of model-scale units. All measured accelerations are given in g's; all displacements are given in inches; all pore water pressures are given in pounds per square inch; and all loads are given in pounds. The centrifuge revolutions-per-minute (RPM) values for each shaking event are shown in Table 7. The

centrifugal accelerations in the model were calculated using an effective radius of 28.4 feet, which was determined by calculating the radial distance to one-third the average height of the sloping soil profiles. Centrifugal acceleration values for each of the loading events are given in Table 7.

Table 7: Centrifuge RPMs and G-Level for Each Loading Event

Shaking Event	RPM	Centrifugal Acceleration (g's)
Static Pull #1	68.2*	45.0
Shake #1	68.4	45.3
Shake #2	68.2	45.0
Shake #3	68.2	45.0
Shake #4	68.4	45.3
Static Pull #2	68.2*	45.0

*Note: The centrifuge RPMs fluctuate slightly over time, which causes slight variations in the centrifuge g-level during the longer loading events (Static Pull #1 and Static Pull #2). The RPM values shown are the average RPM values for the entire loading event.

If desired, the scale factors shown in Table 8 can be used to convert the data from model units to prototype units. The scaling factor N that should be used to convert from model to prototype units is equal to the centrifugal acceleration value for each loading event that is listed in Table 7.

Table 8: Scale Factors for Converting Model Data to Prototype Units (Kutter, 1992)

Quantity	Model Dimension / Prototype Dimension
Time (dynamic)	1/N
Displacement, Length	1/N
Acceleration, Gravity	N
Force	$1/N^2$
Pressure, Stress	1/1
Time (diffusion)*	$1/N^2$

*Note: The diffusion time scale factor depends on whether the diffusion coefficient (e.g. coeffiecient of consolidation) is scaled. For this test, since the same soil was used in the model as the prototype, use $1/N^2$.

SLIDING BLOCK MODEL DISSECTION

Upon completion of the centrifuge test, the sliding block models were removed from the rigid container and dissected to examine shear localization and shear plane behavior. The appearances of the preformed slickensided failure plane for the 10.5 degree slope and the 12 degree slope sliding block models are shown in Figure 13 and Figure 14, respectively. The appearances of the vertical kaolinite markers for the 10.5 degree slope and the 12 degree slope sliding block models are shown in Figure 15 and Figure 16, respectively.

Figure 13: Slickensided failure plane for the 10.5 degree slope sliding block model.

Figure 14: Slickensided failure plane for the 12 degree slope sliding block model.

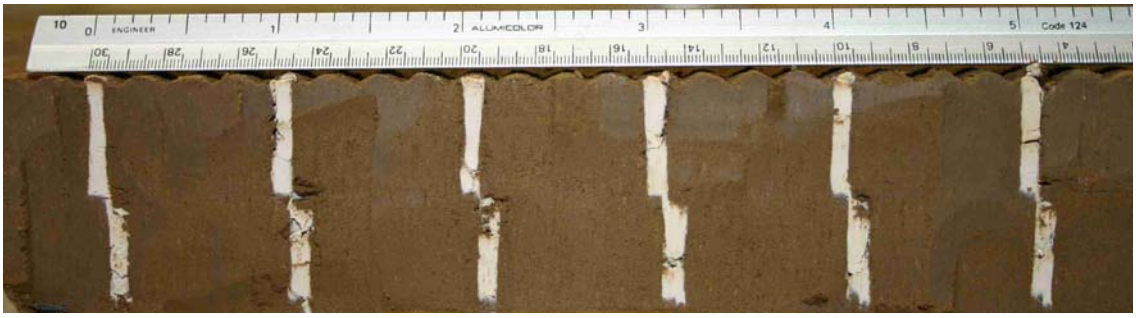

Figure 15: Excavated kaolinite columns from the 10.5 degree slope.

Figure 16: Excavated kaolinite columns from the 12 degree slope.

KNOWN LIMITATIONS OF RECORDED DATA AND MODEL

The relative clay thicknesses on either side of the shearing plane are not exactly 0.5 inches, as shown in the design drawings. Since it was not exactly clear how much polishing would be needed to sufficiently prepare each of the clay specimens prior to assembly, it was necessary to start at a thickness above 0.5 inches and polish the specimen back as needed. Additionally, due to the varying surface geometry of the upper and lower steel plates, the specimen thickness at any given point will vary slightly. The measured overall thicknesses for each of the polished clay and steel specimen halves are given in Table 9. The measured thickness of the porous plastic layer is approximately 0.25 inches, and the thickness of the Monterey sand layer is 0.125 inches. The resulting clay thicknesses given in Table 9 were calculated by subtracting out the thickness of the steel plates, the porous plastic, and the Monterey sand.

Table 9: Clay Thicknesses on Either Side of the Preformed Slickensided Plane

Quantity	Measured Overall Thickness (inches)	Calculated Clay Thickness* (inches)
10.5 degree slope, upper portion	1.534	0.53
10.5 degree slope, lower portion	1.520	0.65
12 degree slope, upper portion	1.556	0.56
12 degree slope, lower portion	1.504	0.63

*Note: The calculated clay thicknesses are only approximate values and will vary across the area of the specimen.

During Static Loading #2, the maximum tensile capacity of the static load cables was exceeded, causing the cables to break, which resulted in an immediate reduction in static load on the slopes. For the 10.5 degree slope model, the static loading cable broke at 8:37 PM during the first fast loading stage. Consequently, the slow loading stage and the second fast loading stage that were described in the TESTING THE MODEL IN THE CENTRIFUGE section were not applied to the 10.5 degree model slope. For the 12 degree slope model, the static loading cable broke at 10:32 PM, during the second fast loading stage. Consequently, a steady-state value of pulling resistance for the second fast loading stage could not be measured.

Additionally, during Static Loading #2 for the 12 degree slope, some of the load data that was recorded is not representative of the actual load applied to the sliding block model. During the initial loading for the first fast loading stage, the load was higher than previously recorded, which caused the voltage readings to go outside the 5 V maximum cap that had been set in the data acquisition system for that channel. Once this discontinuity between the recorded data and the actual data was discovered, the slope was unloaded, the data acquisition system was reconfigured, and the slope was loaded again. For purposes of analysis, the flat cap in load that occurred around 1000 pounds (around 5 V) during the first fast loading stage of Static Loading #2 should be disregarded.

During the static loading phases, there was some variation in the applied loading rate. This behavior was caused by the presence of a porous plastic filter that was added in-line to the hydraulic actuator system. When the load on the actuator changed significantly, the differential pressure driving the hydraulic fluid through the porous plastic filter changed, resulting in a change in the flow rate of hydraulic fluid throughout the system. This caused a change in the displacement rate of the hydraulic piston. As a result of this phenomenon, the hydraulic actuators did not apply true displacement-controlled loading during the test. The magnitude of the change in applied loading rate can be evaluated by looking at the change in slope of a displacement versus time plot for each steel plate. At the residual condition, this effect is relatively insignificant due to the fact that the applied pulling force was not changing significantly over time.

The externally mounted base accelerometers, A1 and A2, show recorded acceleration motions that are inconsistent with the rest of the accelerometer data recorded throughout the model. These accelerometers were both wired through a separate three channel decouple amplifier, and it is believed that this amplifier experienced electrical problems during the test, resulting in inaccurate voltage readings for these instruments. For purposes of analysis, the accelerations measured parallel and perpendicular to the lower steel plate can be used. The data recorded for instruments A1 and A2 can be found in the raw data files; however, to avoid confusion, this data is not plotted in Appendix C.

Due to the very small magnitudes of relative displacement that are recorded during the centrifuge test, the displacement transducers are susceptible to two sources of error: the first is sticking of the sliding core within the housing of the displacement transducer, and the second is flexion or shifting of the flags mounted to the lower steel plate. Sticking of the displacement transducer core is characterized by poor displacement tracking followed by a sudden large jump in displacement that can be seen when redundant displacement transducer measurements are compared. Instrument D8, a 4-inch linear pot, exhibited sticking of the sliding core and should not be considered a reliable instrument for purposes of data analysis. Flexion of the flags mounted to the lower steel plate is characterized by differing measured values of relative displacement after spin-up, followed by consistent relative displacement measurements throughout the rest of the test. Instrument D1 (when compared with instruments D2, D3, and D4) exhibited flag shifting, and should not be used for analysis without offsetting its relative displacement value to match the relative displacement measured by instruments D2, D3, and D4 after spin-up. Upon dissection of the model, it was

observed that instrument D10 had experienced some lateral displacement at its connection point due to a lateral stretching of the shrink tubing joint on the flag, as shown in Figure 17.

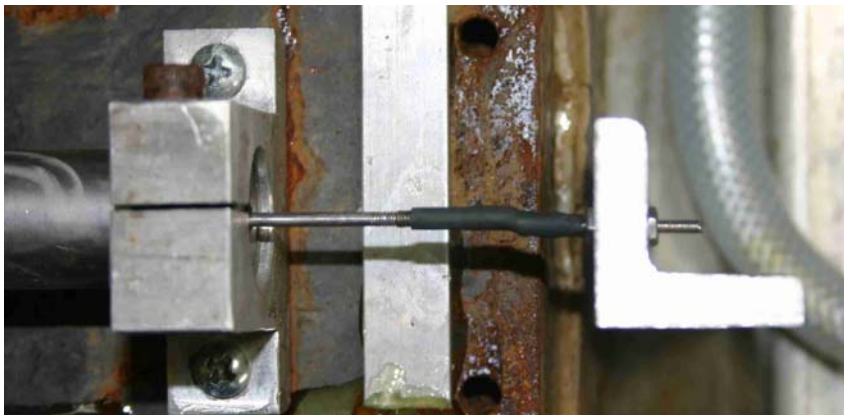

Figure 17: Lateral flexion at the connection point for instrument D10.

Analysis of the fast data files has indicated that there is a phase lag that is introduced to the LVDT measurements of relative displacement during the dynamic loading events. Since the LPs do not exhibit this characteristic phase lag, comparison between the measured LP and LVDT displacements during dynamic loading can be used to evaluate the magnitude of the LVDT phase lag. The best measurements of relative displacement can be made by combining the relative displacements from the LVDT and accelerometer data using signal processing techniques. The resulting values can then be compared with the displacements measured by the LPs.

During consolidation, some of the pore pressure transducers exhibited unusual behavior. Pore pressure transducers P3, P4, P11, and P13 all measured pore pressures that suddenly and unexpectedly deviated from expected pore pressure values. It is not clear what caused this sudden change in pore pressures. One possible explanation is that there was arching of soil stresses around the pore pressure transducer, due to the fact that the pore pressure transducer is relatively large compared to the thickness of the consolidating clay layer. Another possible explanation is that the outer shell of the PPT experienced a small amount of deflection under the relatively large lateral force, which caused a slight distortion of the PPT diaphragm, resulting in the measurement of erroneous pore pressure values.

During the centrifuge test, a number of the pore pressure transducers did not exhibit any response to clear changes in pore water pressure. For example, during spin-up of the centrifuge, all of the pore pressure transducers should have responded by measuring some increase in pore water pressure as a result of the increase in applied total stress. Pore pressure transducers P4, P5, P11, P12, P13, and P16 all exhibited unexplained pore pressure responses during spin-up, and should not be treated as reliable instruments for purposes of data analysis. The unusual response of these instruments is most likely due to a loss of saturation in the porous stone that separates the diaphragm of the PPT from the surrounding soil.

Upon excavation, it was discovered that a portion of the protective outer wire casing for instrument P15 was missing. This is the likely explanation for the larger-than-typical amounts of noise that were measured for this instrument during fast data acquisition. Caution should be used when interpreting data for this instrument.

Pore pressure transducer locations may be slightly different than shown in Figure A10, due to shifting and tilting of the pore pressure transducers during consolidation. If desired, information regarding the final orientation of the PPTs can found in the picture files posted on the NEES central website (http://central.nees.org).

ORGANIZATION OF DATA FILES AND PLOTS

During centrifuge test CLM02, all voltage data from the accelerometers, displacement transducers, pore pressure transducers, and load cells were acquired using Labview. The conversion factors shown in Table 4 were then used to convert recorded voltage values to the appropriate engineering units for each instrument. Plots of the data acquired for each instrument can be found in Appendix C, presented in the appropriate engineering units. All measured accelerations are given in g's; all displacements are given in inches; all pore water pressures are given in pounds per square inch; and all loads are given in pounds. No filtering of data was performed during file conversion; therefore, all the data that is presented is in unfiltered units.

Information regarding each loading event that the slopes were subjected to during centrifuge test CLM02 can be found in Table 5. Information regarding the centrifuge RPMs and corresponding g-level for each loading event can be found in Table 7.

As shown in Table 5, each model slope was first sheared statically, then subjected to a series of dynamic shaking events, and then sheared statically again. Table 10 outlines the organization of the data plots that are presented in Appendix C for the 1st static shearing phase. Table 11 outlines the organization of the data plots that are presented in Appendix C for each seismic shaking event. Table 12 outlines the organization of the data plots that are presented in Appendix C for the 2nd static shearing phase. In Appendix C, pages labeled: file = "CLM02_S1" correspond to the first static shearing phase; pages labeled: file = "CLM02_01" through file = "CLM02_04" correspond to dynamic shaking events; and pages labeled: file = "CLM02_S2" correspond to the second static shearing phase.

Table 10: Organization of Data Plots for the 1st Static Shearing Phase. (See Appendix C for data plots).

Page #	Page Name	Instruments
1	10.5 & 12 Degree Slope, Load Cells Pulling force applied to each plate over time	L1 & L2
2	10.5 Degree Slope, Displacement Transducers 4 measurements of downslope displacement 2 measurements of transverse displacement	D1, D2, D3, D4 & D5, D6
3	10.5 Degree Slope, Pore Pressure Transducers Measurement of pore pressures at 8 locations	P1, P2, P3, P4, P5, P6, P7, P8
4	12 Degree Slope, Displacement Transducers 4 measurements of downslope displacement 2 measurements of transverse displacement	D7, D8, D9, D10 & D11, D12
5	12 Degree Slope, Pore Pressure Transducers Measurement of pore pressures at 8 locations and 1 external transducer to measure ambient barometric pressure	P9, P10, P11, P12, P13, P14, P15, P16, & P17

Table 11: Organization of Data Plots for Each Seismic Shaking Event. (See Appendix C for data plots).

Page #	Page Name	Instruments
1	10.5 Degree Slope, Accelerometers – Base Plate (parallel & perpendicular at 4 locations)	A3 & A4, A5 & A6, A7 & A8, A9 & A10
2	10.5 Degree Slope, Accelerometers – Top Plate (parallel & perpendicular at 4 locations)	A11 & A12, A13 & A14, A15 & A16, A17 & A18
3	10.5 Degree Slope, Displacement Transducers 4 measurements of downslope displacement 2 measurements of transverse displacement	D1, D2, D3, D4 & D5, D6
4	10.5 Degree Slope, Pore Pressure Transducers Measurement of pore pressures at 8 locations	P1, P2, P3, P4, P5, P6, P7, P8
5	12 Degree Slope, Accelerometers – Base Plate (parallel & perpendicular at 4 locations)	A19 & A20, A21 & A22, A23 & A24, A25 & A26
6	12 Degree Slope, Accelerometers – Top Plate (parallel & perpendicular at 4 locations)	A27 & A28, A29 & A30, A31 & A32, A33 & A34
7	12 Degree Slope, Displacement Transducers 4 measurements of downslope displacement 2 measurements of transverse displacement	D7, D8, D9, D10 & D11, D12
8	12 Degree Slope, Pore Pressure Transducers Measurement of pore pressures at 8 locations and 1 external transducer to measure ambient barometric pressure	P9, P10, P11, P12, P13, P14, P15, P16 & P17

Table 12: Organization of Data Plots for the 2nd Static Shearing Phase. (See Appendix C for data plots).

Page #	Page Name	Instruments
1	10.5 & 12 Degree Slope, Load Cells Pulling force applied to each plate over time	L1 & L2
2	10.5 Degree Slope, Displacement Transducers 4 measurements of downslope displacement 2 measurements of transverse displacement	D1, D2, D3, D4 & D5, D6
3	10.5 Degree Slope, Pore Pressure Transducers Measurement of pore pressures at 7 locations	P1, P2, P3, P4, P5, P6, P7, P8
4	12 Degree Slope, Displacement Transducers 4 measurements of downslope displacement 2 measurements of transverse displacement	D7, D8, D9, D10 & D11, D12
5	12 Degree Slope, Pore Pressure Transducers Measurement of pore pressures at 8 locations and 1 external transducer to measure ambient barometric pressure	P9, P10, P11, P12, P13, P14, P15, P16 & P17

Each figure presented in Appendix C contains the following data fields:

- file = "CLM02_S1": Specifies the loading event that is plotted on that page and refers to the raw data file name.
- each_tick = … units: Refers to the model-unit increment (in appropriate units) represented by the distance between tick marks on the ordinate axis.
- inst_from_top = (…): Designates a list of instruments for which data is plotted on that page, where left-to-right listing corresponds to top-to-bottom order of instruments in the plot.
- pk_to_pk = (…): Gives the peak-to-peak response, in model units, of each instrument for which data is plotted on that page. The peak-to-peak responses are listed in the same order as the instruments are listed in the "inst_from_top" field.

For plotting purposes, each instrument's data was zeroed at the beginning of the time history for each event. On the plots, the recorded data oscillates about an offset "zero" line. Adjacent instrument signals on the plots have been offset so as not to overlap on each figure. The time axis in the plots is in model-scale seconds and in some cases has been truncated to show only a portion of the time histories for an event.

REFERENCES

Kutter, B. L. (1992). "Dynamic centrifuge modeling of geotechnical structures." *Transportation Research Record*, 1336, 24-30.

APPENDIX A

CENTRIFUGE MODEL DRAWINGS

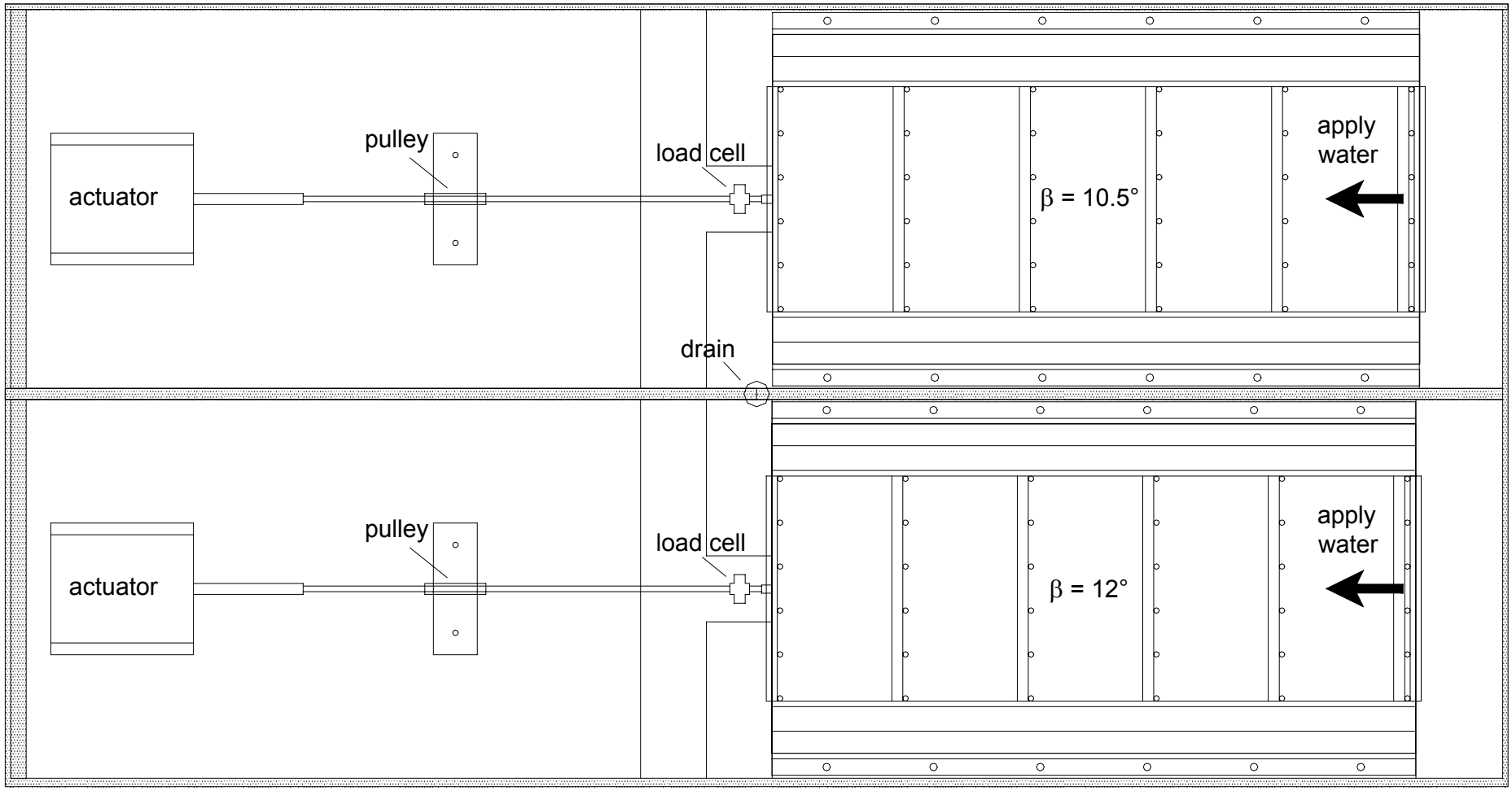

Figure A1 – Overall Concept – Plan View

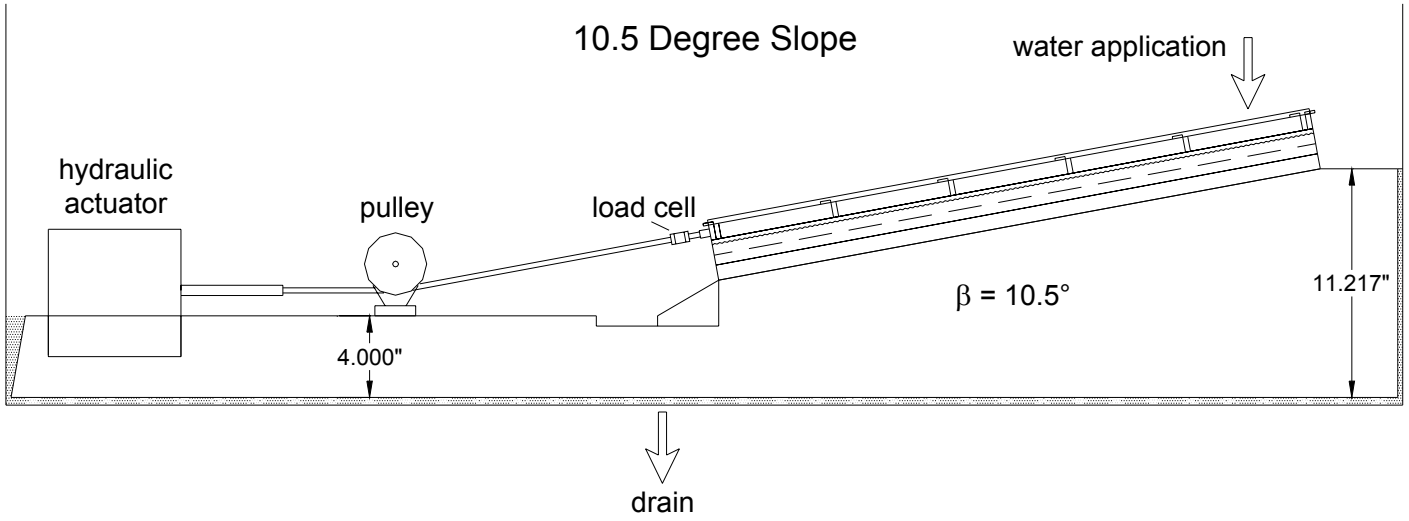

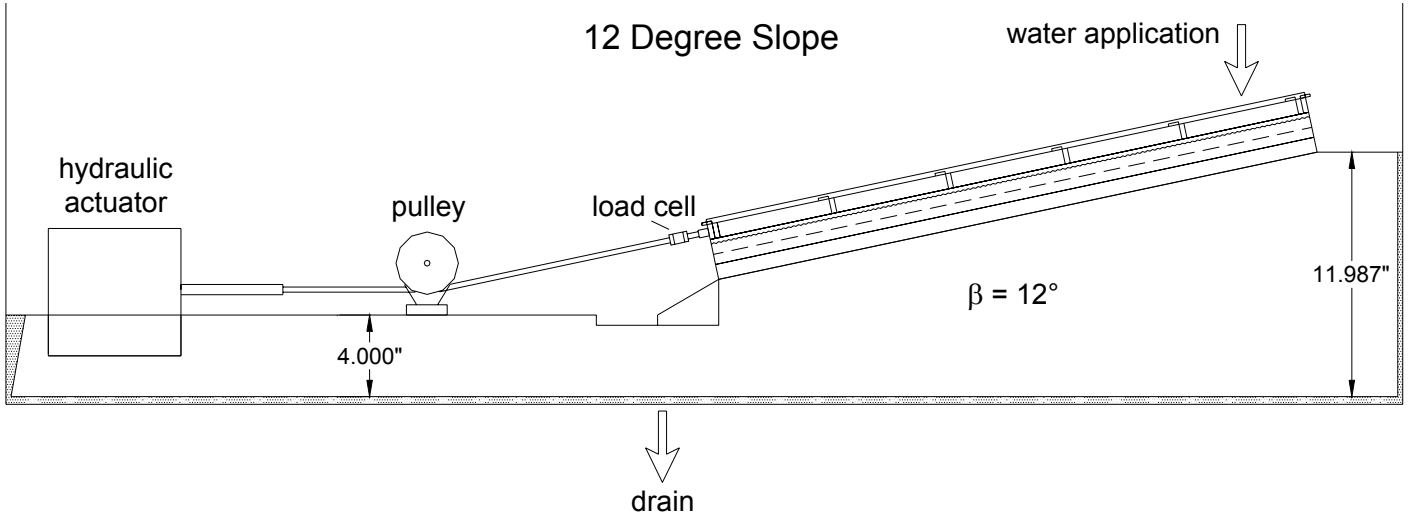

Figure A2 – Overall Concept – Side View

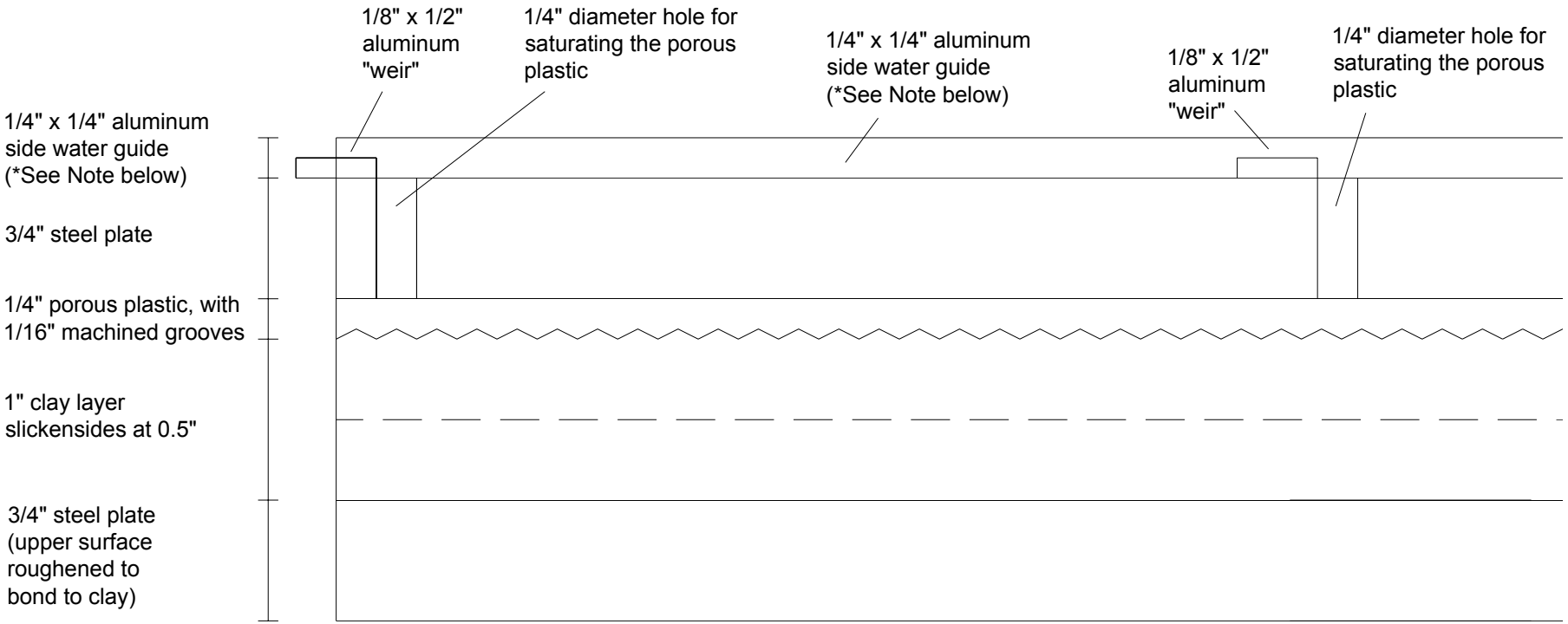

*Note: aluminum side water guide is 1/4" wide by 1/2" tall on the outside edges of the model, to account for the curvature of the water's surface that results from the curvature of the g-field across the width of the specimen.

Figure A3 – Detailed Side View of Specimen During Test

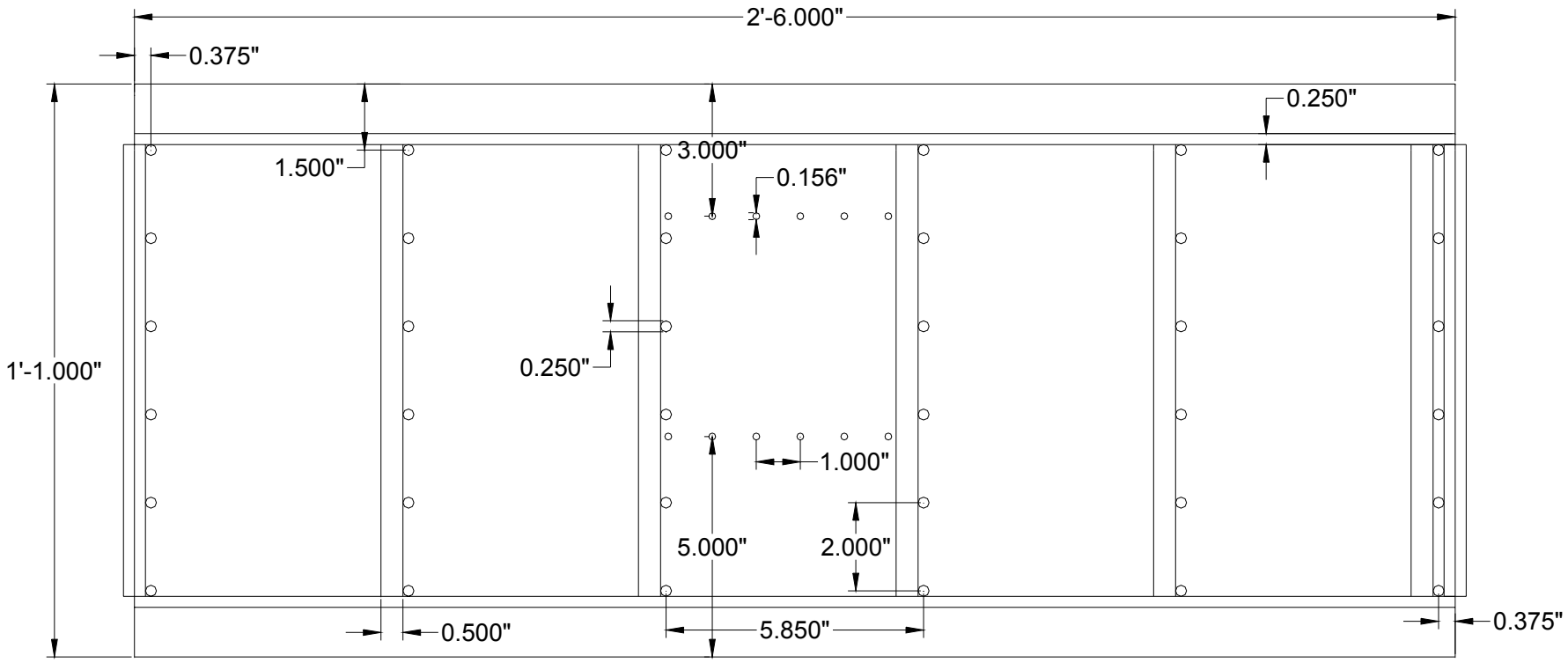

Figure A4 – Detailed View of Upper Steel Plate

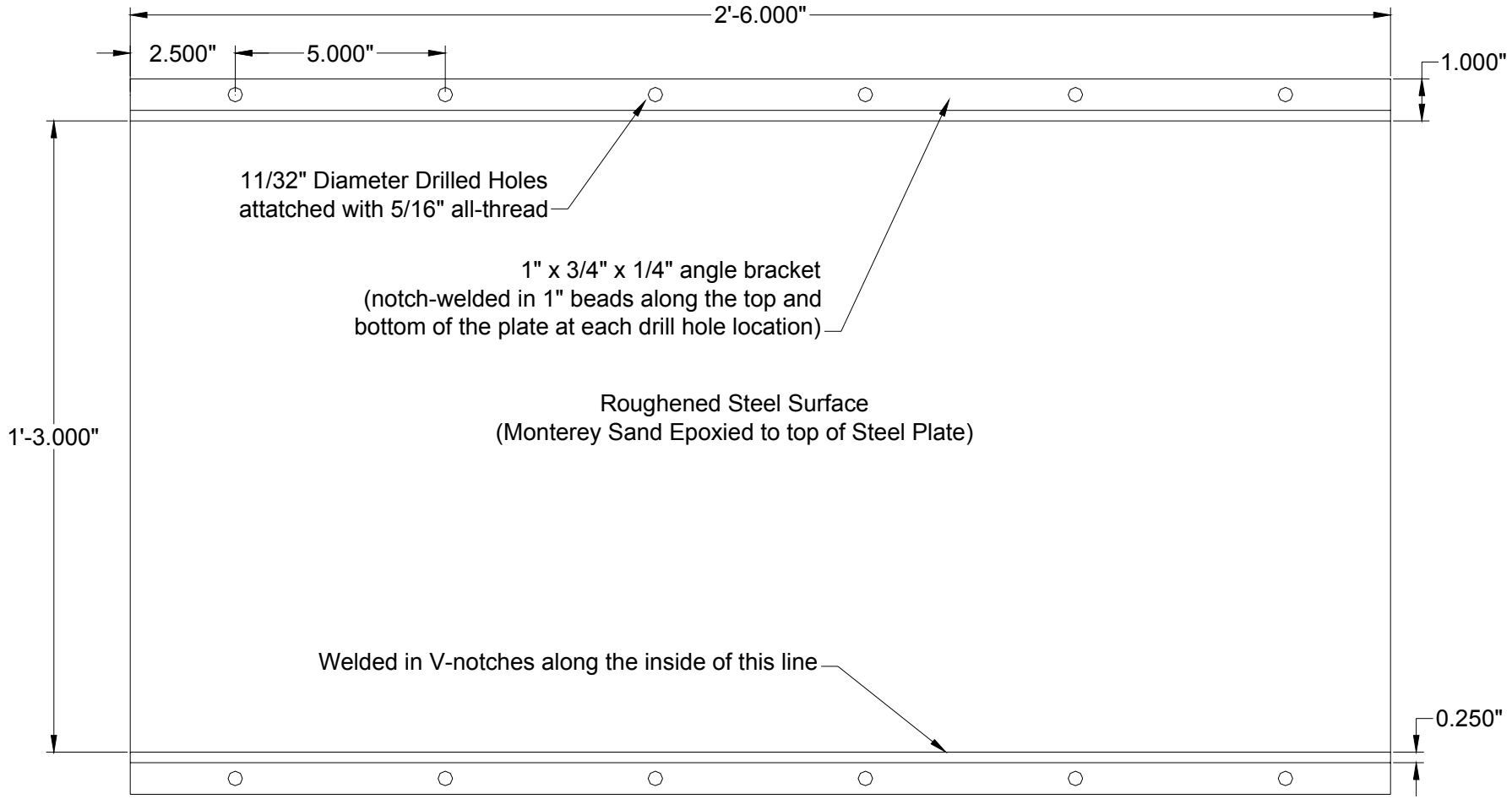

Figure A5 – Detailed View of Lower Steel Plate

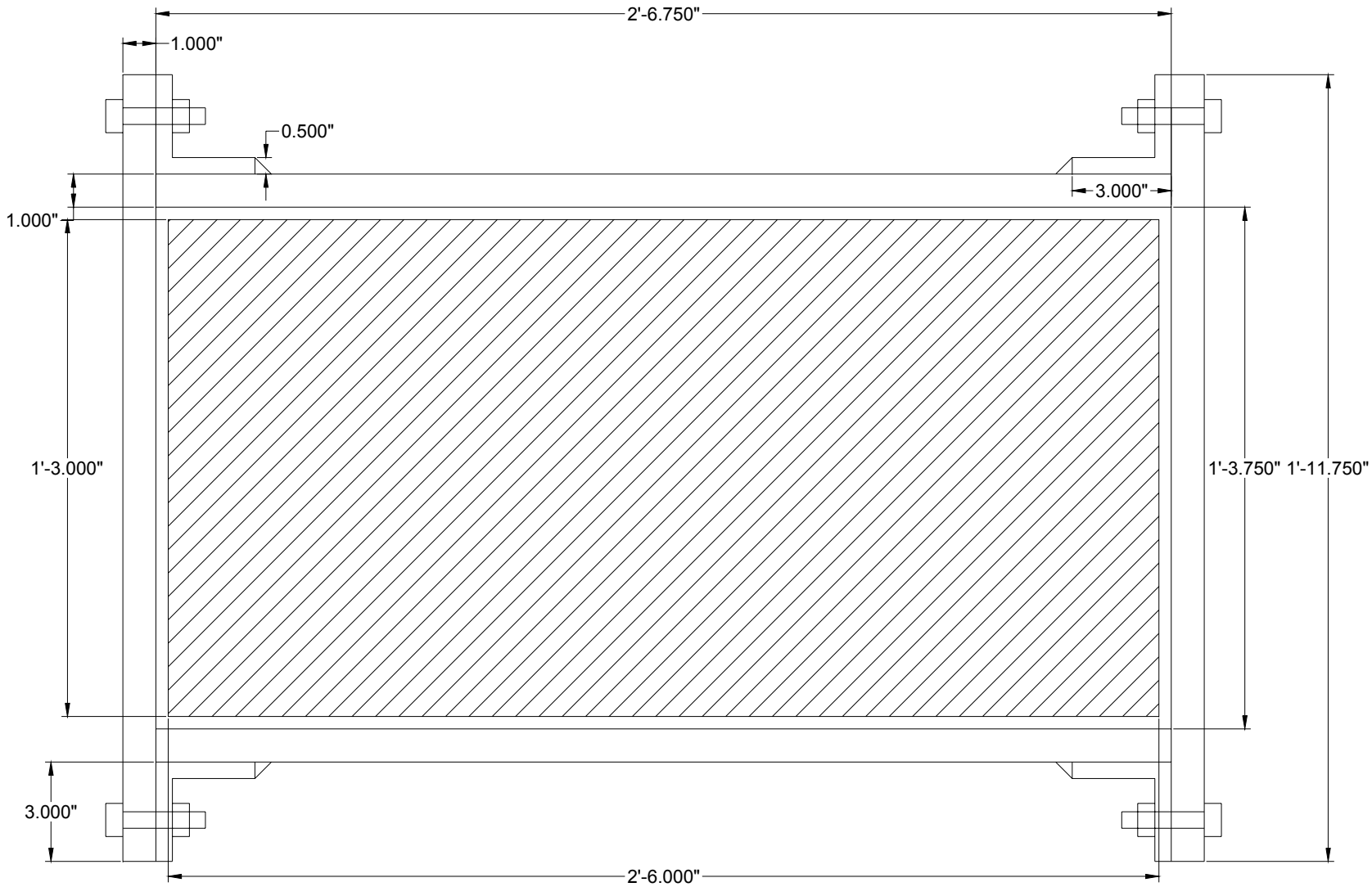

Figure A6 – Consolidation Mold, Plan View

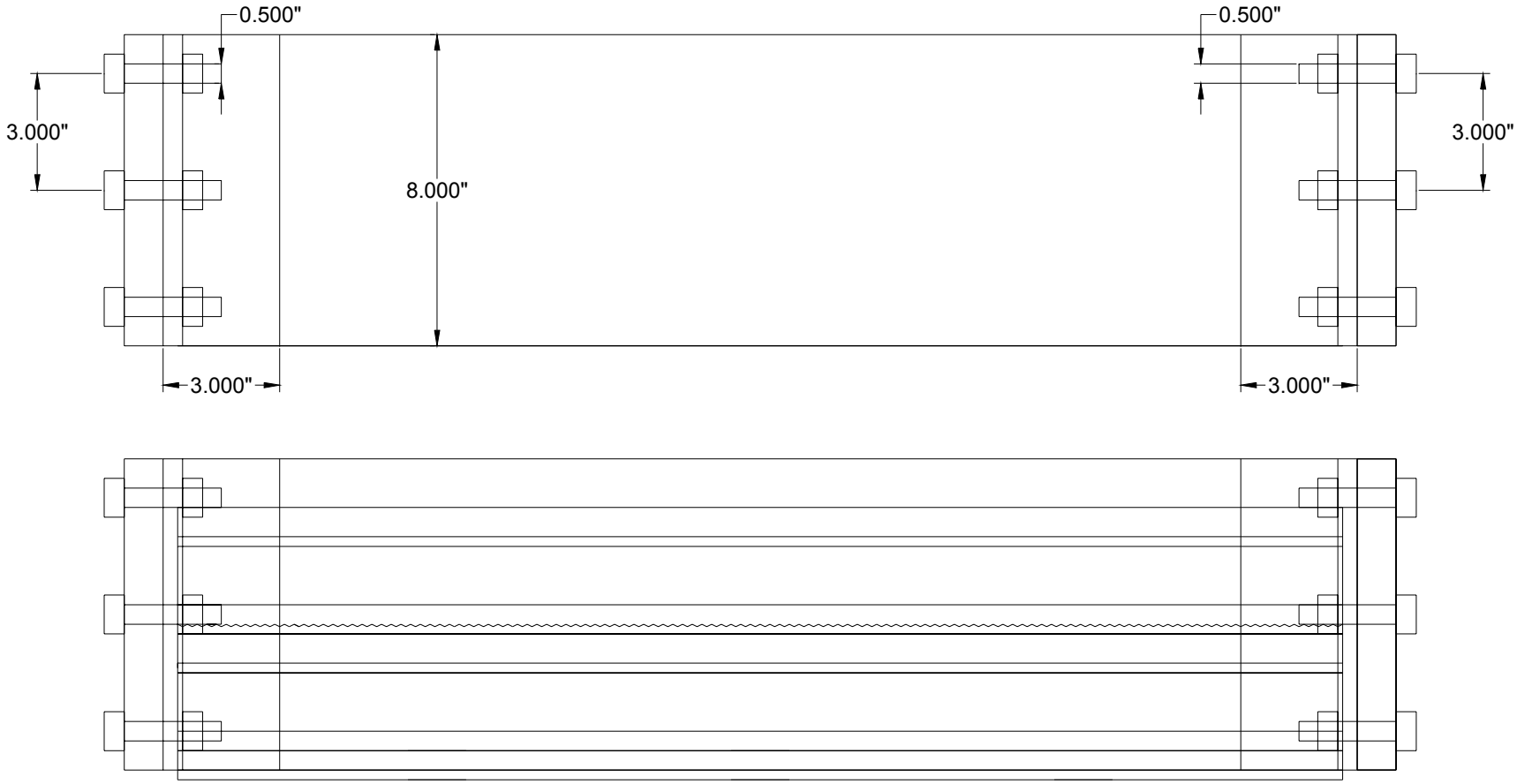

Figure A7 – Consolidation Mold, Side View

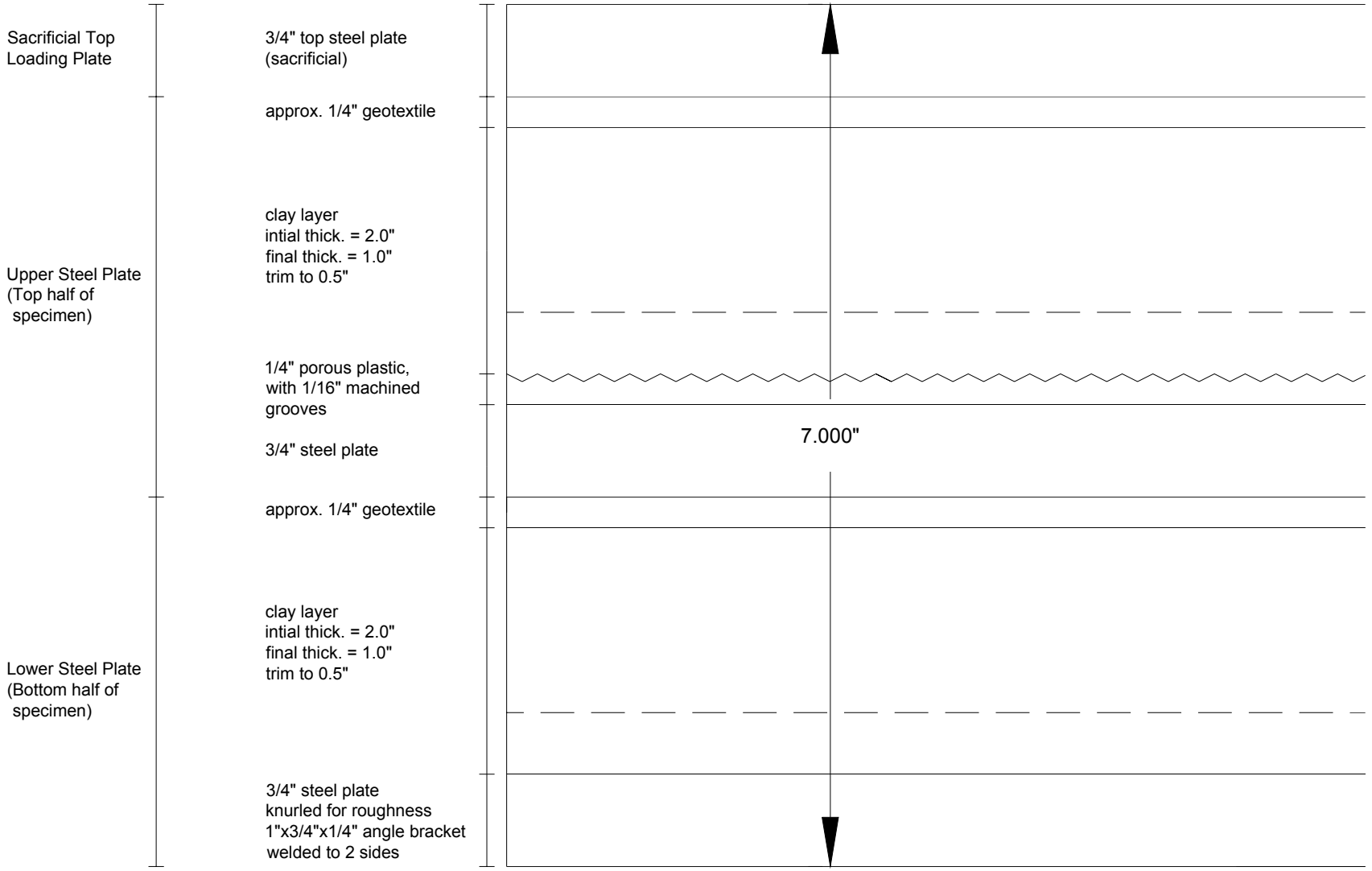

Figure A8 – Consolidation Layer System, Detail View

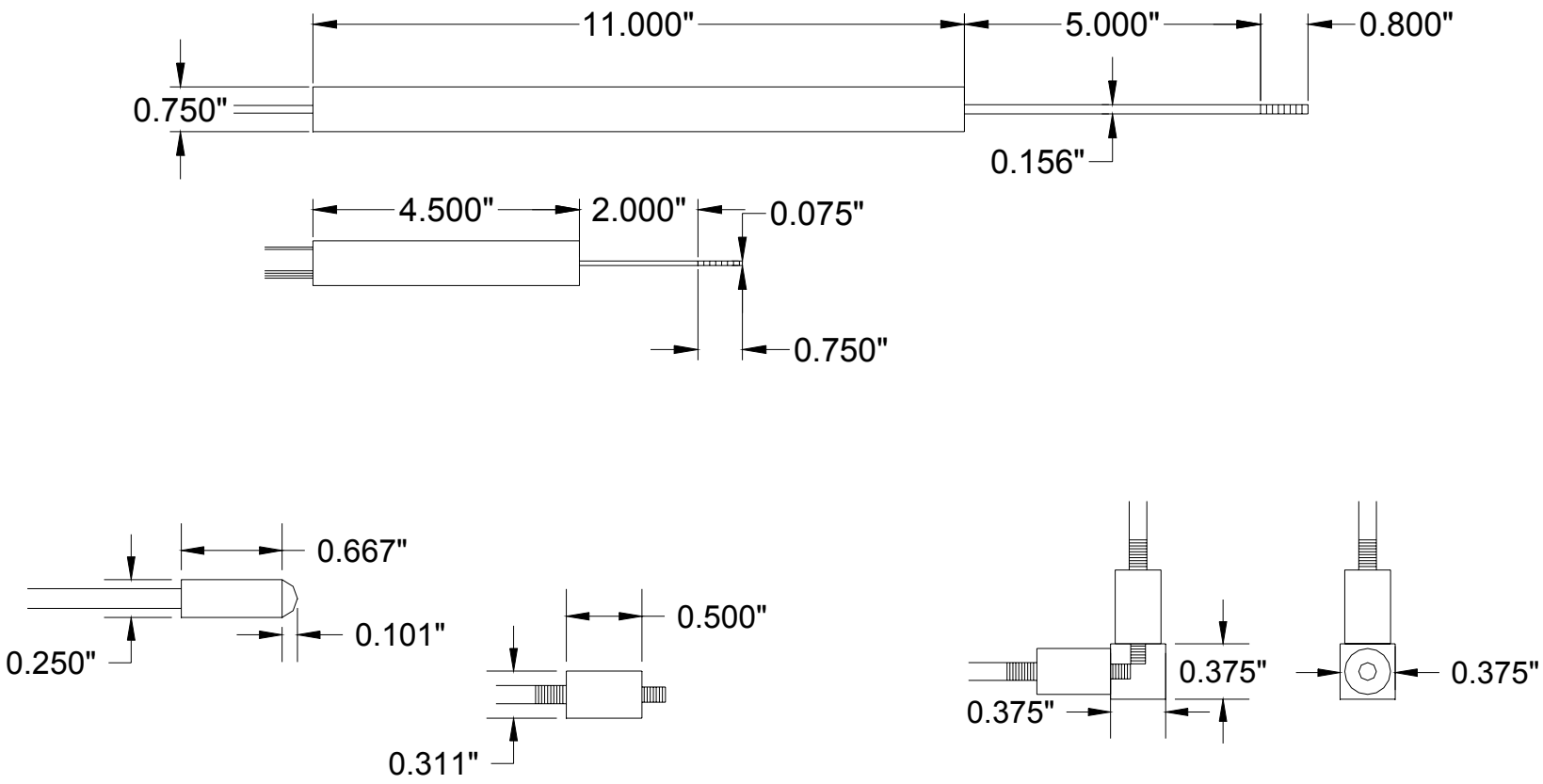

Figure A9 – Approximate Instrument Sizes and Dimensions
(Not to Scale)

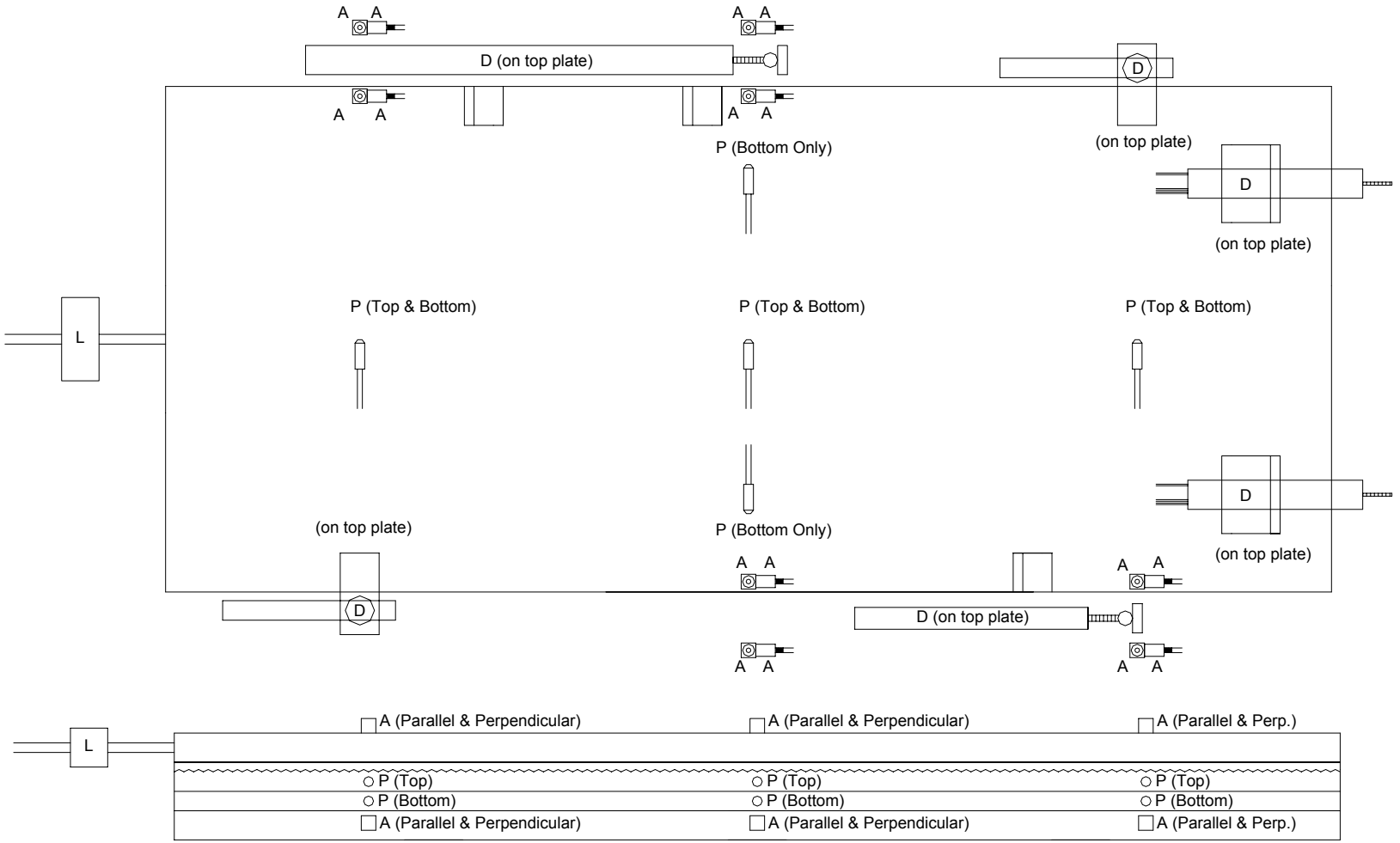

KEY: A = Accelerometer
P = Pore Pressure Transducer
D = Displacement Transducer (LP or LVDT)
L = Load Cell

SCALE (inches) 0 1 2 3 4 5

Figure A10 – Location of Instruments on Each Plate

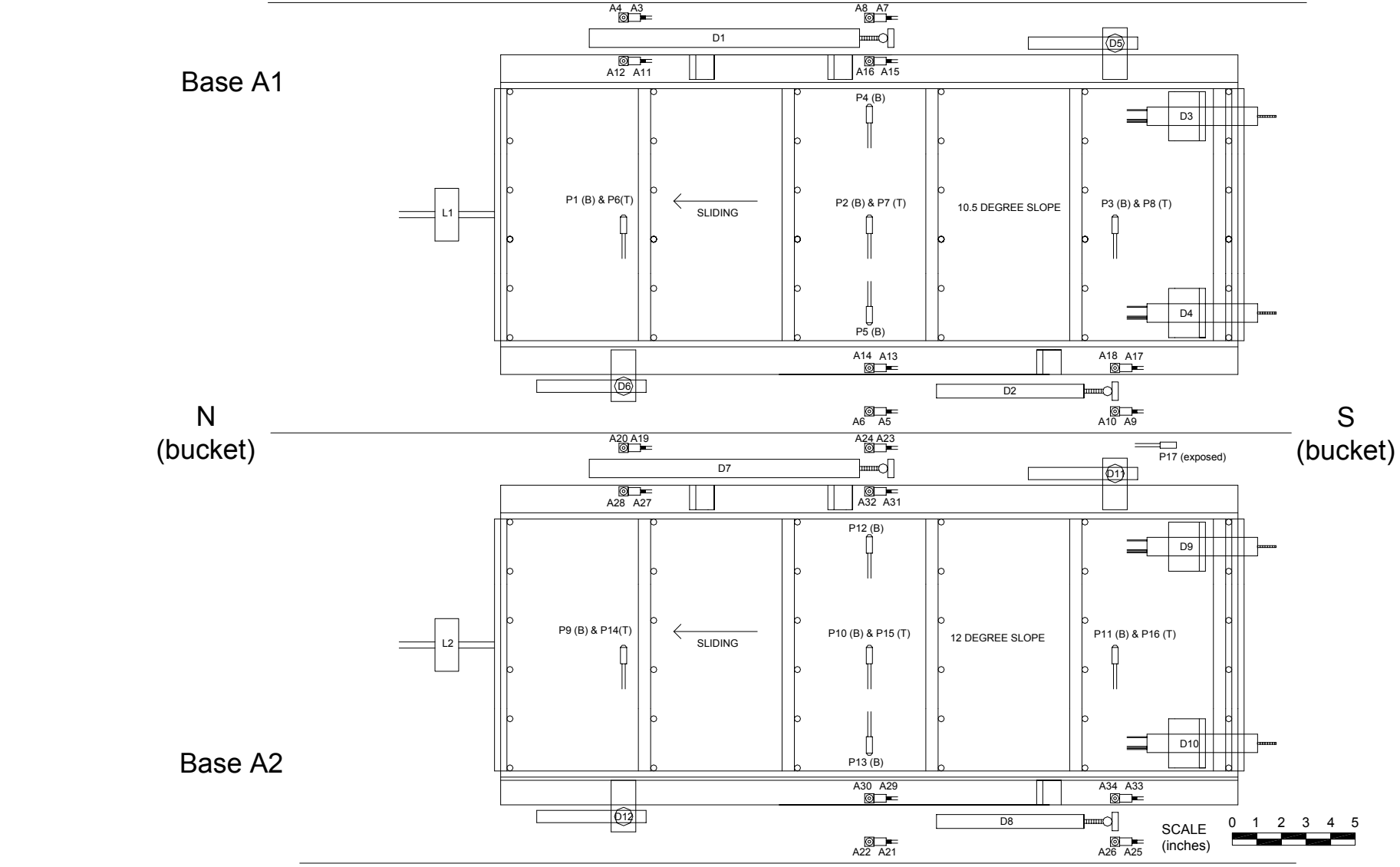

Figure A11 – Instrument Numbering Scheme

APPENDIX B

CONSOLIDATION DATA

Load Steps Used to Consolidate the Rancho Solano Clay

Load Step	Date	Time	Load Step Description	Hydraulic Pressure (psi)	Load on Upper Plate (lbs)	Load on Lower Plate (lbs)	Area (square feet)	Pressure on Upper Plate (psf)	Pressure on Lower Plate (psf)
1	8-Jul	17:00	plate, clay, plate, I-beams		160	340	3.125	51	109
2	11-Jul	9:29	1st ram step	55	1307	1485	3.125	418	475
3	11-Jul	16:00	2nd ram step	110	2613	2791	3.125	836	893
4	12-Jul	8:49	3rd ram step	220	5227	5405	3.125	1673	1730
5	12-Jul	13:09	4th ram step	440	10454	10632	3.125	3345	3402
6	13-Jul	9:12	5th ram step	900	21382	21560	3.125	6842	6899
7	13-Jul	12:27	6th ram step	1900	45141	45319	3.125	14445	14502

Load Step 2

10.5 Degree Slope				12 Degree Slope			
Time (min.)	Left Rear Dial Reading (in.)	Time (min.)	Right Front Dial Reading (in.)	Time (min.)	Left Rear Dial Reading (in.)	Time (min.)	Right Front Dial Reading (in.)
0.25	0.11	0.5	0.128	0.1	0.109	0.1	0.133
0.5	0.135	1	0.145	0.25	0.113	0.25	0.142
1	0.156	2	0.16	0.5	0.121	0.5	0.156
2	0.171	4.1	0.176	1	0.13	1	0.167
4.1	0.189	8.5	0.198	2	0.138	2	0.179
8.5	0.21	16	0.222	4.1	0.149	4.1	0.196
16	0.233	30	0.255	8.5	0.163	8.5	0.215
30	0.261	65	0.31	16	0.181	16	0.238
65	0.313	128	0.377	30	0.206	30	0.271
128	0.377	240	0.43	65	0.248	65	0.322
240	0.431	384	0.459	128	0.2985	128	0.382
384	0.46			240	0.338	240	0.427
				384	0.361	384	0.45

Load Step 3

10.5 Degree Slope				12 Degree Slope			
Time (min.)	Left Rear Dial Reading (in.)	Time (min.)	Right Front Dial Reading (in.)	Time (min.)	Left Rear Dial Reading (in.)	Time (min.)	Right Front Dial Reading (in.)
0.1	0.103	0.1	0.105	0.1	0.104	0.1	0.105
0.3	0.107	0.25	0.111	0.25	0.11	0.25	0.11
0.5	0.113	0.5	0.1215	0.5	0.118	0.5	0.117
1	0.119	1.0	0.13	1	0.124	1	0.123
2.0	0.125	2	0.137	2	0.13	2	0.129
4	0.132	4	0.147	4.0	0.139	4.0	0.137
8	0.143	8	0.159	8	0.151	8	0.1475
16	0.157	16	0.1775	16	0.166	16	0.163
31	0.176	31	0.201	31	0.186	31	0.183
58	0.2	58	0.228	58	0.209	58	0.202
994	0.271	994	0.305	994	0.288	994	0.2795

Load Step 4

10.5 Degree Slope				12 Degree Slope			
Time (min.)	Left Rear Dial Reading (in.)	Time (min.)	Right Front Dial Reading (in.)	Time (min.)	Left Rear Dial Reading (in.)	Time (min.)	Right Front Dial Reading (in.)
0.1	0.106	0.1	0.11	0.1	0.112	0.1	0.112
0.3	0.112	0.25	0.118	0.25	0.118	0.25	0.117
0.5	0.116	0.5	0.1235	0.5	0.122	0.5	0.1205
1	0.12	1.0	0.128	1	0.126	1	0.1245
2.0	0.124	2	0.1345	2	0.132	2	0.1295
4	0.13	4	0.1425	4.0	0.14	4.0	0.136
8	0.1395	8	0.153	8	0.1505	8	0.1455
16	0.1515	16	0.168	16	0.1645	16	0.1585
32	0.168	32	0.187	32	0.183	32	0.176
60	0.187	60	0.208	60	0.2035	60	0.196
120	0.209	120	0.2315	120	0.2255	120	0.218
254	0.227	254	0.249	254	0.244	254	0.235

Load Step 5

10.5 Degree Slope				12 Degree Slope			
Time (min.)	Left Rear Dial Reading (in.)	Time (min.)	Right Front Dial Reading (in.)	Time (min.)	Left Rear Dial Reading (in.)	Time (min.)	Right Front Dial Reading (in.)
0.1	0.115	0.1	0.124	0.1	0.121	0.1	0.123
0.3	0.128	0.25	0.133	0.25	0.129	0.25	0.129
0.5	0.132	0.5	0.1395	0.5	0.133	0.5	0.1345
1	0.138	1.0	0.145	1	0.139	1	0.14
2.0	0.145	2	0.1515	2	0.146	2	0.147
4	0.153	4	0.161	4.0	0.156	4.0	0.1565
8	0.1645	8	0.174	8	0.169	8	0.169
20	0.1875	20	0.198	20	0.193	20	0.193
40	0.211	40	0.2215	40	0.2165	40	0.2175
72	0.2305	72	0.2415	72	0.2365	72	0.238
146	0.246	146	0.26	146	0.258	146	0.257
268	0.255	268	0.27	268	0.271	268	0.267
1186	0.2635	1186	0.279	1186	0.282	1186	0.2755

Load Step 6

10.5 Degree Slope				12 Degree Slope			
Time (min.)	Left Rear Dial Reading (in.)	Time (min.)	Right Front Dial Reading (in.)	Time (min.)	Left Rear Dial Reading (in.)	Time (min.)	Right Front Dial Reading (in.)
0.1	0.132	0.1	0.122	0.1	0.132	0.1	0.123
0.3	0.145	0.25	0.136	0.25	0.139	0.25	0.132
0.5	0.157	0.5	0.142	0.5	0.148	0.5	0.138
1	0.164	1.0	0.148	1	0.153	1	0.144
2.0	0.171	2	0.155	2	0.16	2	0.1515
4	0.182	4	0.164	4.0	0.17	4.0	0.161
8	0.1955	8	0.176	8	0.1835	8	0.174
16	0.213	16	0.192	16	0.201	16	0.192
30	0.231	30	0.21	30	0.218	30	0.2105
63	0.2535	63	0.231	63	0.239	63	0.233
138	0.2685	138	0.25	138	0.259	138	0.252
190	0.275	190	0.256	190	0.266	190	0.257

Load Step 7

10.5 Degree Slope				12 Degree Slope			
Time (min.)	Left Rear Dial Reading (in.)	Time (min.)	Right Front Dial Reading (in.)	Time (min.)	Left Rear Dial Reading (in.)	Time (min.)	Right Front Dial Reading (in.)
0.1	0.14	0.1	0.125	0.1	0.13	0.1	0.141
0.3	0.165	0.25	0.148	0.25	0.152	0.25	0.157
0.5	0.179	0.5	0.159	0.5	0.164	0.5	0.166
1	0.191	1.0	0.169	1	0.178	1	0.174
2.0	0.203	2	0.181	2	0.19	2	0.185
4	0.216	4	0.195	4.0	0.205	4.0	0.197
8	0.232	8	0.2115	8	0.221	8	0.2125
16	0.2505	16	0.232	16	0.2415	16	0.232
26	0.2645	26	0.2485	26	0.257	26	0.249
60	0.294	60	0.2765	60	0.285	60	0.2785
127	0.314	127	0.297	127	0.3065	127	0.298
286	0.3255	286	0.312	286	0.3215	286	0.31
1235	0.3335	1235	0.3225	1235	0.3315	1235	0.318

Pore Pressures Measured During Consolidation for the 10.5 Degree Slope Model:

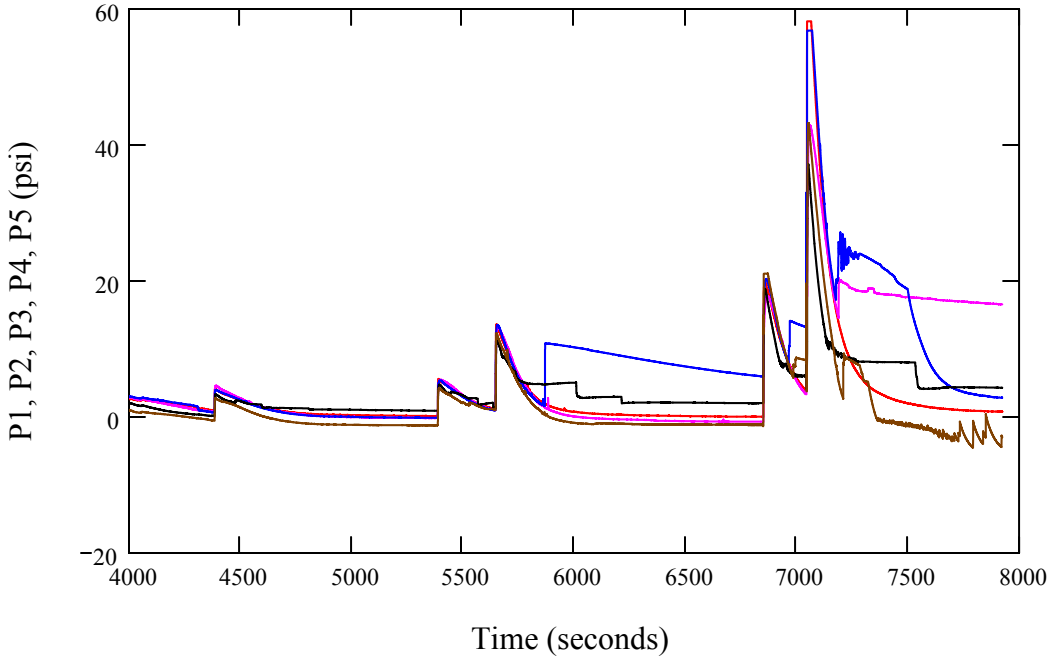

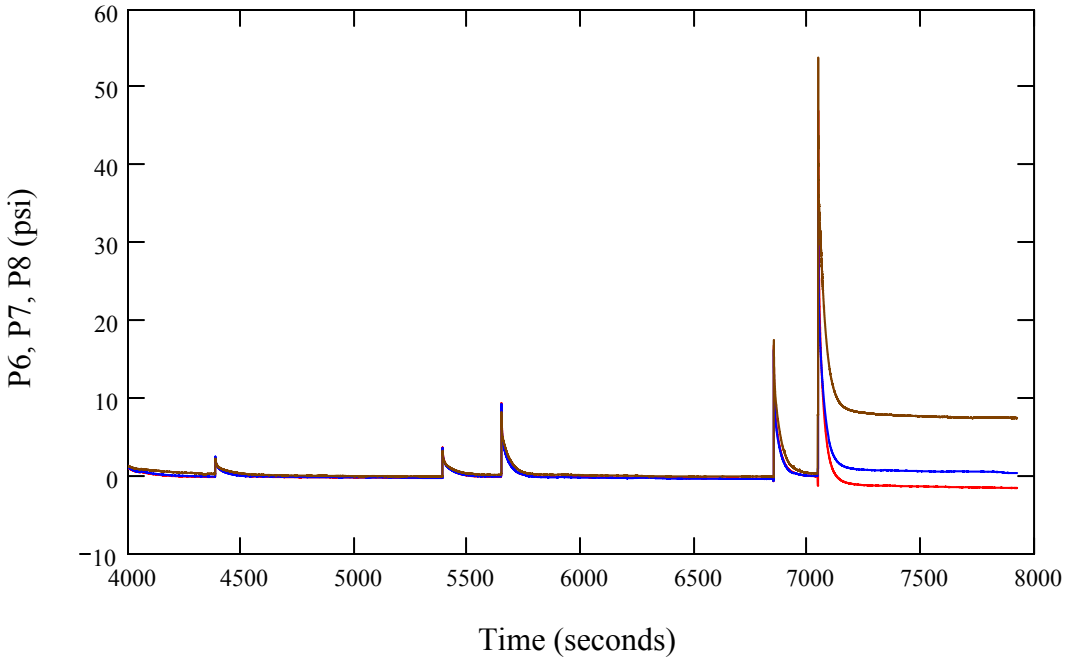

Pore Pressures Measured During Consolidation for the 12 Degree Slope Model:

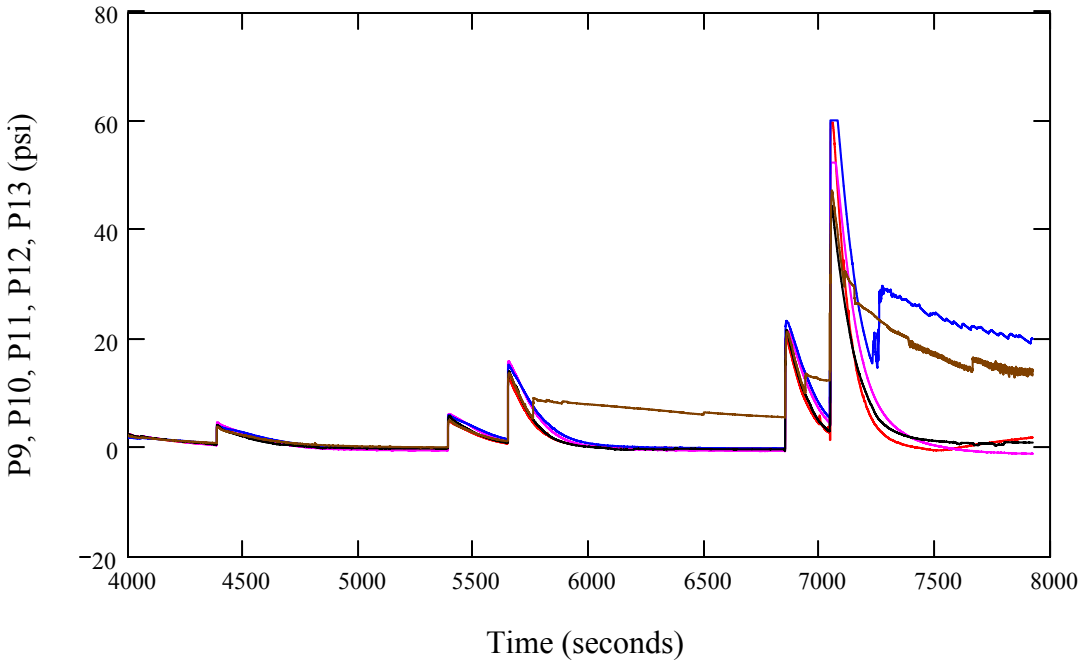

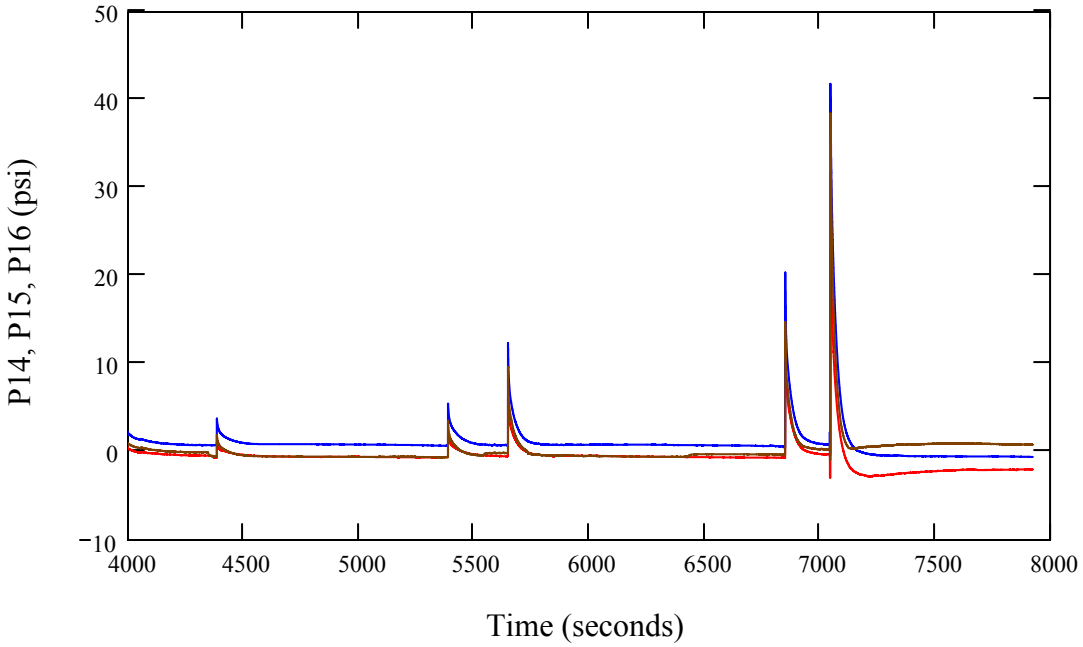

APPENDIX C

CENTRIFUGE DATA PLOTS

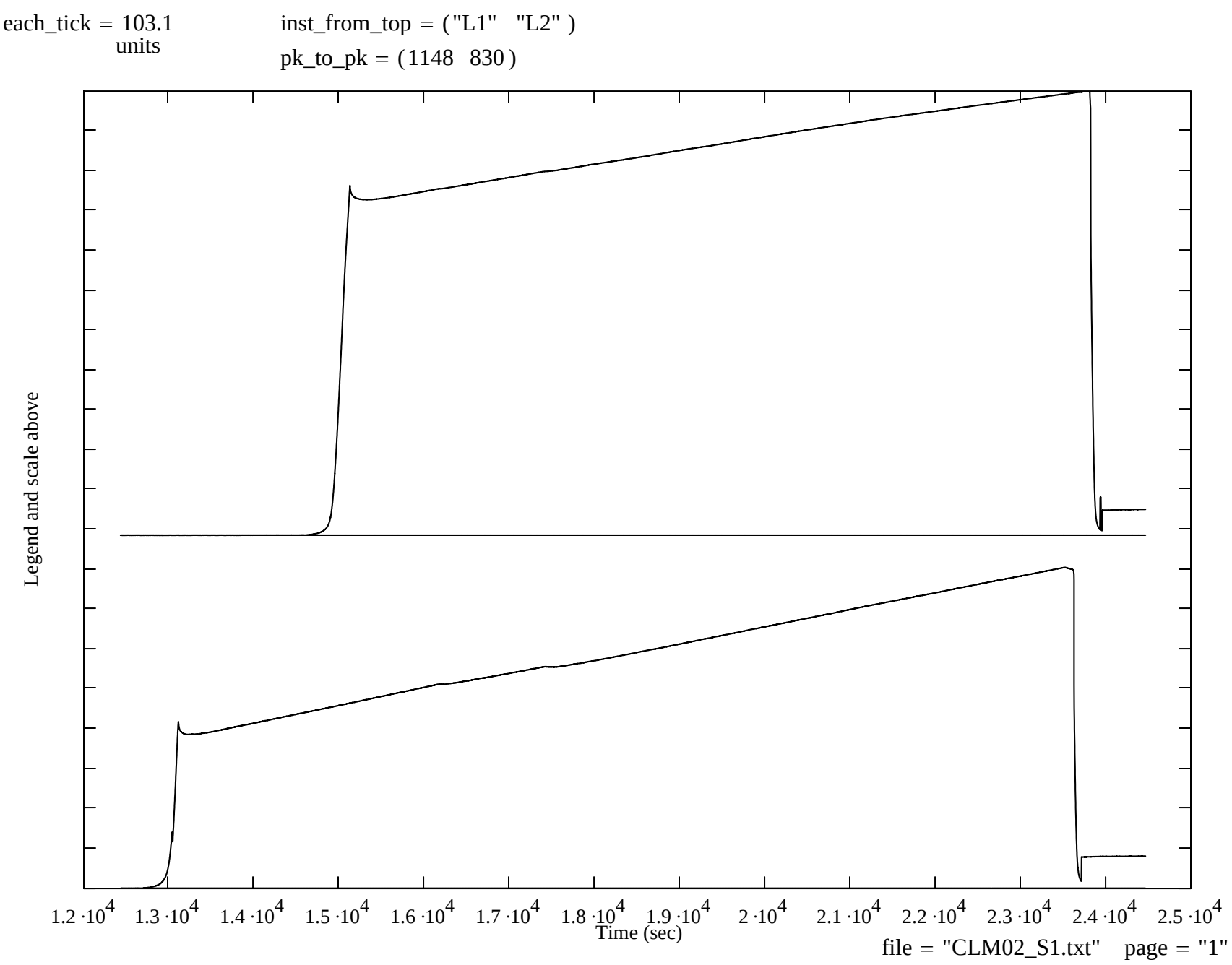
each_tick = 103.1
units
inst_from_top = ("L1" "L2")
pk_to_pk = (1148 830)
Legend and scale above
1.2 ·10^4
1.3 ·10^4
1.4 ·10^4
1.5 ·10^4
1.6 ·10^4
1.7 ·10^4
1.8 ·10^4
1.9 ·10^4
2 ·10^4
2.1 ·10^4
2.2 ·10^4
2.3 ·10^4
2.4 ·10^4
2.5 ·10^4
Time (sec)
file = "CLM02_S1.txt" page = "1"

each_tick = 0.013
units

inst_from_top = ("D1" "D2" "D3" "D4" "D5" "D6")

pk_to_pk = (0.048 0.064 0.061 0.063 0.005 0.006)

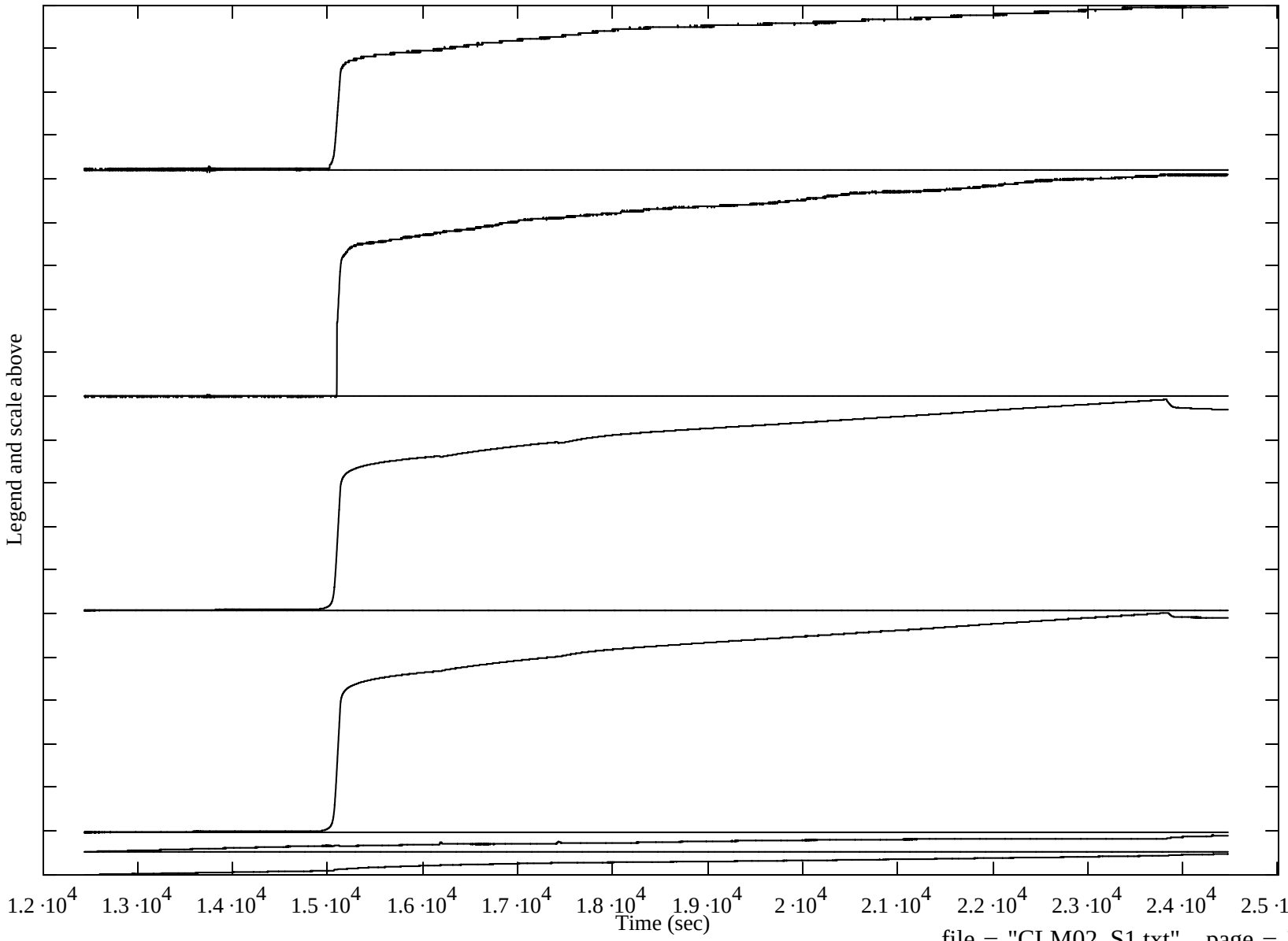

file = "CLM02_S1.txt" page = "2"

each_tick = 0.98
units

inst_from_top = ("P1" "P2" "P3" "P4" "P5" "P6" "P7" "P8")

pk_to_pk = (2.83 2.86 5.18 2.33 0.03 2.96 1.25 1.72)

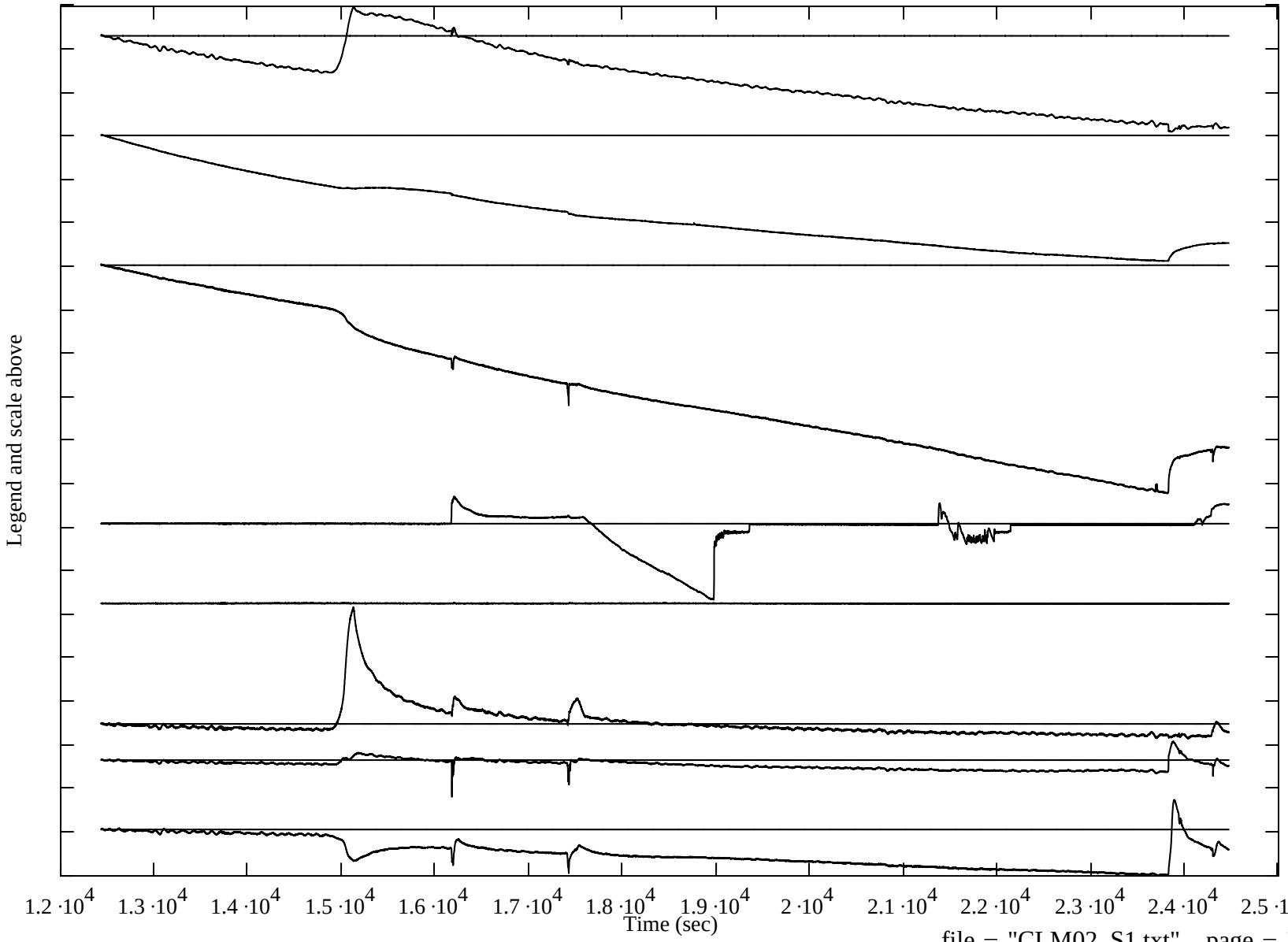

file = "CLM02_S1.txt" page = "3"

each_tick = 0.017
units

inst_from_top = ("D7" "D8" "D9" "D10" "D11" "D12")

pk_to_pk = (0.102 0.001 0.109 0.110 0.008 0.003)

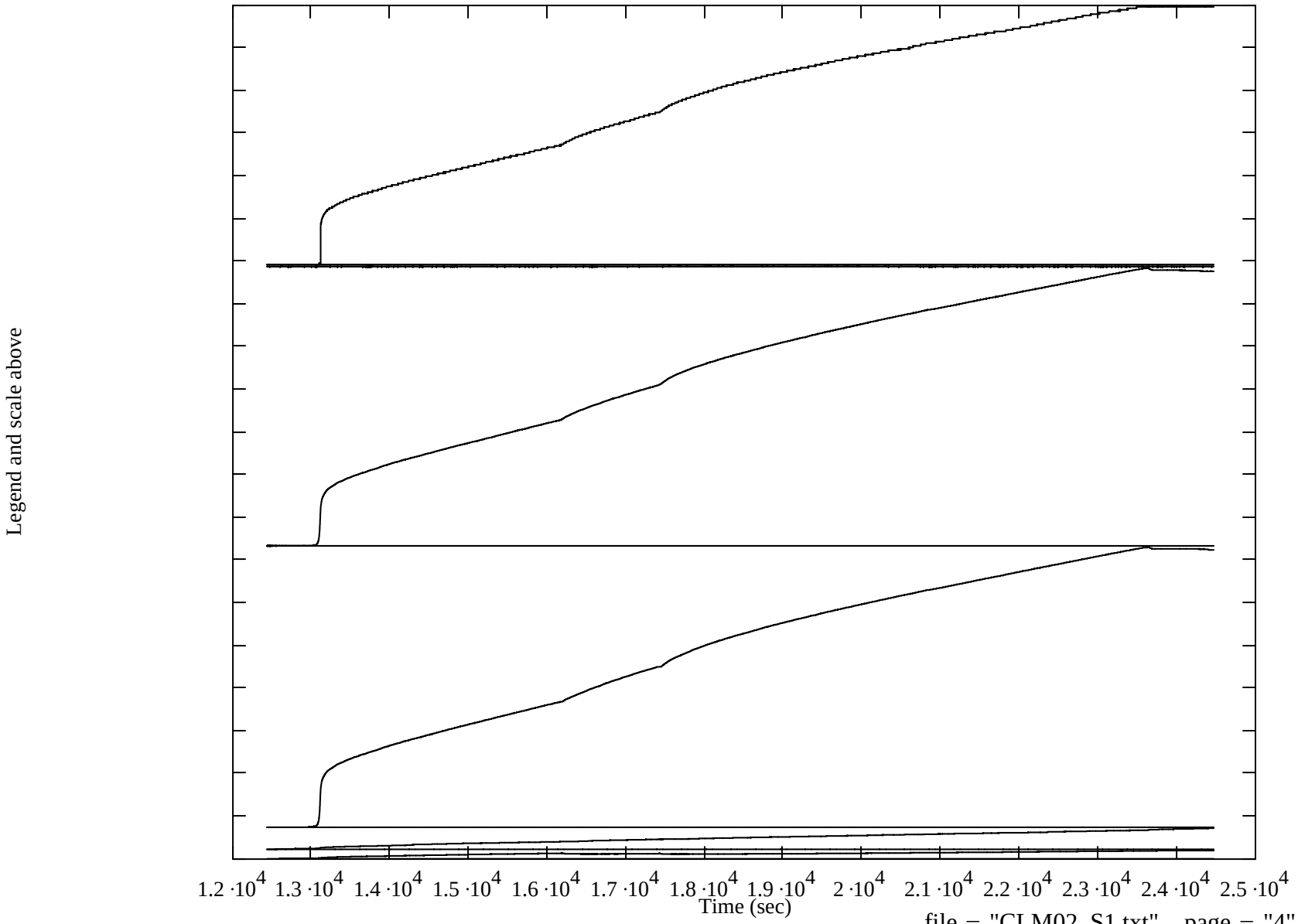

file = "CLM02_S1.txt" page = "4"

each_tick = 0.45
units

inst_from_top = ("P9" "P10" "P11" "P12" "P13" "P14" "P15" "P16" "P17")

pk_to_pk = (3.25 2.11 1.00 0.16 0.17 0.84 0.54 0.92 0.04)

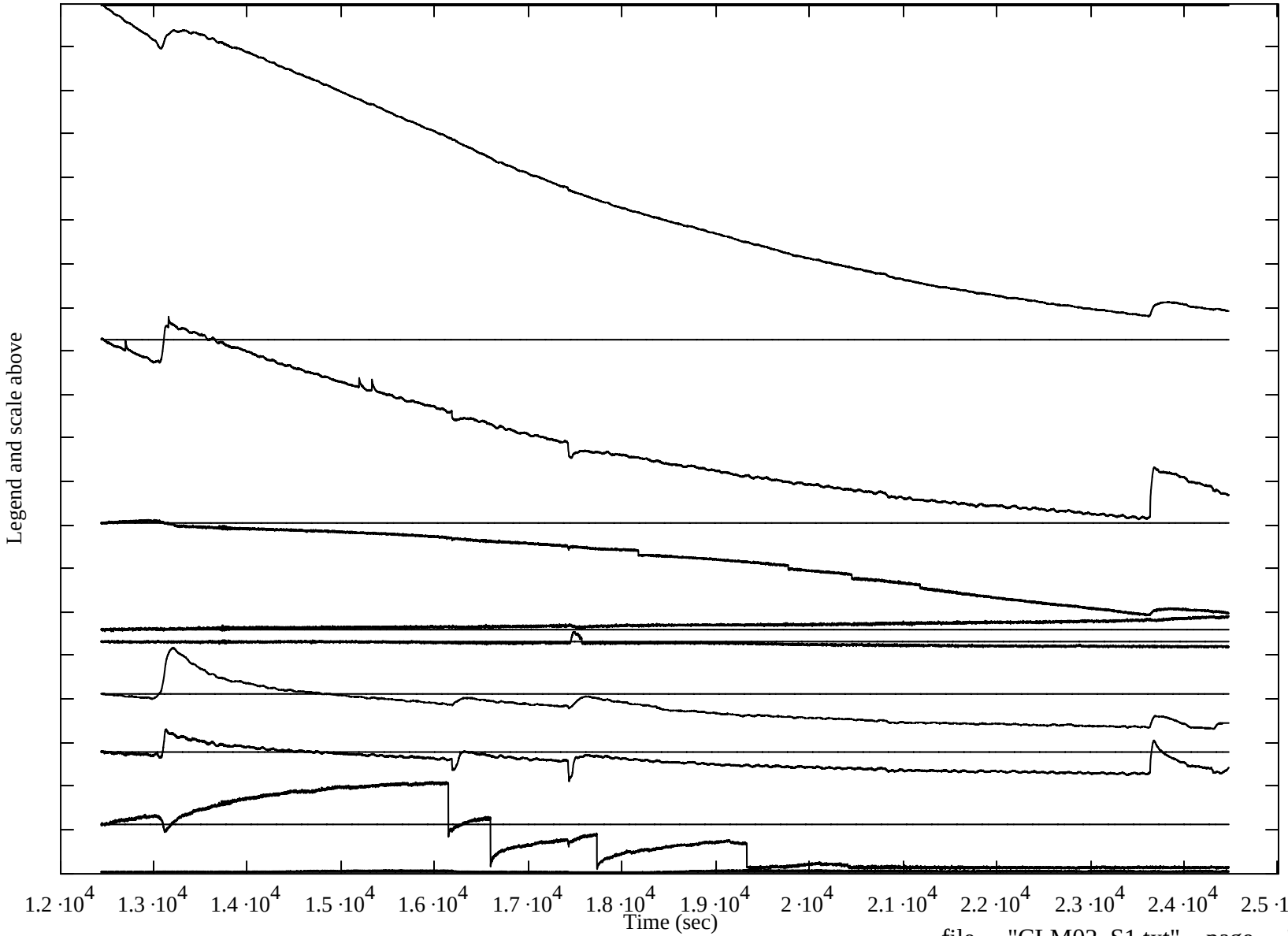

file = "CLM02_S1.txt" page = "5"

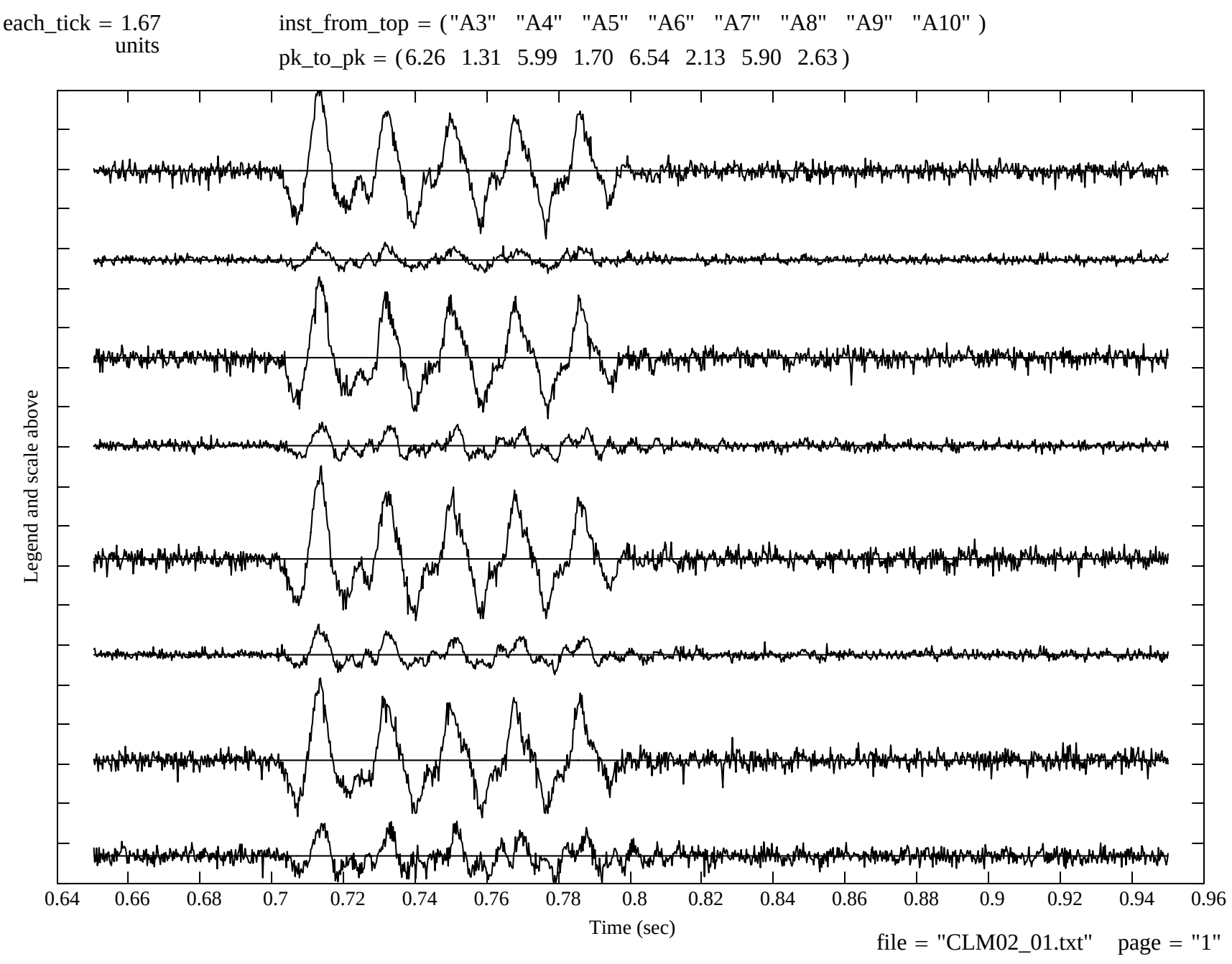
each_tick = 1.67
units
inst_from_top = ("A3" "A4" "A5" "A6" "A7" "A8" "A9" "A10")
pk_to_pk = (6.26 1.31 5.99 1.70 6.54 2.13 5.90 2.63)
Legend and scale above
0.64
0.66
0.68
0.7
0.72
0.74
0.76
0.78
0.8
0.82
0.84
0.86
0.88
0.9
0.92
0.94
0.96
Time (sec)
file = "CLM02_01.txt" page = "1"

each_tick = 1.91 units

inst_from_top = ("A11" "A12" "A13" "A14" "A15" "A16" "A17" "A18")

pk_to_pk = (7.47 1.76 6.77 2.42 7.14 1.98 6.65 2.92)

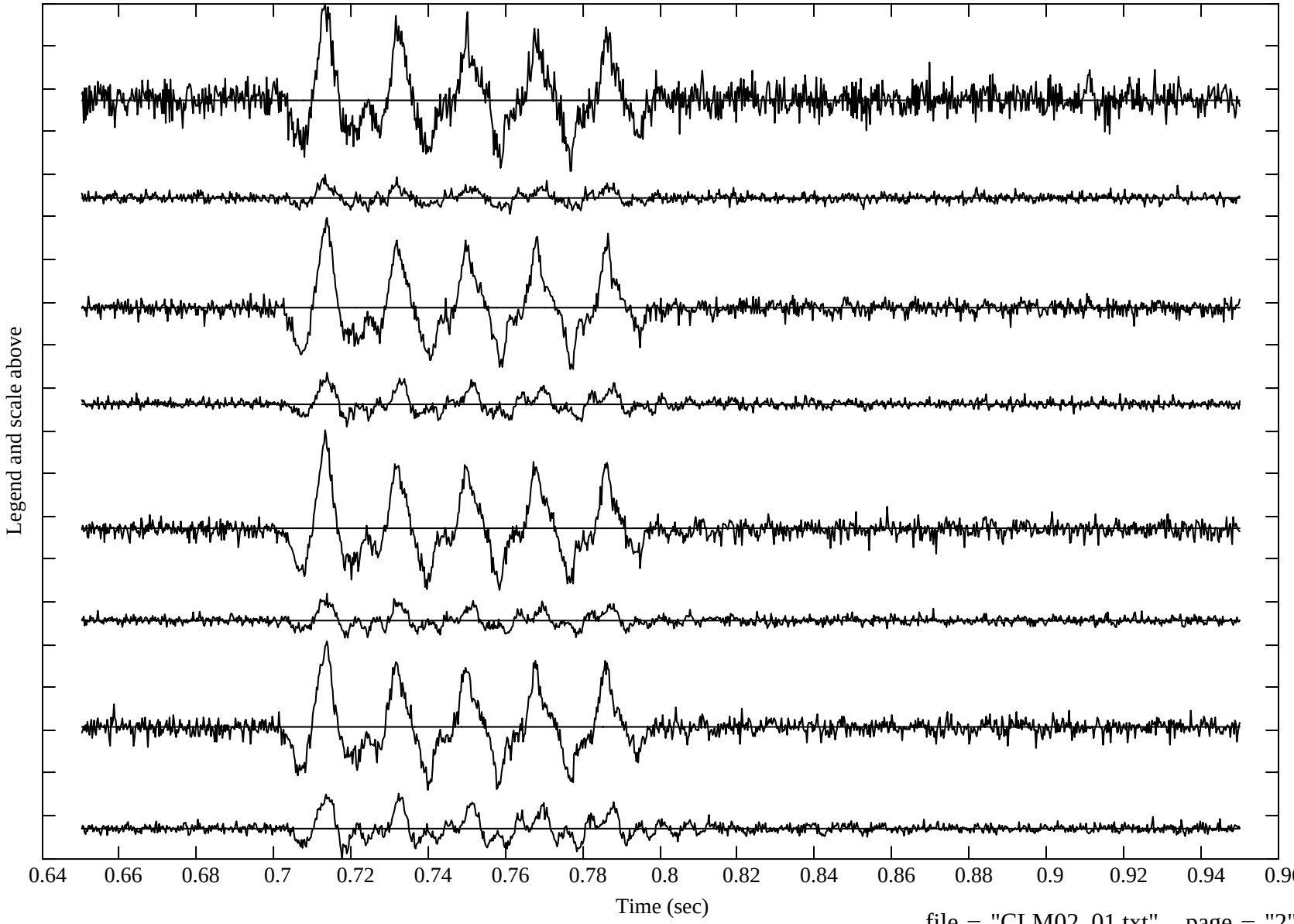

file = "CLM02_01.txt" page = "2"

each_tick = 0.012
units

inst from top = ("D1" "D2" "D3" "D4" "D5" "D6")

pk_to_pk = $\left(0.155 \quad 0.048 \quad 0.013 \quad 0.013 \quad 7.494 \times 10^{-3} \quad 3.346 \times 10^{-3}\right)$

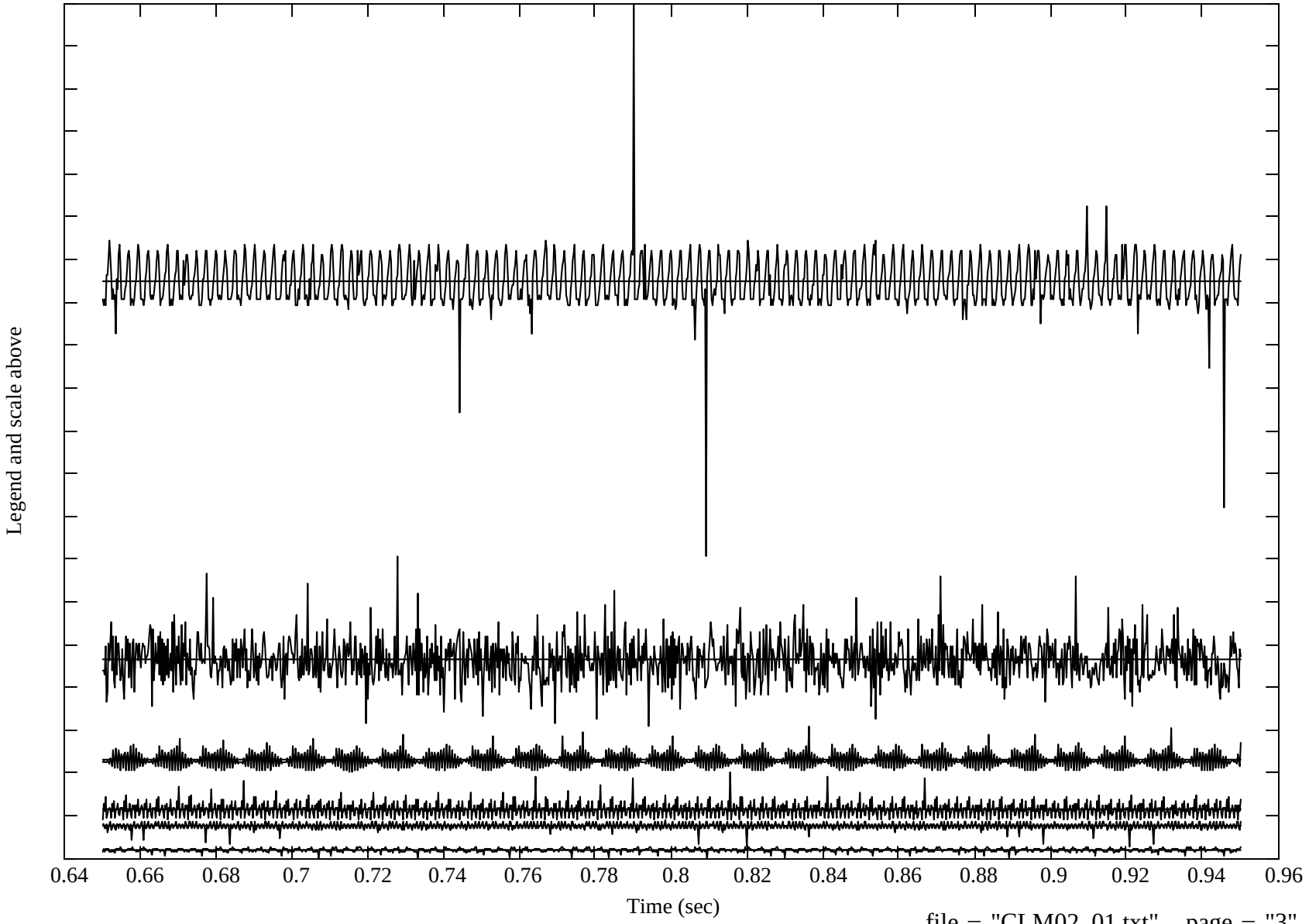

file = "CLM02_01.txt" page = "3"

each_tick = 0.76
units

inst_from_top = ("P1" "P2" "P3" "P4" "P5" "P6" "P7" "P8")

pk_to_pk = (0.55 0.65 2.22 1.73 1.29 3.33 2.36 2.31)

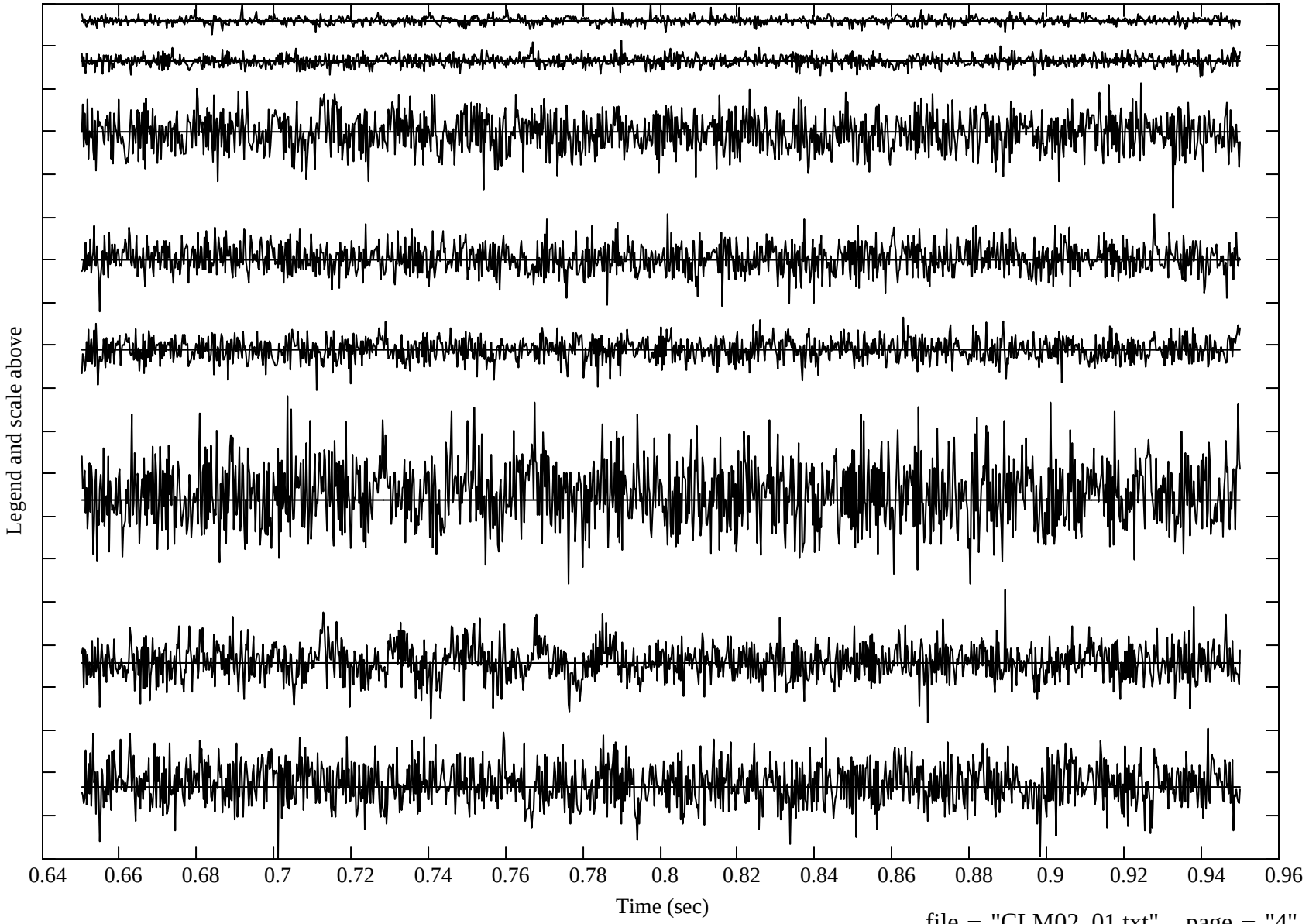

file = "CLM02_01.txt" page = "4"

each_tick = 1.88
units

inst_from_top = ("A19" "A20" "A21" "A22" "A23" "A24" "A25" "A26")

pk_to_pk = (6.82 1.47 6.08 2.27 6.79 2.63 7.20 3.15)

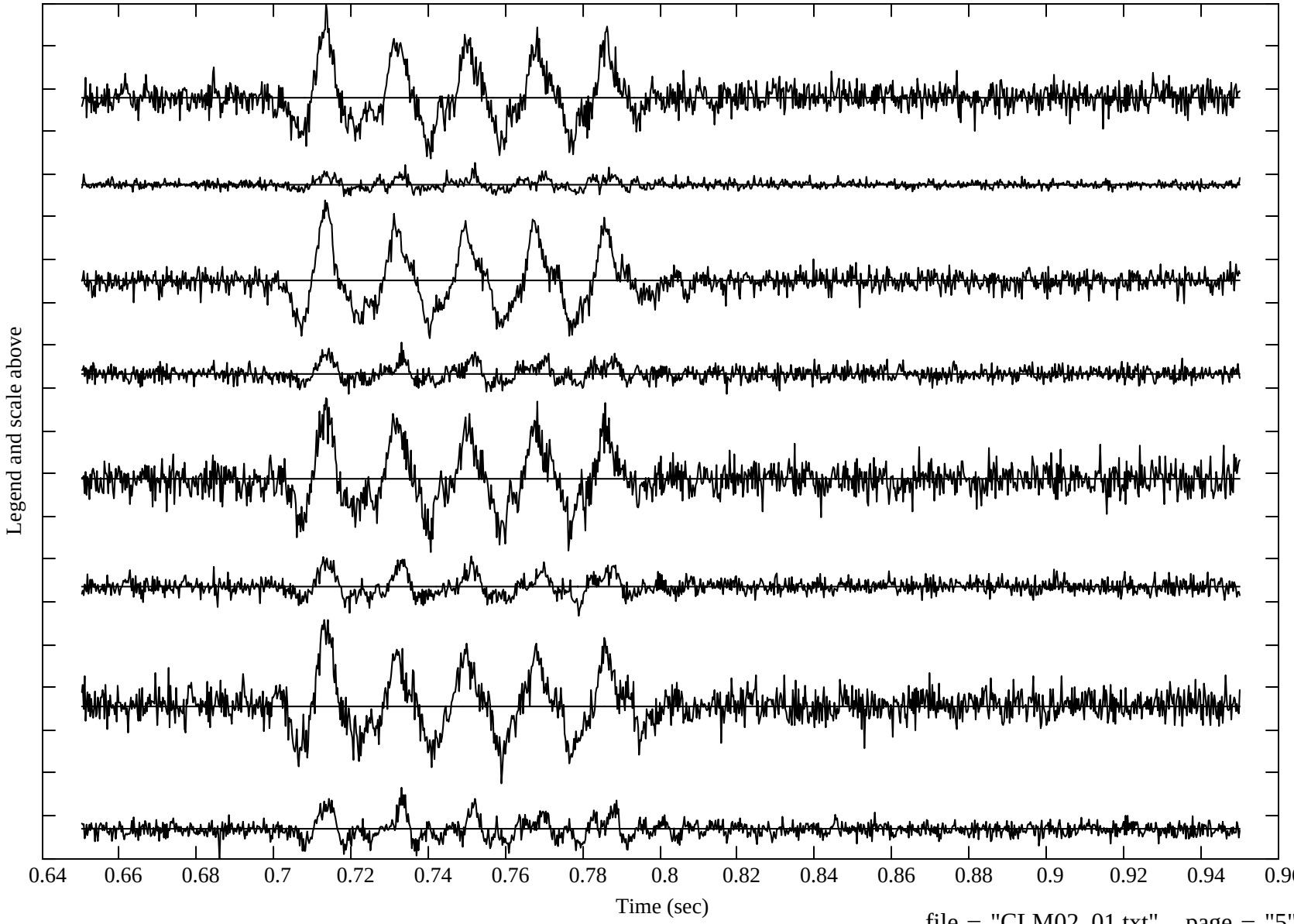

file = "CLM02_01.txt" page = "5"

each_tick = 2.05
units

inst_from_top = ("A27" "A28" "A29" "A30" "A31" "A32" "A33" "A34")

pk_to_pk = (7.55 2.41 7.05 2.95 7.07 2.33 7.26 3.13)

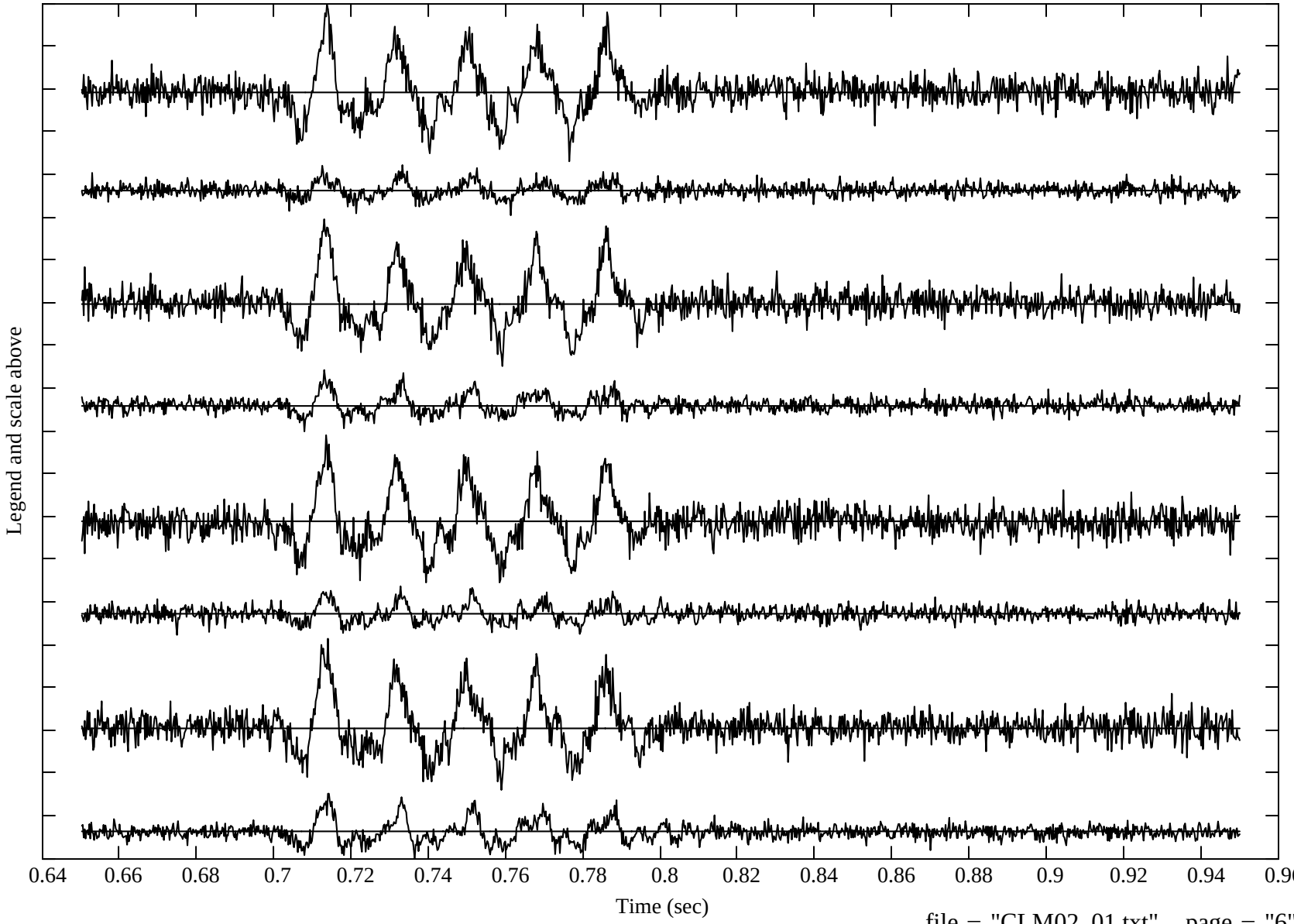

file = "CLM02_01.txt" page = "6"

each_tick = 5.99×10^{-3} units

inst from top = ("D7" "D8" "D9" "D10" "D11" "D12")

pk_to_pk = $\left(0.037 \quad 0.054 \quad 0.013 \quad 0.011 \quad 3.324 \times 10^{-3} \quad 1.956 \times 10^{-3}\right)$

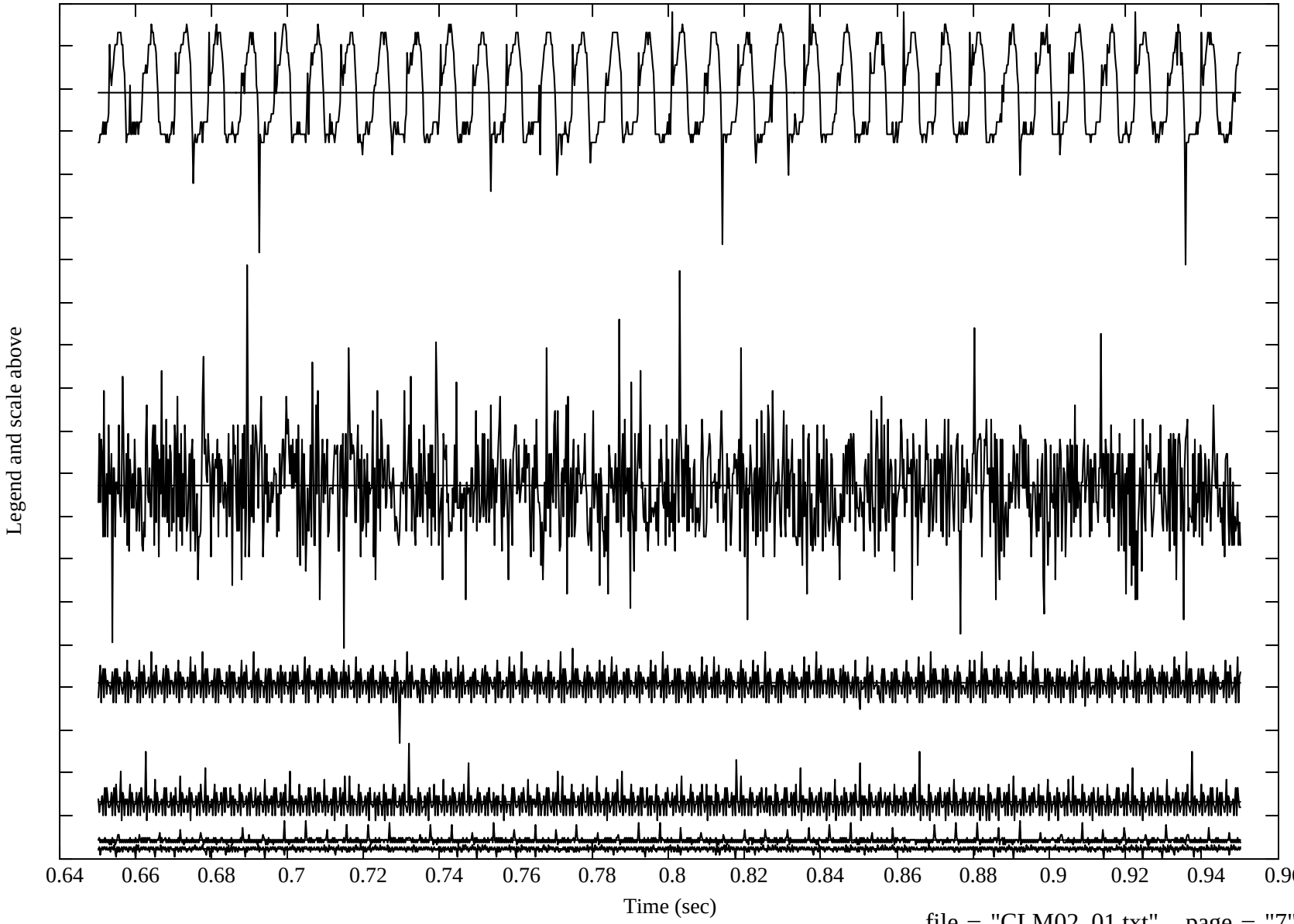

file = "CLM02_01.txt" page = "7"

each_tick = 0.68
units

inst_from_top = ("P9" "P10" "P11" "P12" "P13" "P14" "P15" "P16" "P17")

pk_to_pk = (0.71 0.83 2.08 2.92 1.95 0.46 1.14 2.62 0.63)

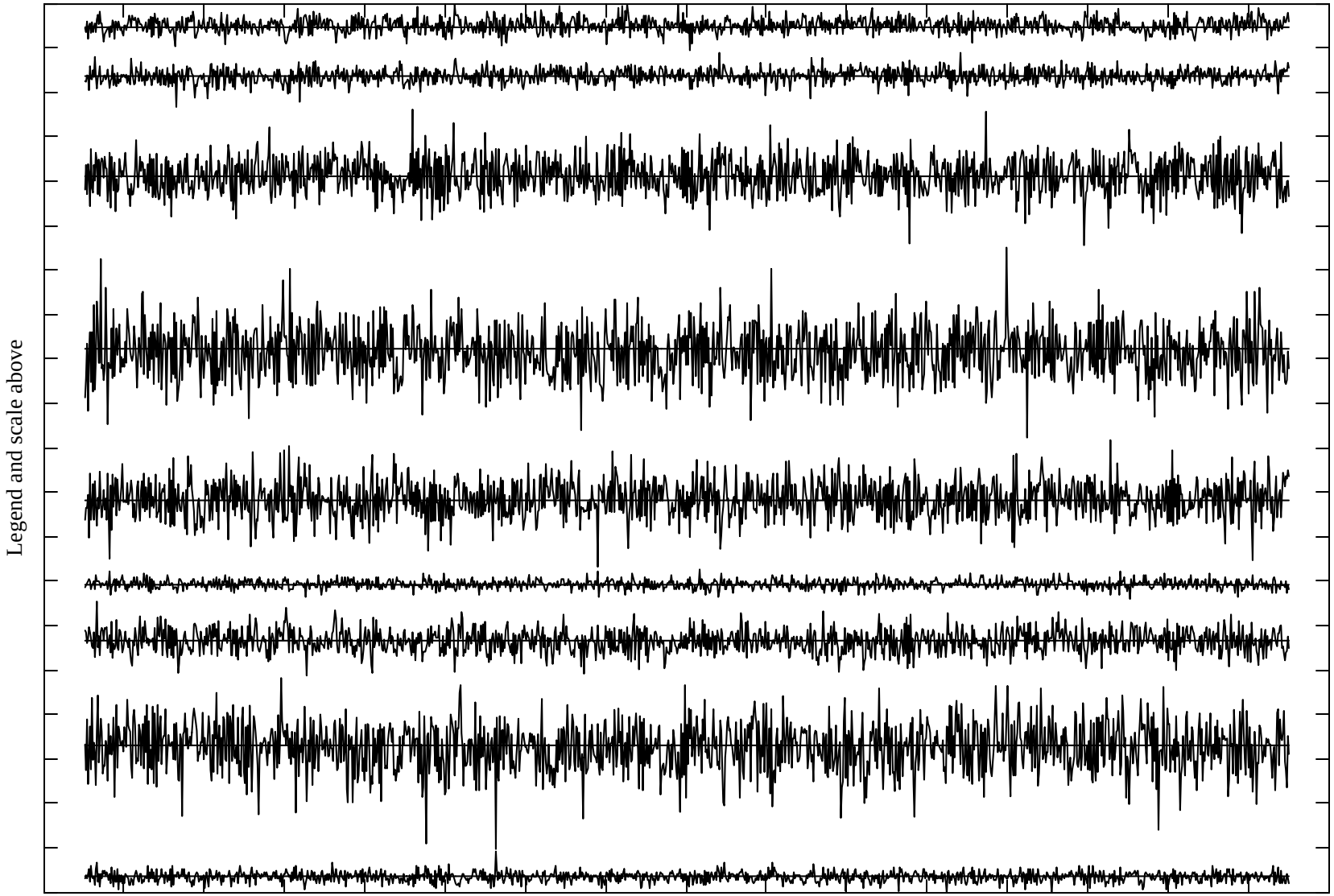

file = "CLM02_01.txt" page = "8"

each_tick = 8.749 units

inst_from_top = ("A3" "A4" "A5" "A6" "A7" "A8" "A9" "A10")

pk_to_pk = (31.04 8.78 29.89 10.97 32.34 11.23 31.55 14.15)

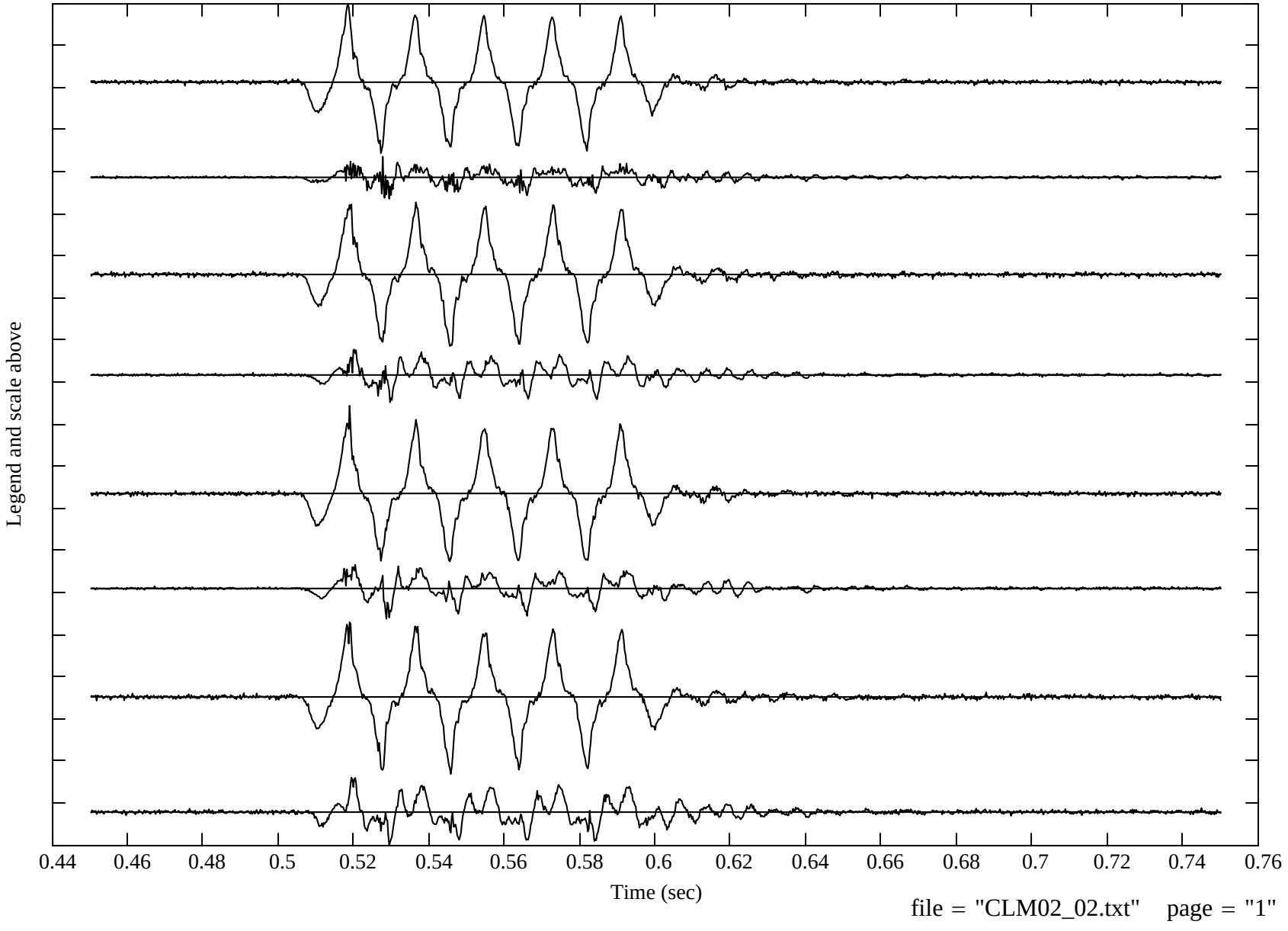

file = "CLM02_02.txt" page = "1"

each_tick = 10.290
units

inst_from_top = ("A11" "A12" "A13" "A14" "A15" "A16" "A17" "A18")

pk_to_pk = (35.98 8.82 38.72 13.92 35.00 12.55 37.09 17.01)

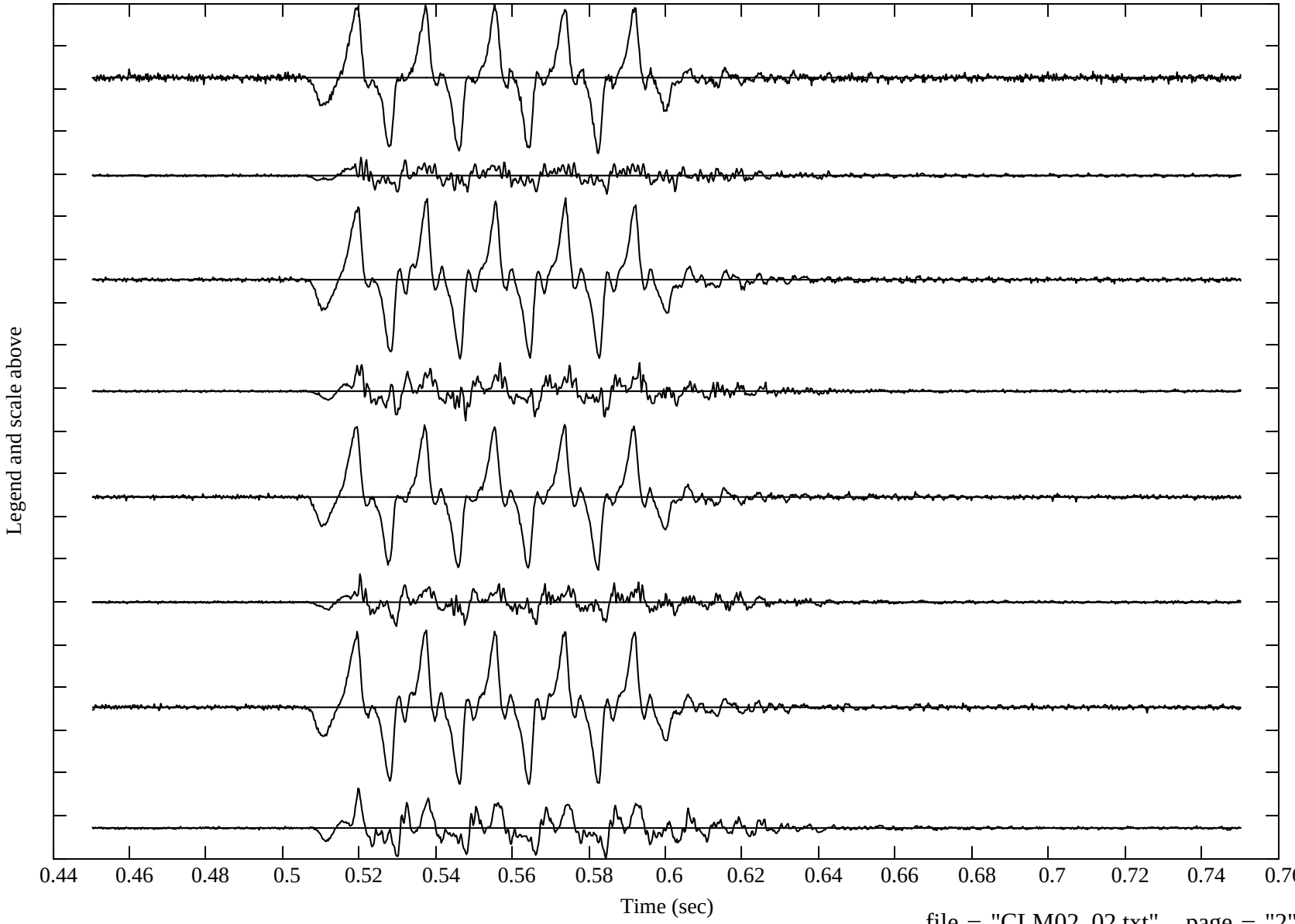

file = "CLM02_02.txt" page = "2"

each_tick = 8.853×10^{-3} units

inst from top = ("D1" "D2" "D3" "D4" "D5" "D6")

pk_to_pk = $(0.090 \quad 0.046 \quad 0.015 \quad 0.015 \quad 6.792 \times 10^{-3} \quad 3.681 \times 10^{-3})$

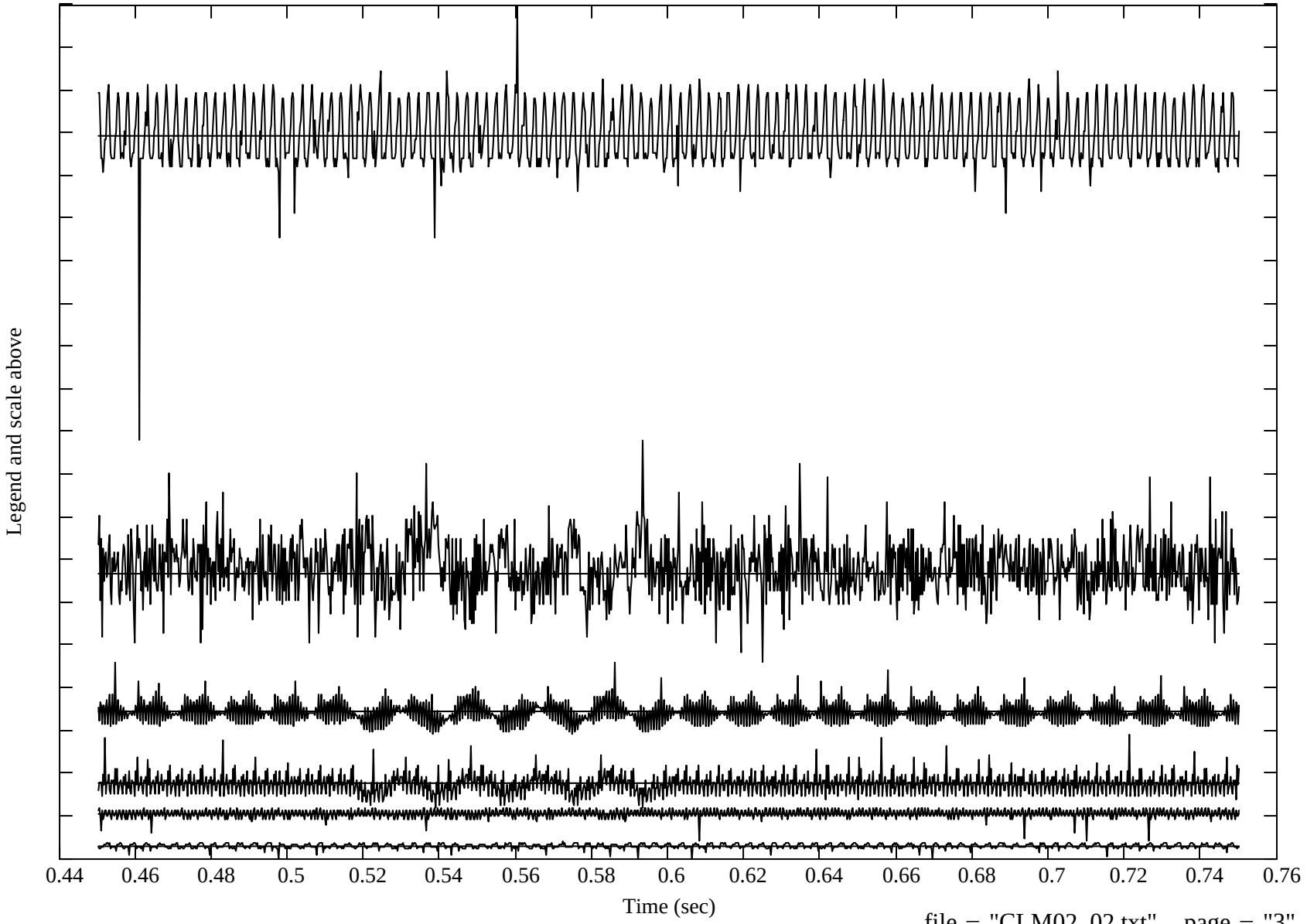

file = "CLM02_02.txt" page = "3"

each_tick = 1.24
units

inst_from_top = ("P1" "P2" "P3" "P4" "P5" "P6" "P7" "P8")

pk_to_pk = (2.02 0.61 3.62 1.88 1.55 5.36 5.86 2.82)

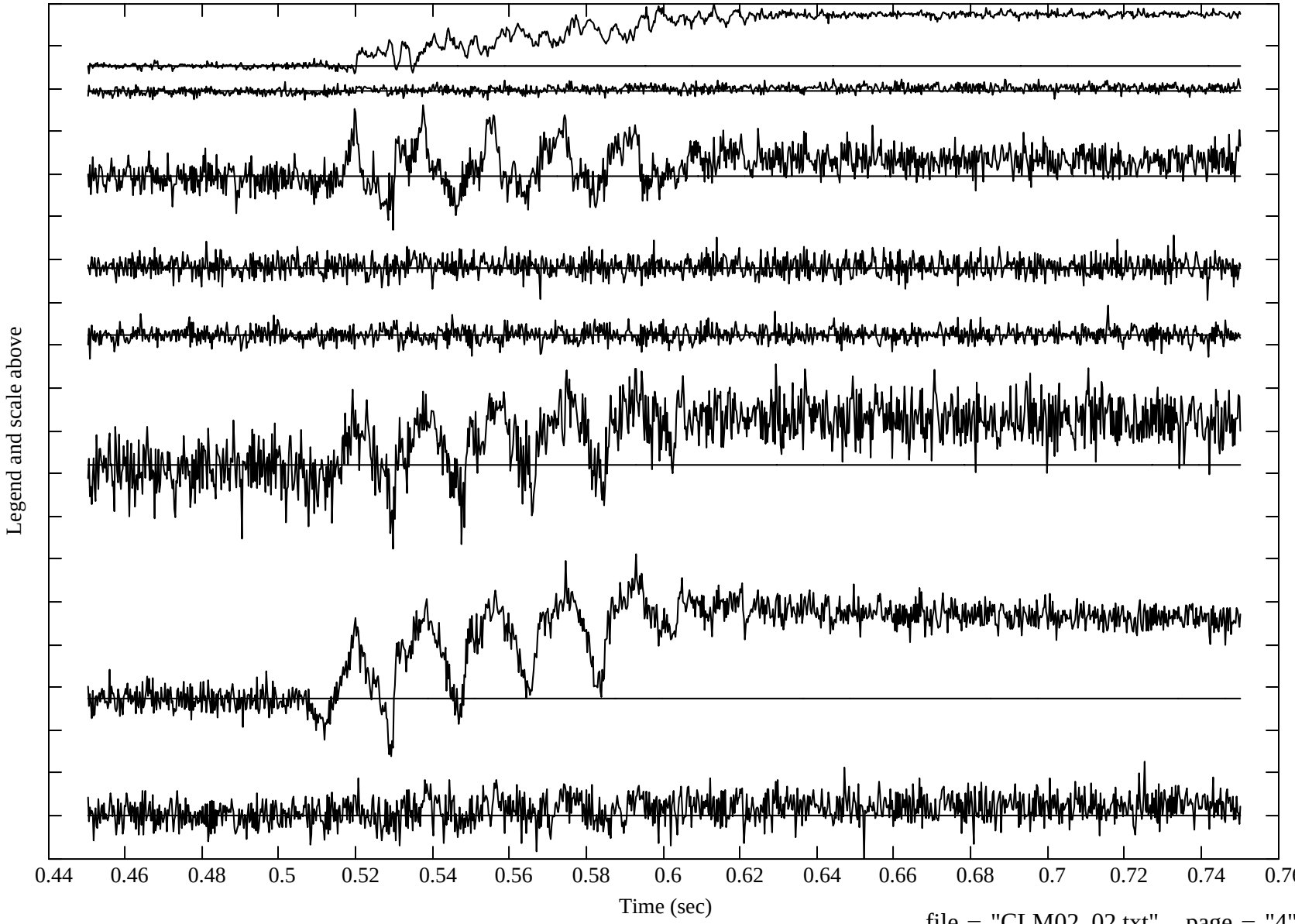

file = "CLM02_02.txt" page = "4"

each_tick = 8.49 units

inst_from_top = ("A19" "A20" "A21" "A22" "A23" "A24" "A25" "A26")

pk_to_pk = (31.33 6.85 31.49 9.28 29.53 11.05 31.19 14.38)

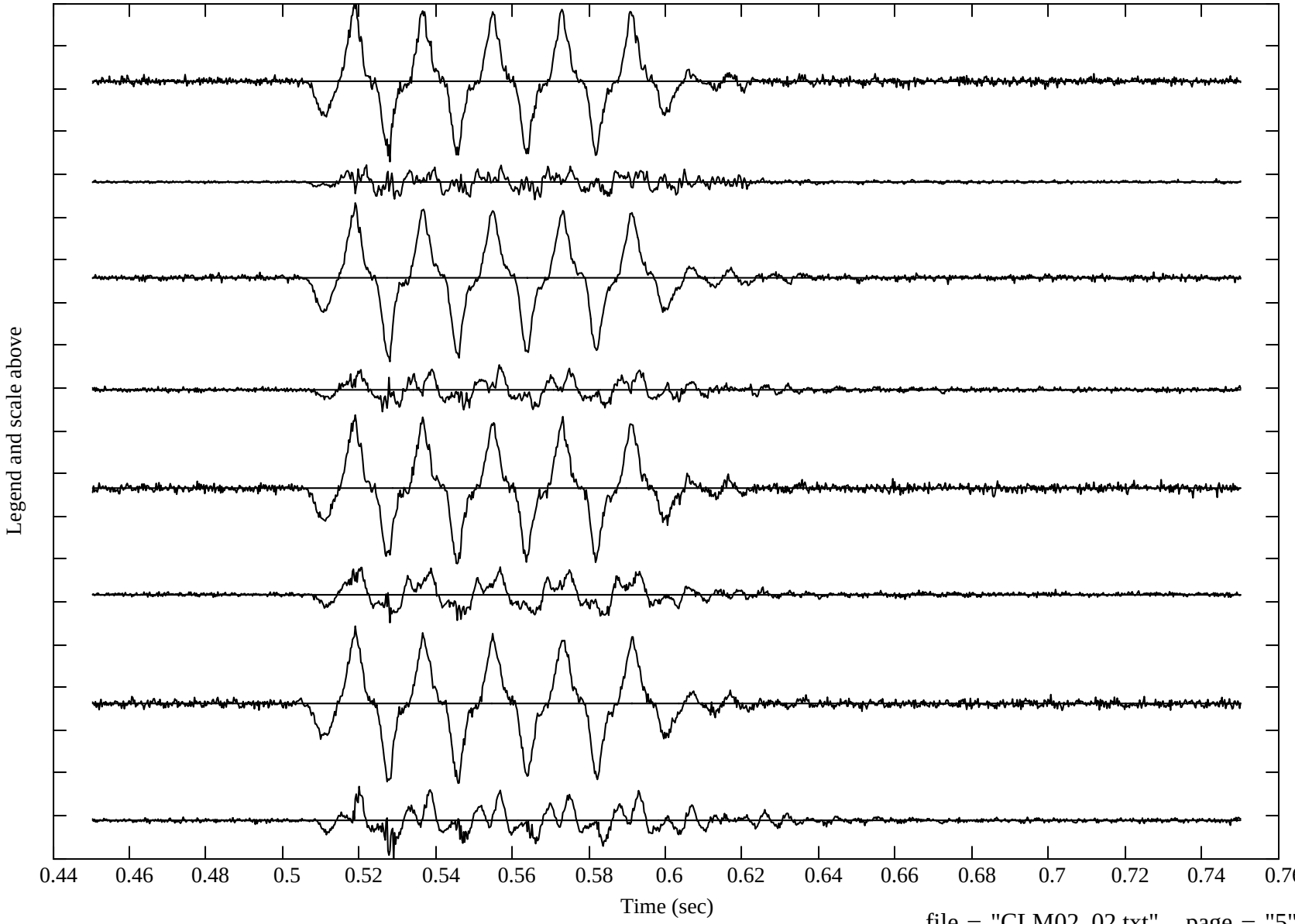

file = "CLM02_02.txt" page = "5"

each_tick = 10.00
units

inst_from_top = ("A27" "A28" "A29" "A30" "A31" "A32" "A33" "A34")

pk_to_pk = (36.02 8.83 37.88 11.13 35.61 11.89 36.51 15.90)

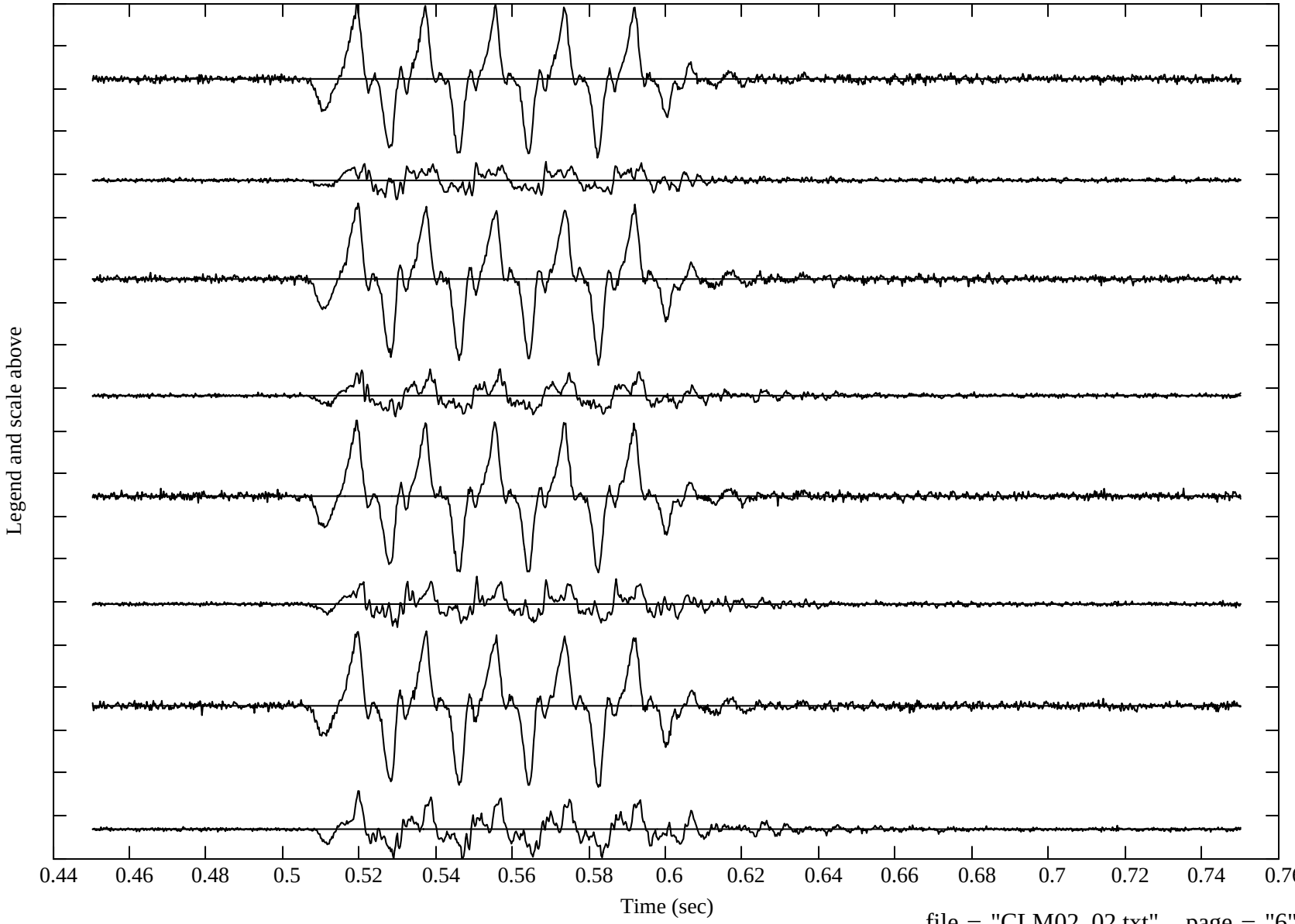

file = "CLM02_02.txt" page = "6"

each_tick = 8.05×10^{-3} units

inst from top = ("D7" "D8" "D9" "D10" "D11" "D12")

pk_to_pk = $\begin{pmatrix} 0.035 & 0.091 & 0.014 & 0.014 & 4.155 \times 10^{-3} & 3.073 \times 10^{-3} \end{pmatrix}$

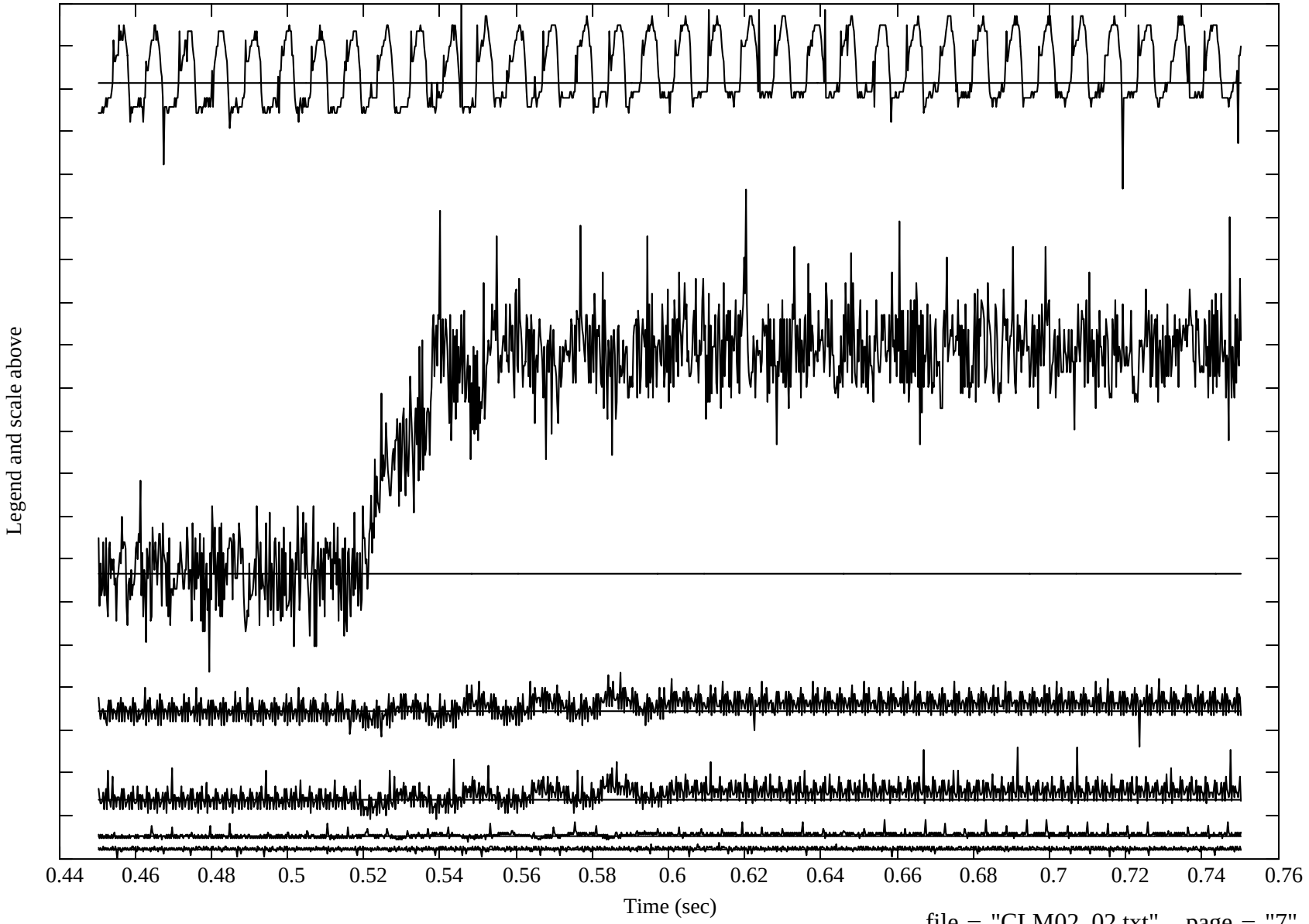

file = "CLM02_02.txt" page = "7"

each_tick = 0.80
units

inst_from_top = ("P9" "P10" "P11" "P12" "P13" "P14" "P15" "P16" "P17")

pk_to_pk = (0.86 1.92 2.01 2.27 2.00 0.64 3.39 2.11 0.58)

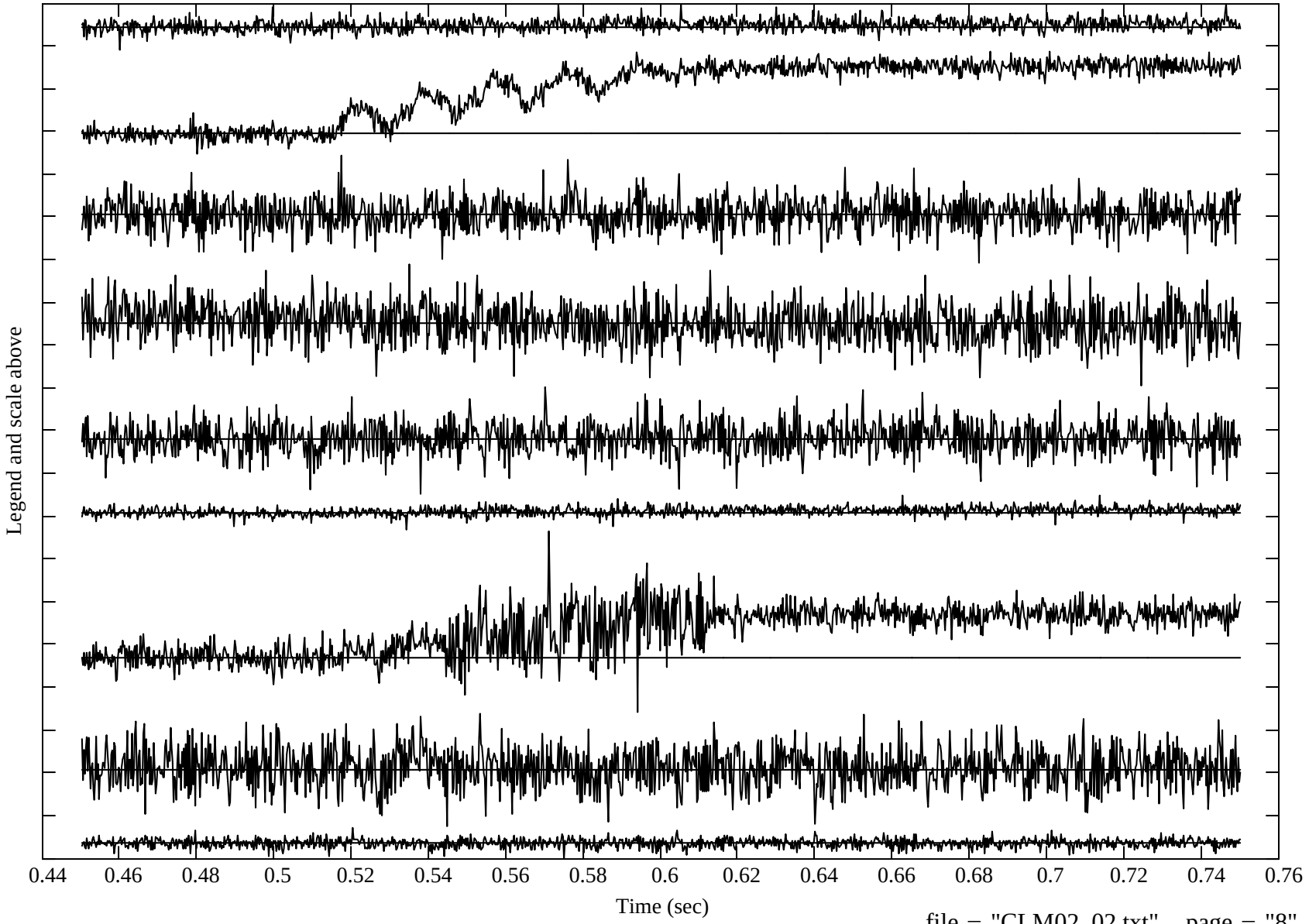

file = "CLM02_02.txt" page = "8"

each_tick = 16.20
units

inst_from_top = ("A3" "A4" "A5" "A6" "A7" "A8" "A9" "A10")

pk_to_pk = (49.65 27.30 56.37 20.38 52.18 23.59 53.45 29.32)

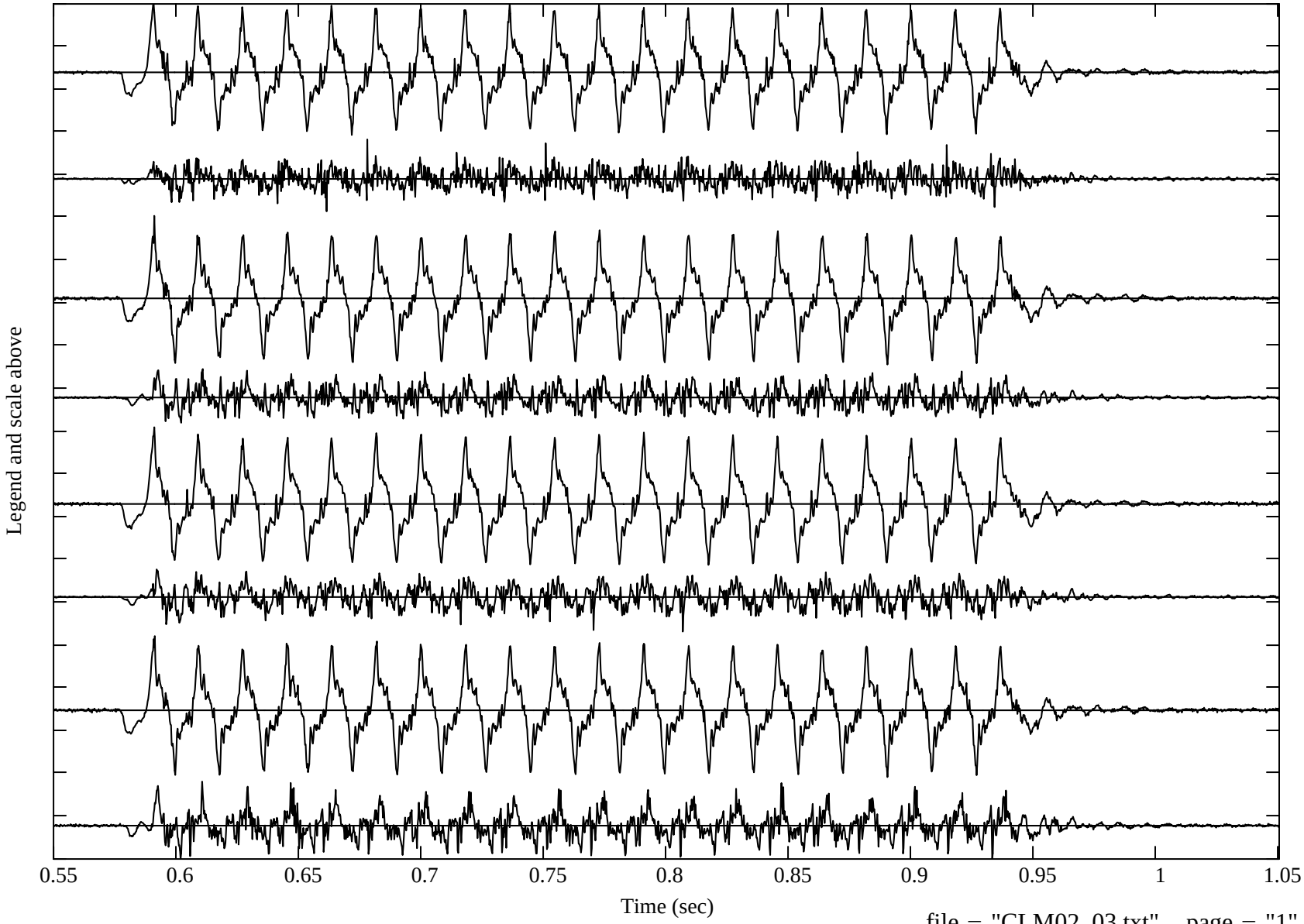

file = "CLM02_03.txt" page = "1"

each_tick = 19.74
units

inst_from_top = ("A11" "A12" "A13" "A14" "A15" "A16" "A17" "A18")

pk_to_pk = (57.72 30.80 63.27 37.38 57.02 32.71 62.83 38.43)

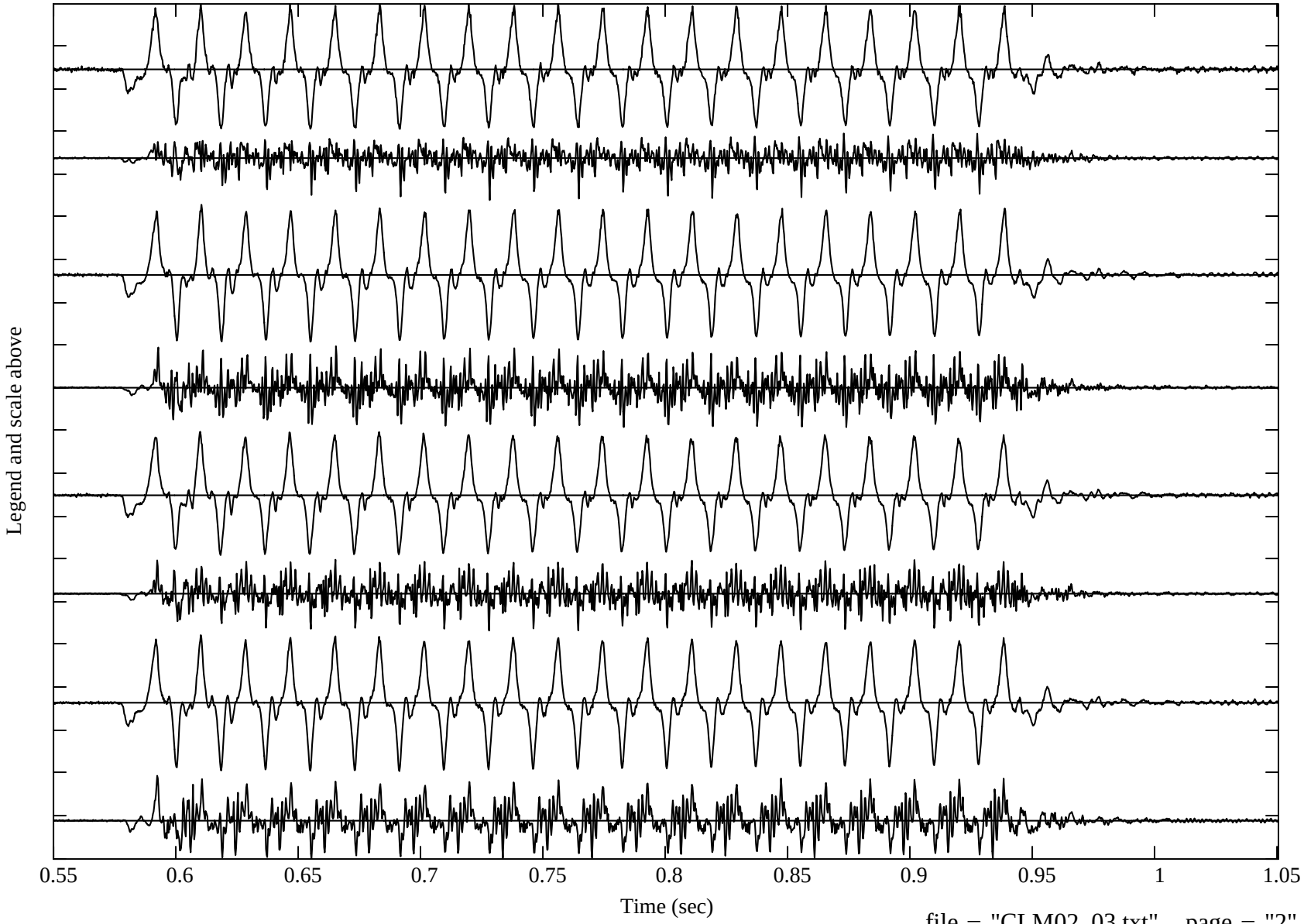

file = "CLM02_03.txt" page = "2"

each_tick = 0.015
units

inst from top = ("D1" "D2" "D3" "D4" "D5" "D6")

pk_to_pk = $\begin{pmatrix} 0.13 & 0.08 & 0.04 & 0.04 & 8.43\times10^{-3} & 4.52\times10^{-3} \end{pmatrix}$

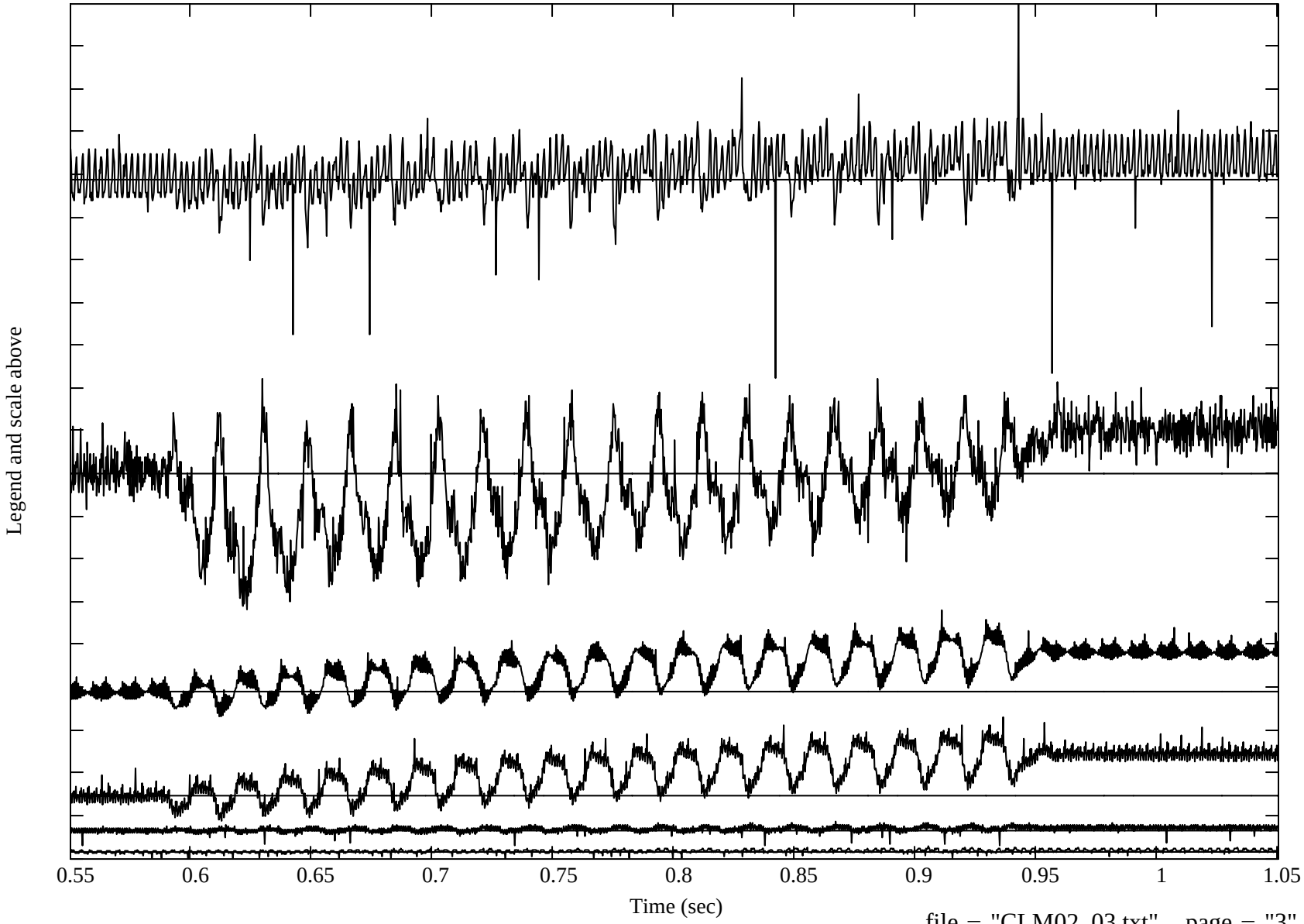

file = "CLM02_03.txt" page = "3"

each_tick = 4.08
units

inst_from_top = ("P1" "P2" "P3" "P4" "P5" "P6" "P7" "P8")

pk_to_pk = (7.03 1.18 3.40 2.09 2.19 17.71 15.59 19.46)

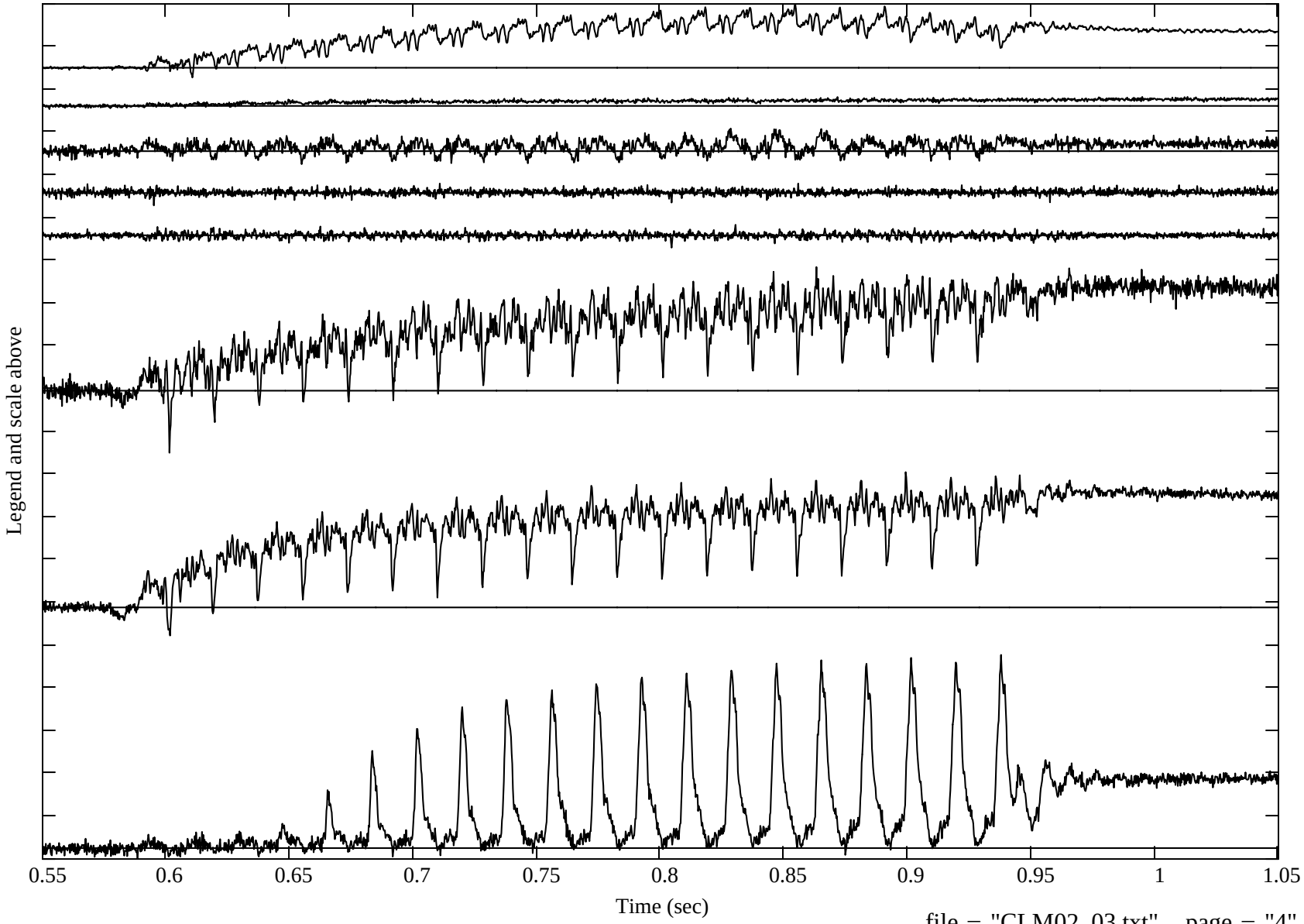

file = "CLM02_03.txt" page = "4"

each_tick = 17.90
units

inst_from_top = ("A19" "A20" "A21" "A22" "A23" "A24" "A25" "A26")

pk_to_pk = (49.09 45.44 49.94 54.06 50.67 26.15 50.19 22.70)

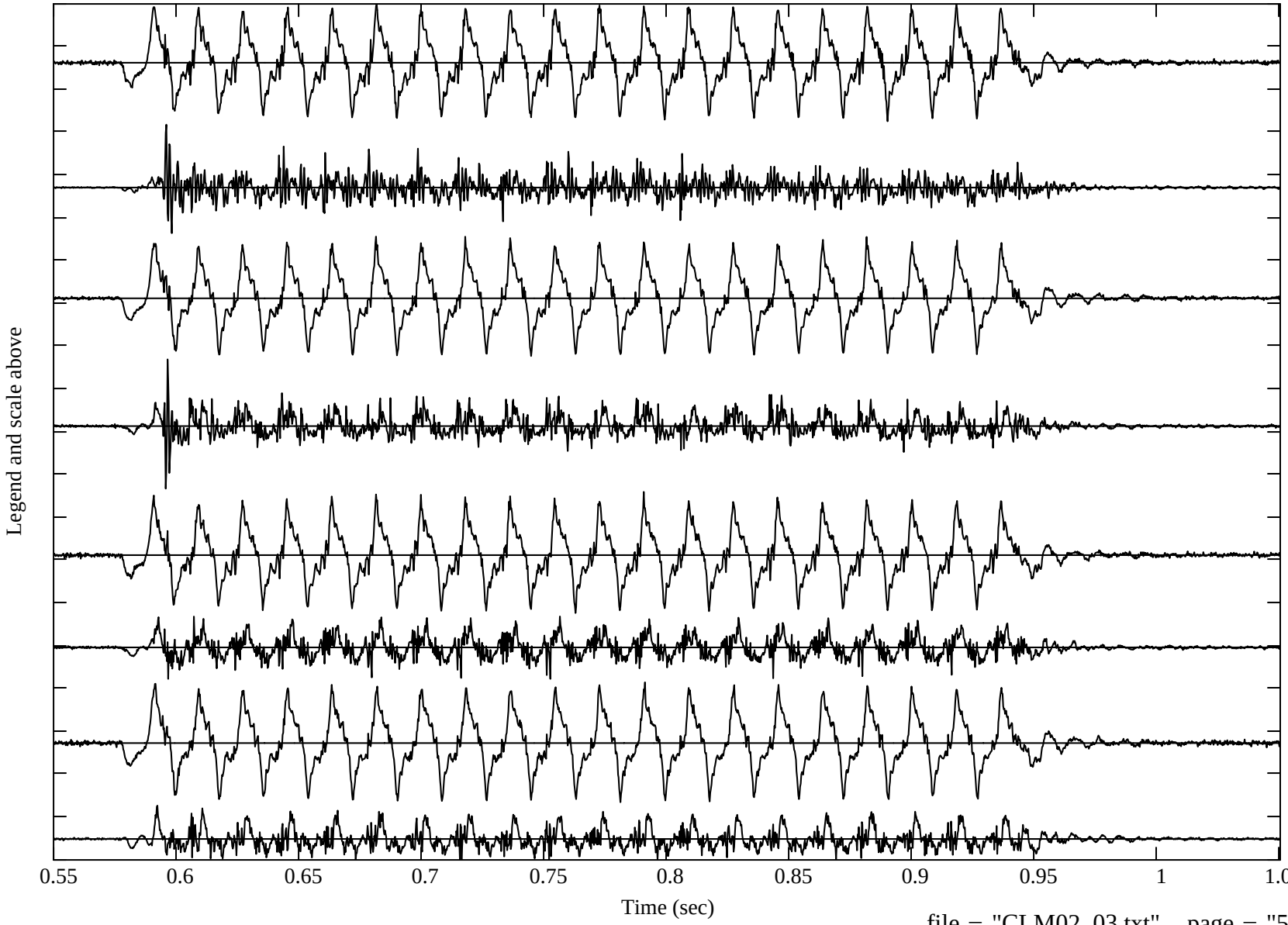

file = "CLM02_03.txt" page = "5"

each_tick = 18.02
units

inst_from_top = ("A27" "A28" "A29" "A30" "A31" "A32" "A33" "A34")

pk_to_pk = (54.90 24.13 60.92 27.31 55.51 30.41 59.94 34.33)

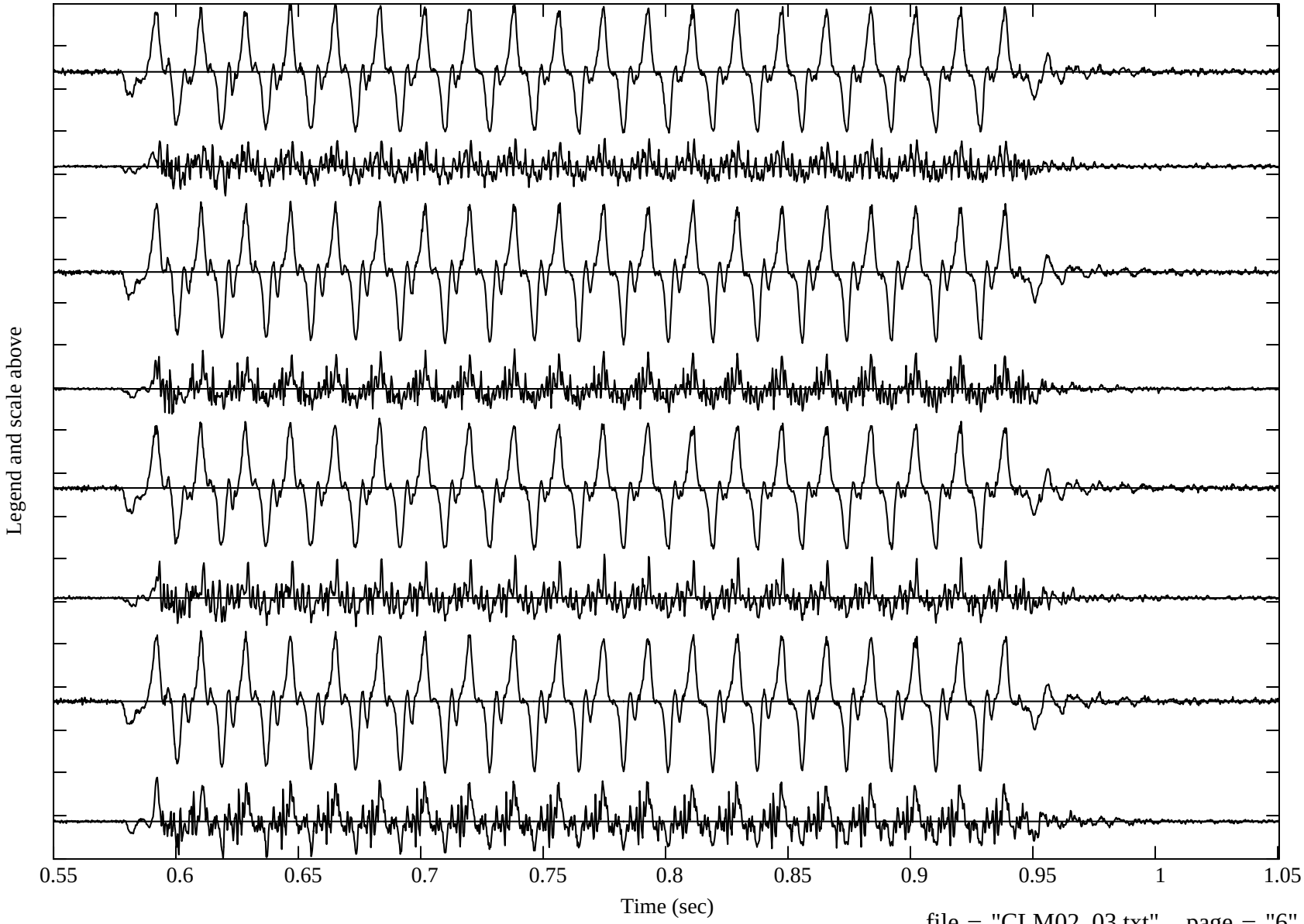

file = "CLM02_03.txt" page = "6"

each_tick = 0.013
units

inst from top = ("D7" "D8" "D9" "D10" "D11" "D12")

pk_to_pk = $\begin{pmatrix} 0.07 & 0.09 & 0.05 & 0.05 & 8.86\times10^{-3} & 4.75\times10^{-3} \end{pmatrix}$

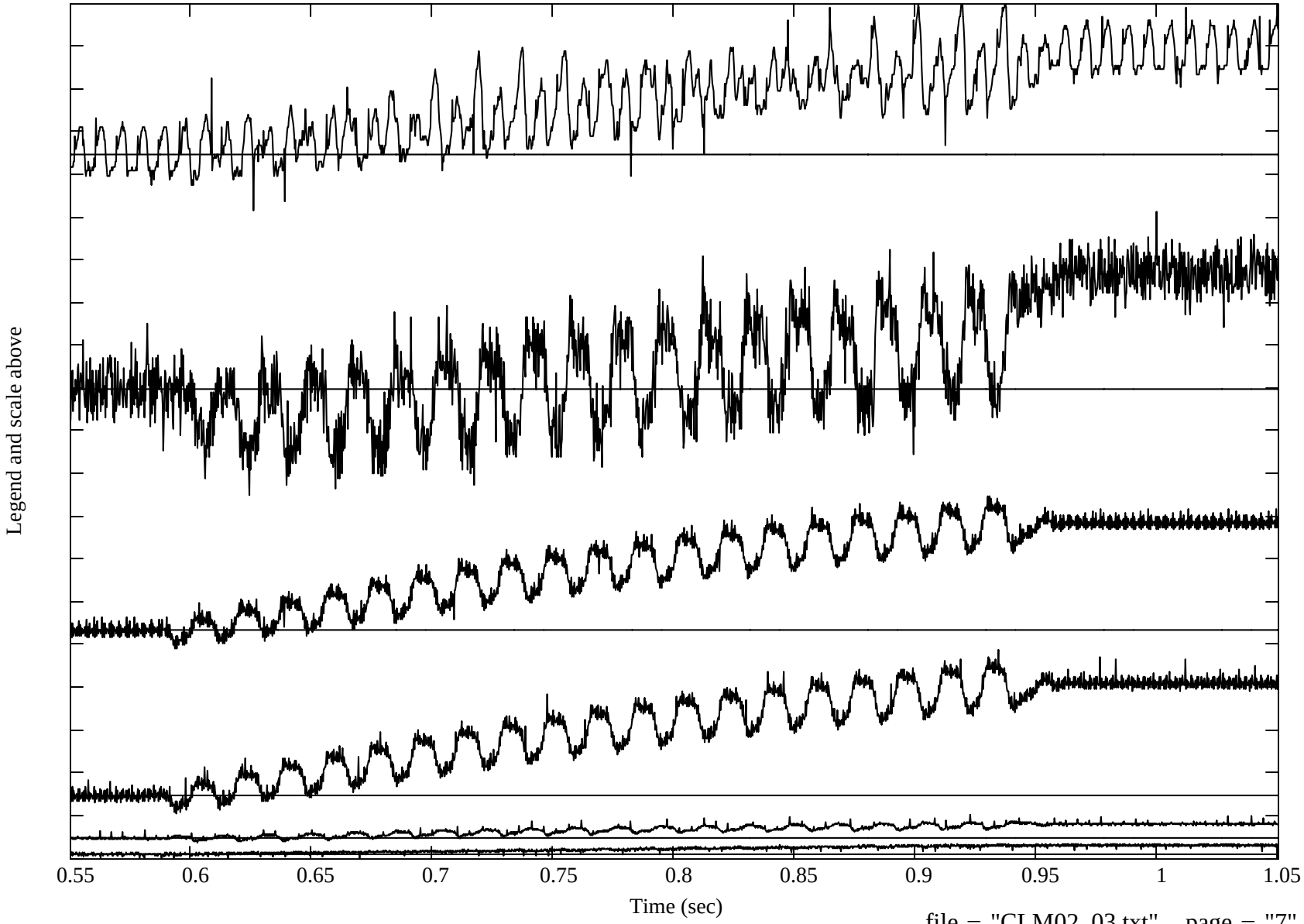

file = "CLM02_03.txt" page = "7"

each_tick = 1.239
units

inst_from_top = ("P9" "P10" "P11" "P12" "P13" "P14" "P15" "P16" "P17")

pk_to_pk = (1.82 3.13 2.15 2.27 2.66 1.28 7.99 2.26 0.85)

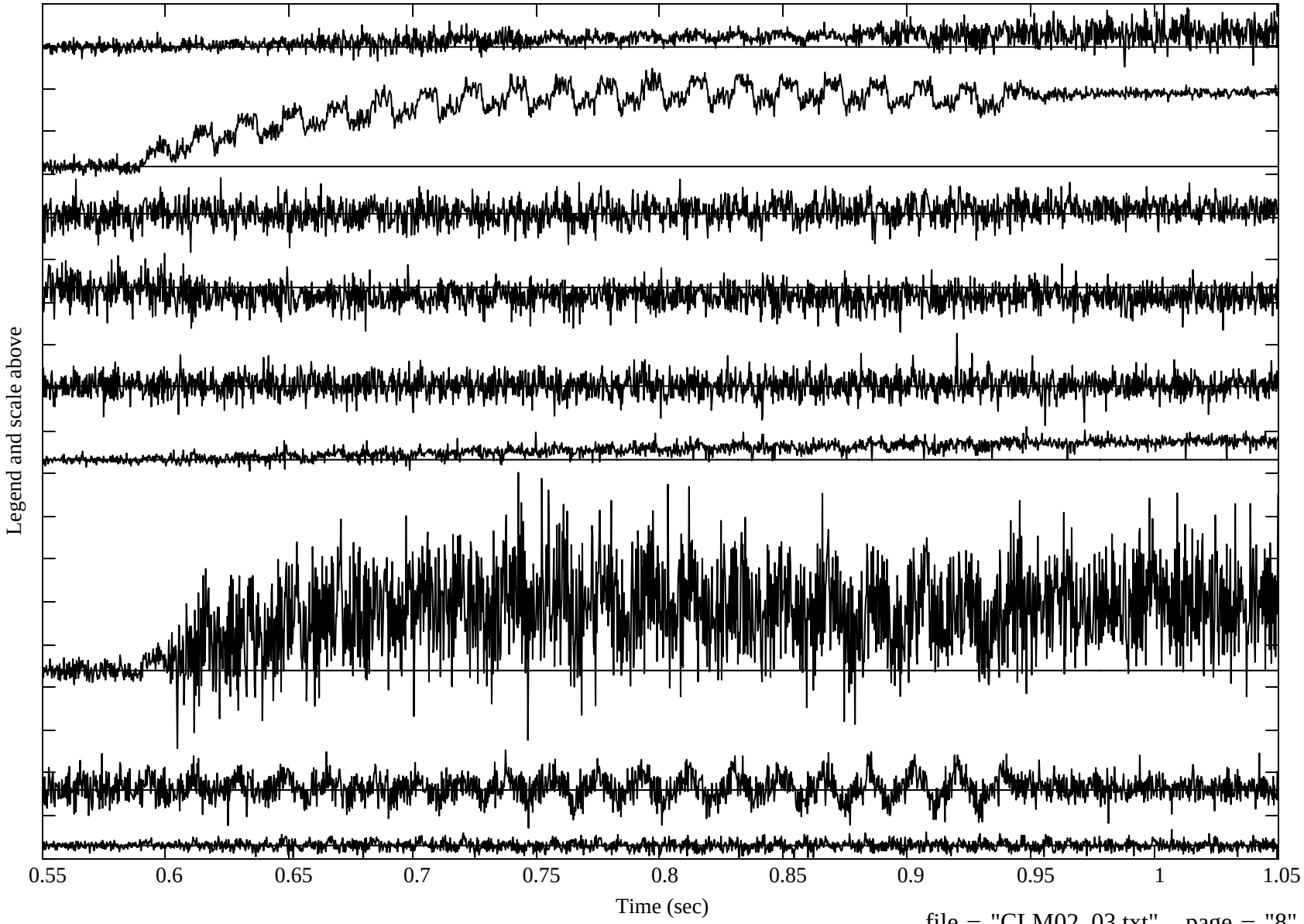

file = "CLM02_03.txt" page = "8"

each_tick = 0.56
units

inst_from_top = ("A3" "A4" "A5" "A6" "A7" "A8" "A9" "A10")

pk_to_pk = (1.60 0.82 2.15 0.84 1.52 0.80 1.42 1.51)

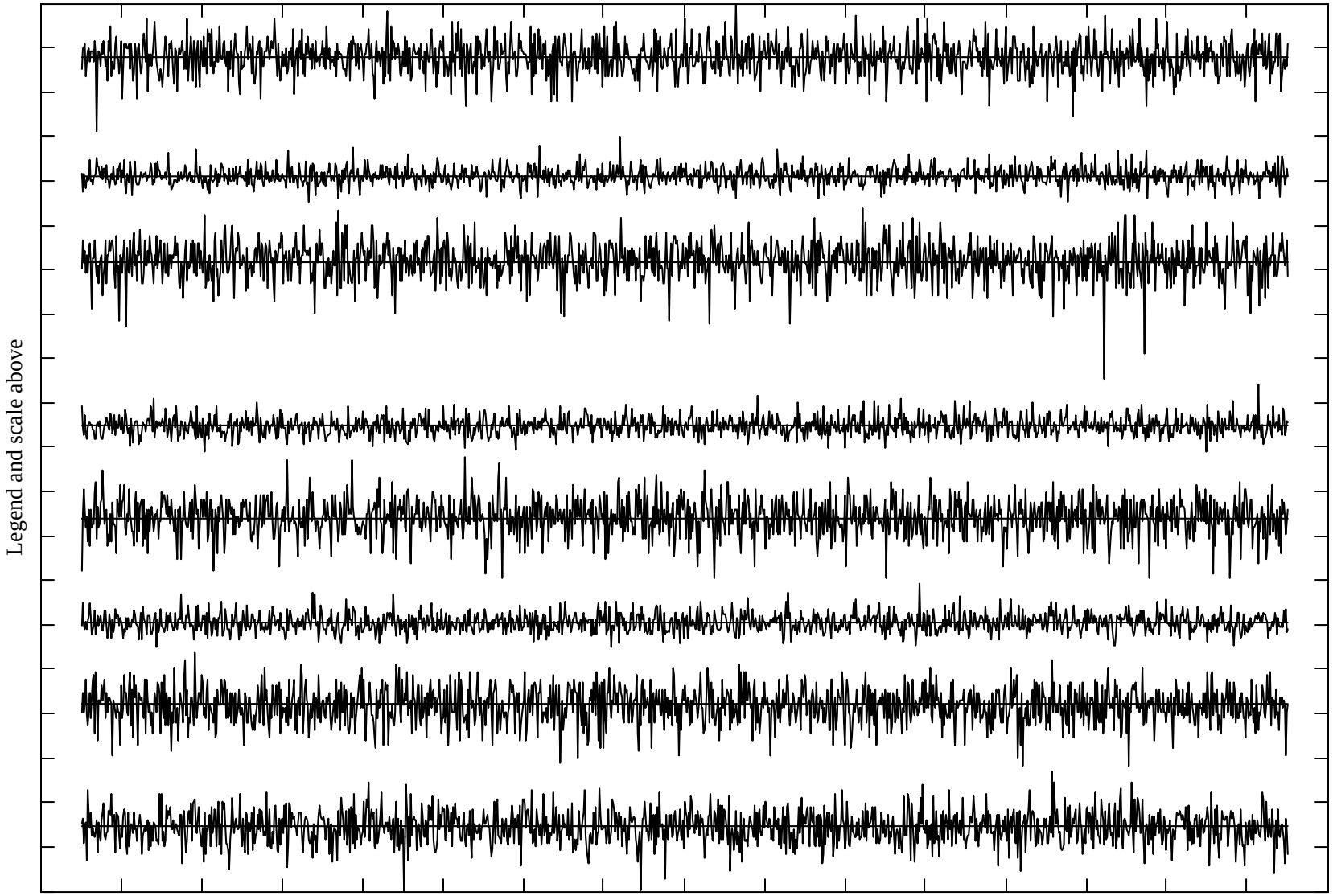

file = "CLM02_04.txt" page = "1"

each_tick = 0.58
units

inst_from_top = ("A11" "A12" "A13" "A14" "A15" "A16" "A17" "A18")

pk_to_pk = (3.04 1.04 1.48 0.81 1.53 0.80 1.78 0.89)

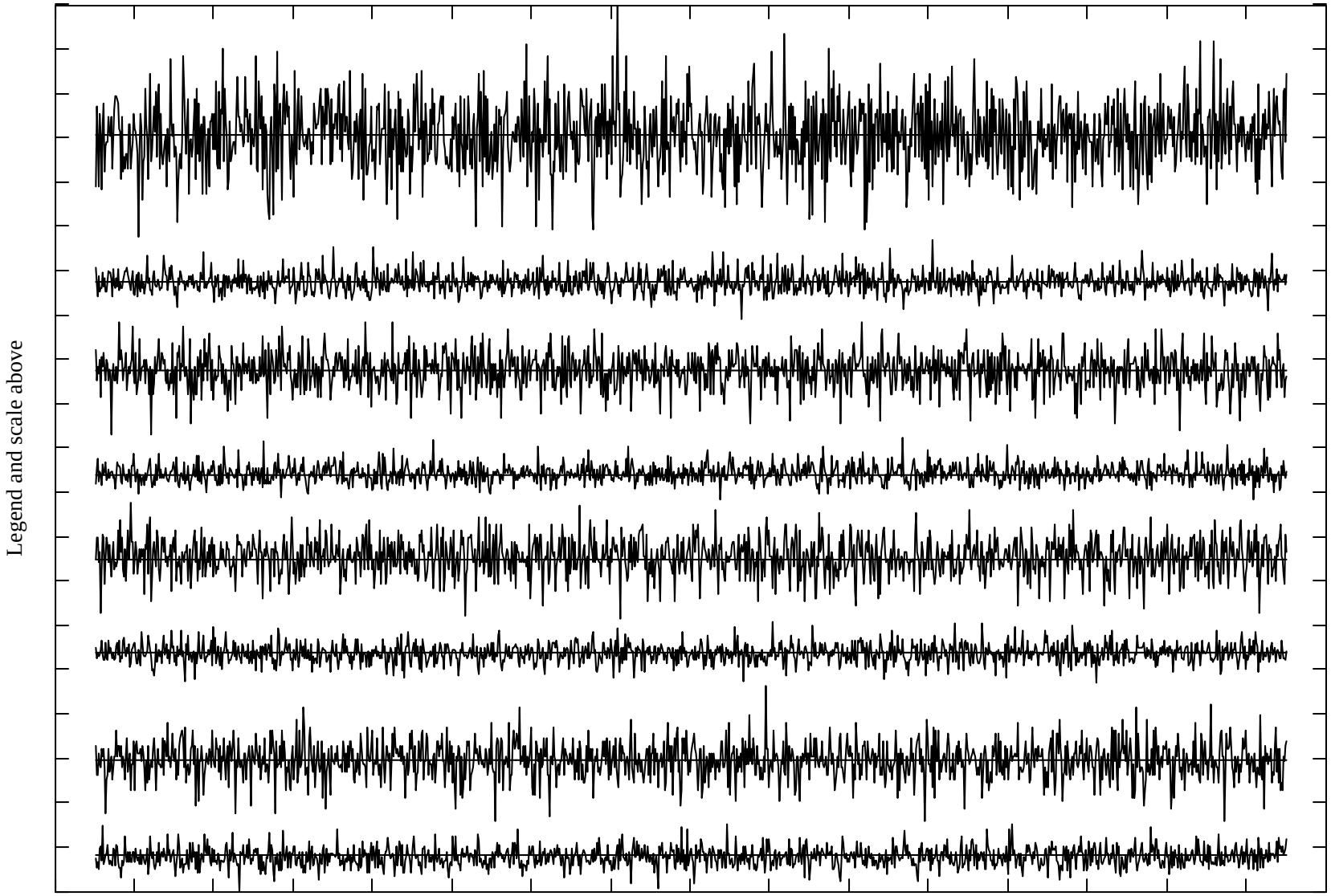

file = "CLM02_04.txt" page = "2"

each_tick = 0.010
units

inst from top = ("D1" "D2" "D3" "D4" "D5" "D6")

pk_to_pk = $\left(0.124 \quad 0.043 \quad 0.013 \quad 0.013 \quad 6.792 \times 10^{-3} \quad 3.179 \times 10^{-3}\right)$

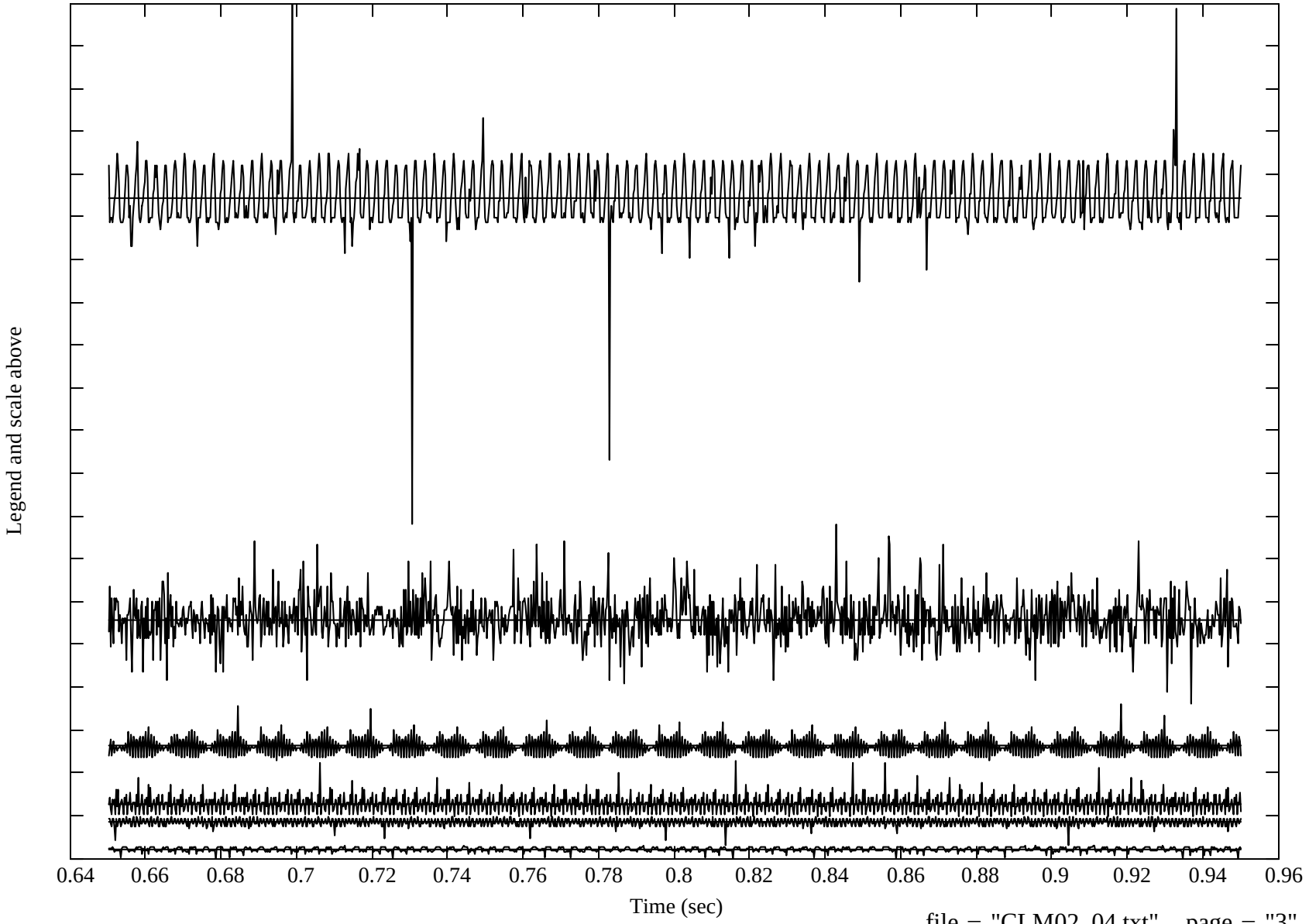

file = "CLM02_04.txt" page = "3"

each_tick = 0.69
units

inst_from_top = ("P1" "P2" "P3" "P4" "P5" "P6" "P7" "P8")

pk_to_pk = (0.48 0.53 2.03 1.76 1.28 3.13 1.93 2.03)

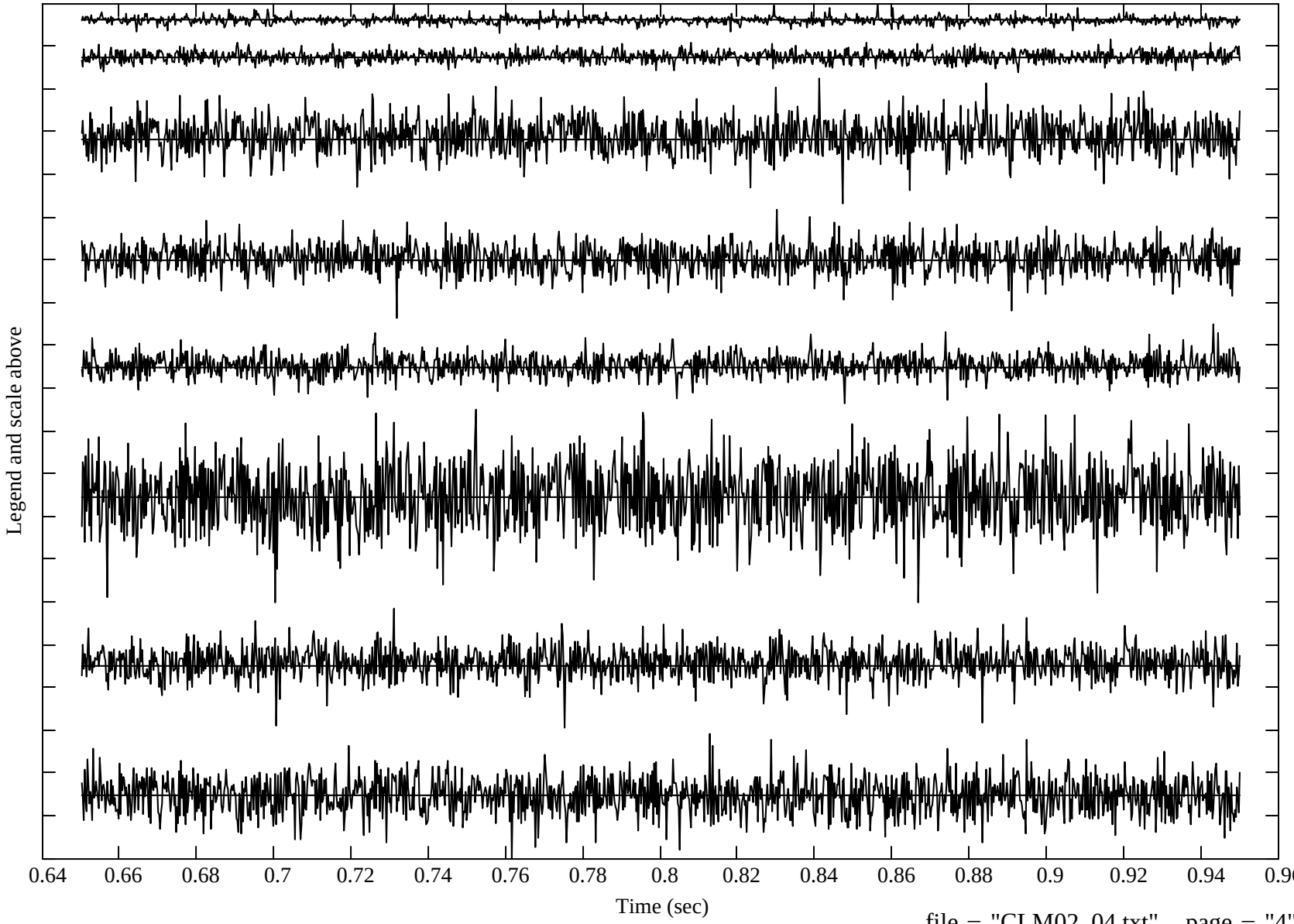

file = "CLM02_04.txt" page = "4"

each_tick = 0.84
units

inst_from_top = ("A19" "A20" "A21" "A22" "A23" "A24" "A25" "A26")

pk_to_pk = (2.62 0.78 2.21 1.61 2.89 1.55 3.01 1.53)

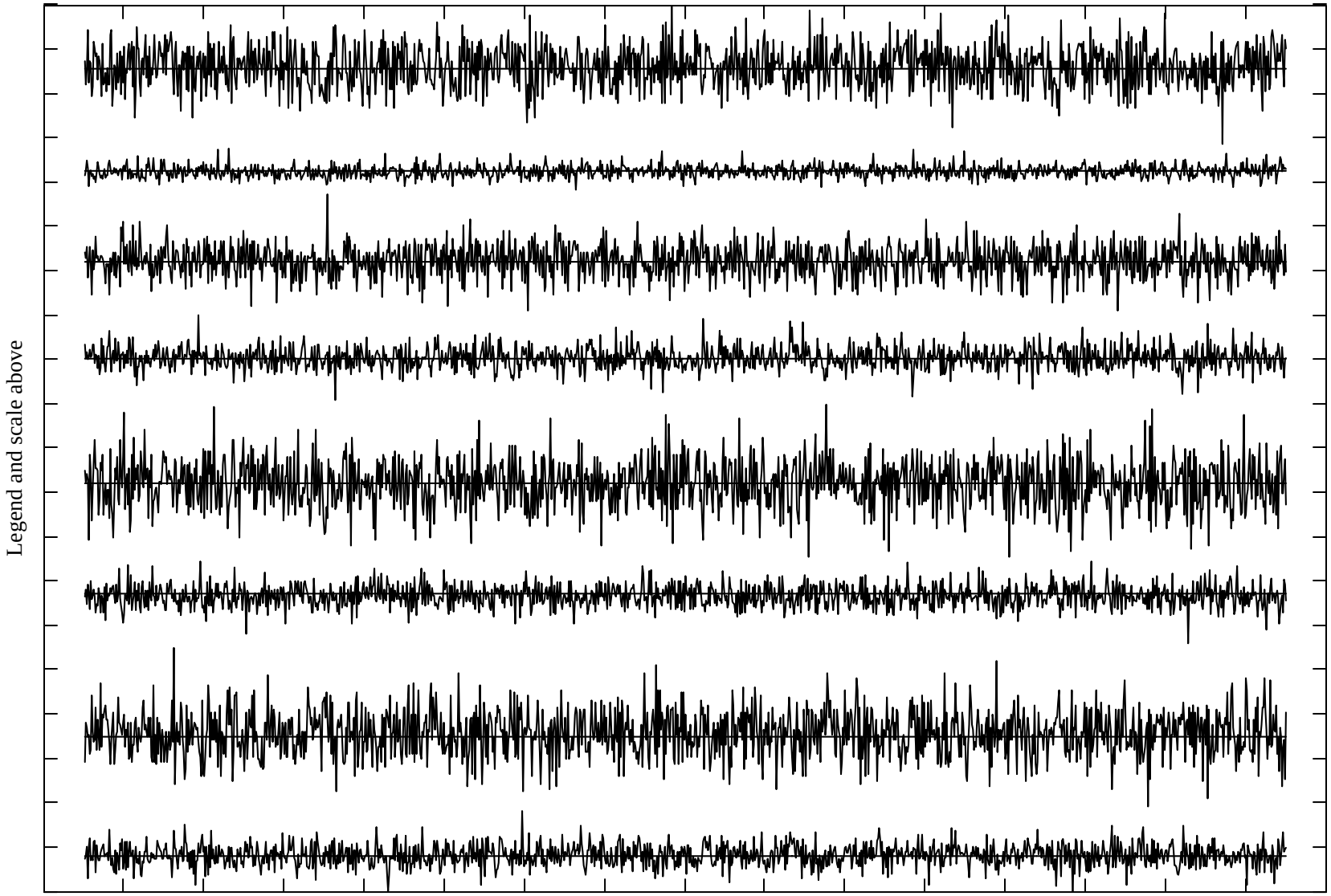

file = "CLM02_04.txt" page = "5"

each_tick = 0.98
units

inst_from_top = ("A27" "A28" "A29" "A30" "A31" "A32" "A33" "A34")

pk_to_pk = (3.33 1.74 3.03 1.63 3.23 1.65 3.06 1.47)

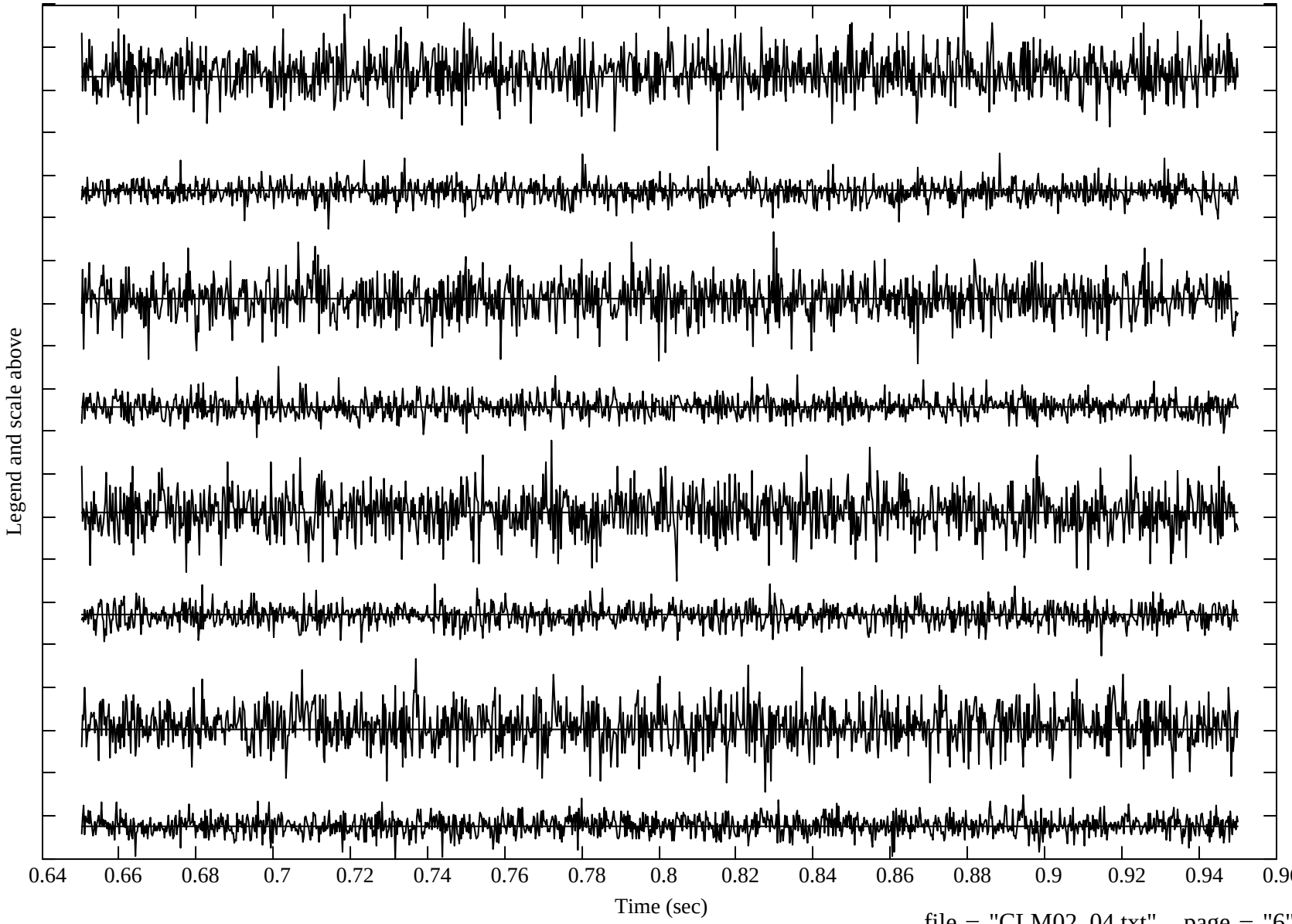

file = "CLM02_04.txt" page = "6"

each_tick = 5.79×10^{-3} units

inst from top = ("D7" "D8" "D9" "D10" "D11" "D12")

pk_to_pk = $\left(0.032 \quad 0.056 \quad 0.010 \quad 0.011 \quad 3.740 \times 10^{-3} \quad 2.515 \times 10^{-3}\right)$

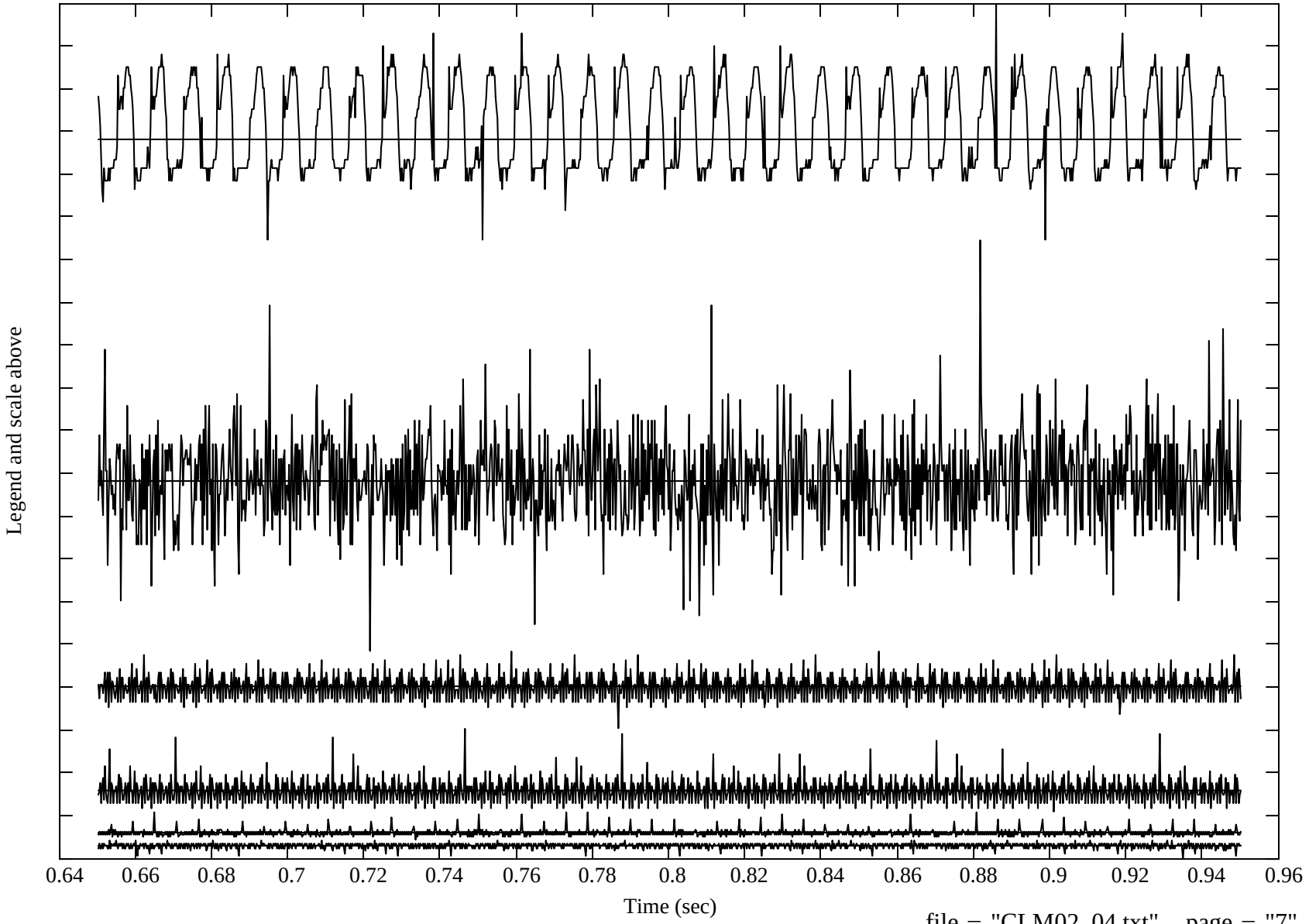

file = "CLM02_04.txt" page = "7"

each_tick = 0.94
units

inst_from_top = ("P9" "P10" "P11" "P12" "P13" "P14" "P15" "P16" "P17")

pk_to_pk = (1.82 0.52 1.68 1.71 2.12 1.13 6.44 2.21 0.81)

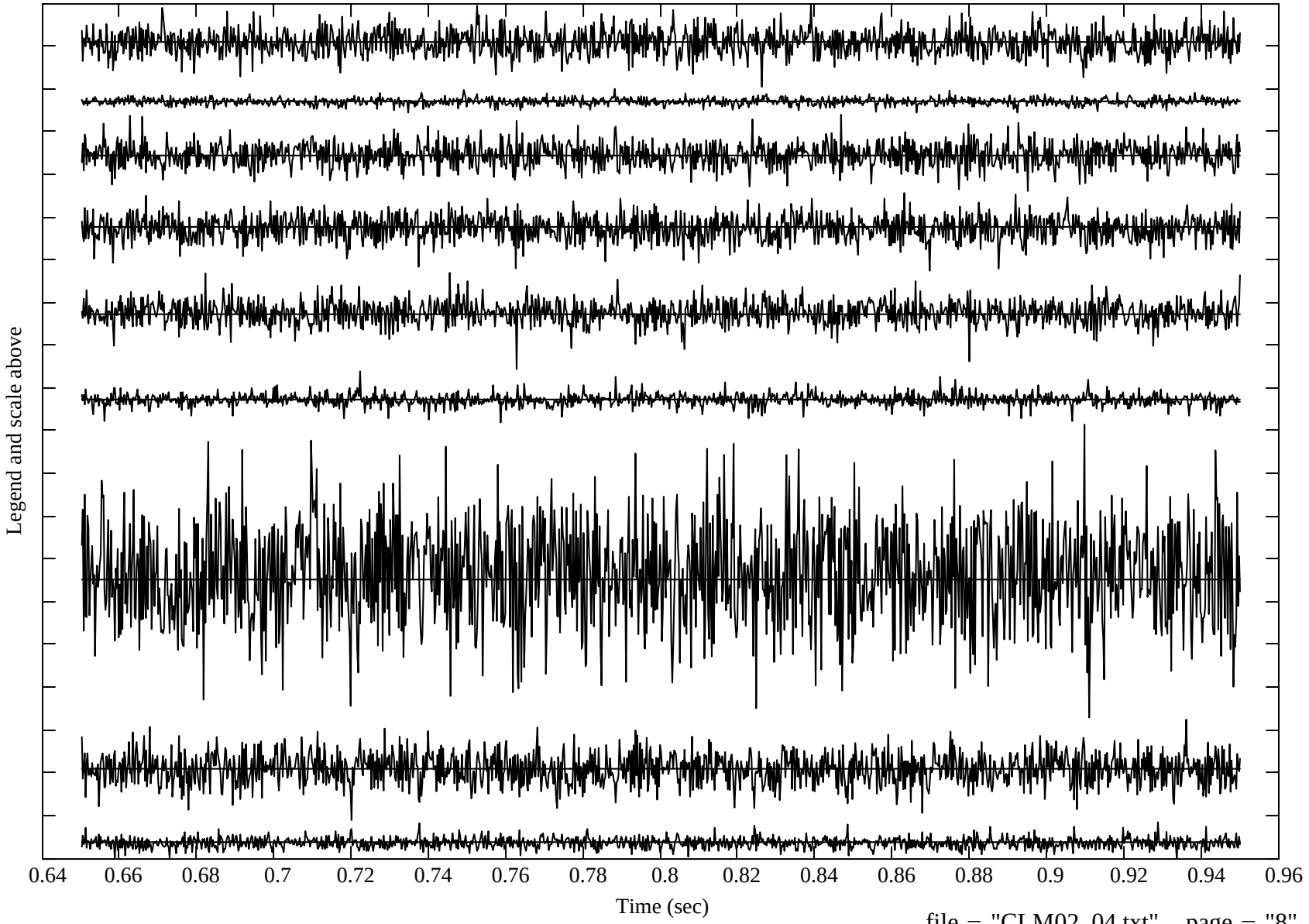

file = "CLM02_04.txt" page = "8"

each_tick = 168
units

inst_from_top = ("L1" "L2")

pk_to_pk = (1652 1558)

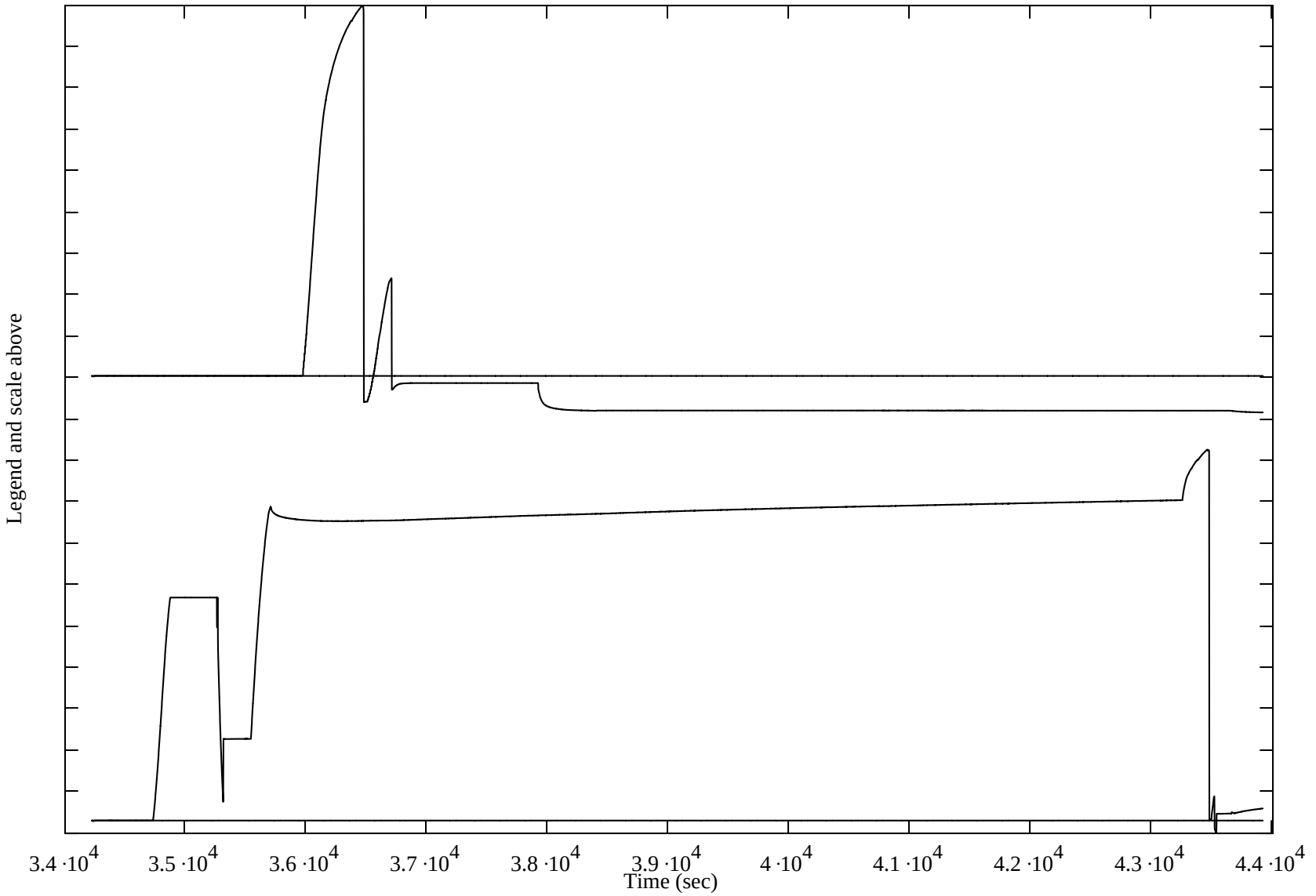

file = "CLM02_S2.txt" page = "1"

each_tick = 0.0023
units

inst_from_top = ("D1" "D2" "D3" "D4" "D5" "D6")

pk_to_pk = (0.0074 0.0104 0.0105 0.0099 0.0028 0.0035)

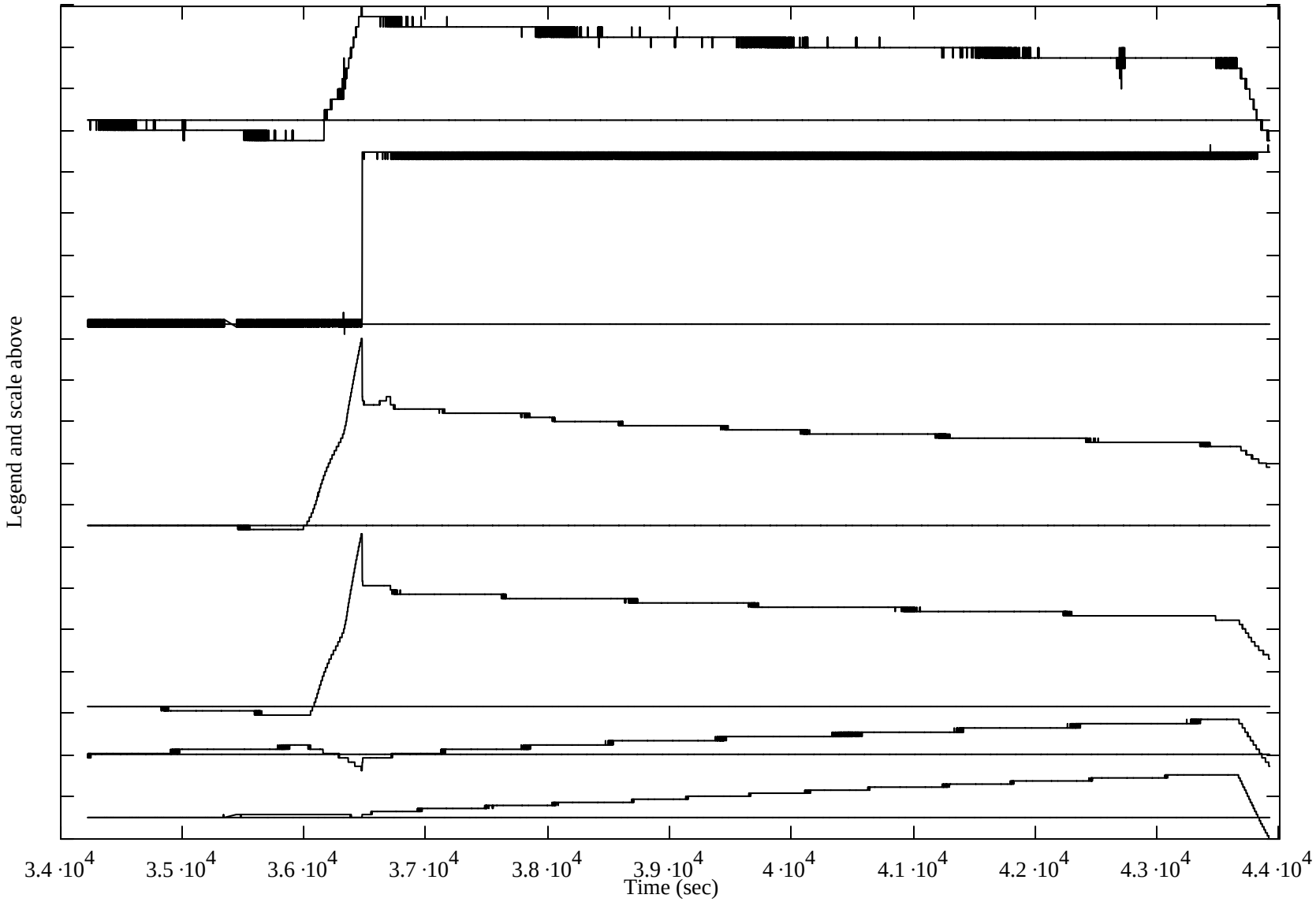

file = "CLM02_S2.txt" page = "2"

each_tick = 1.38
units

inst_from_top = ("P1" "P2" "P3" "P4" "P5" "P6" "P7" "P8")

pk_to_pk = (3.76 2.03 2.83 0.53 0.04 6.14 4.74 7.61)

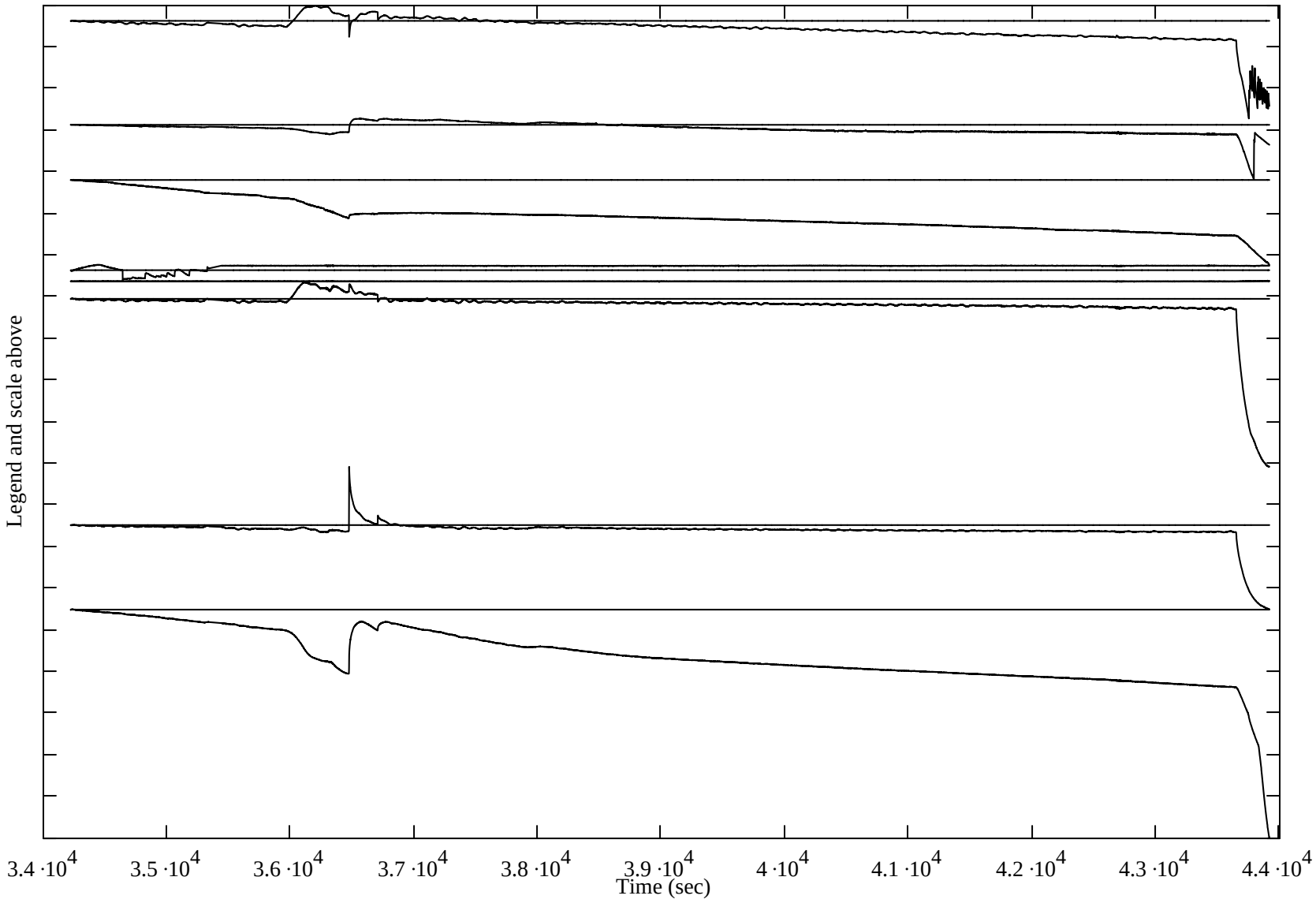

file = "CLM02_S2.txt" page = "3"

each_tick = 0.015
units

inst_from_top = ("D7" "D8" "D9" "D10" "D11" "D12")

pk_to_pk = (0.063 0.074 0.070 0.073 0.003 0.004)

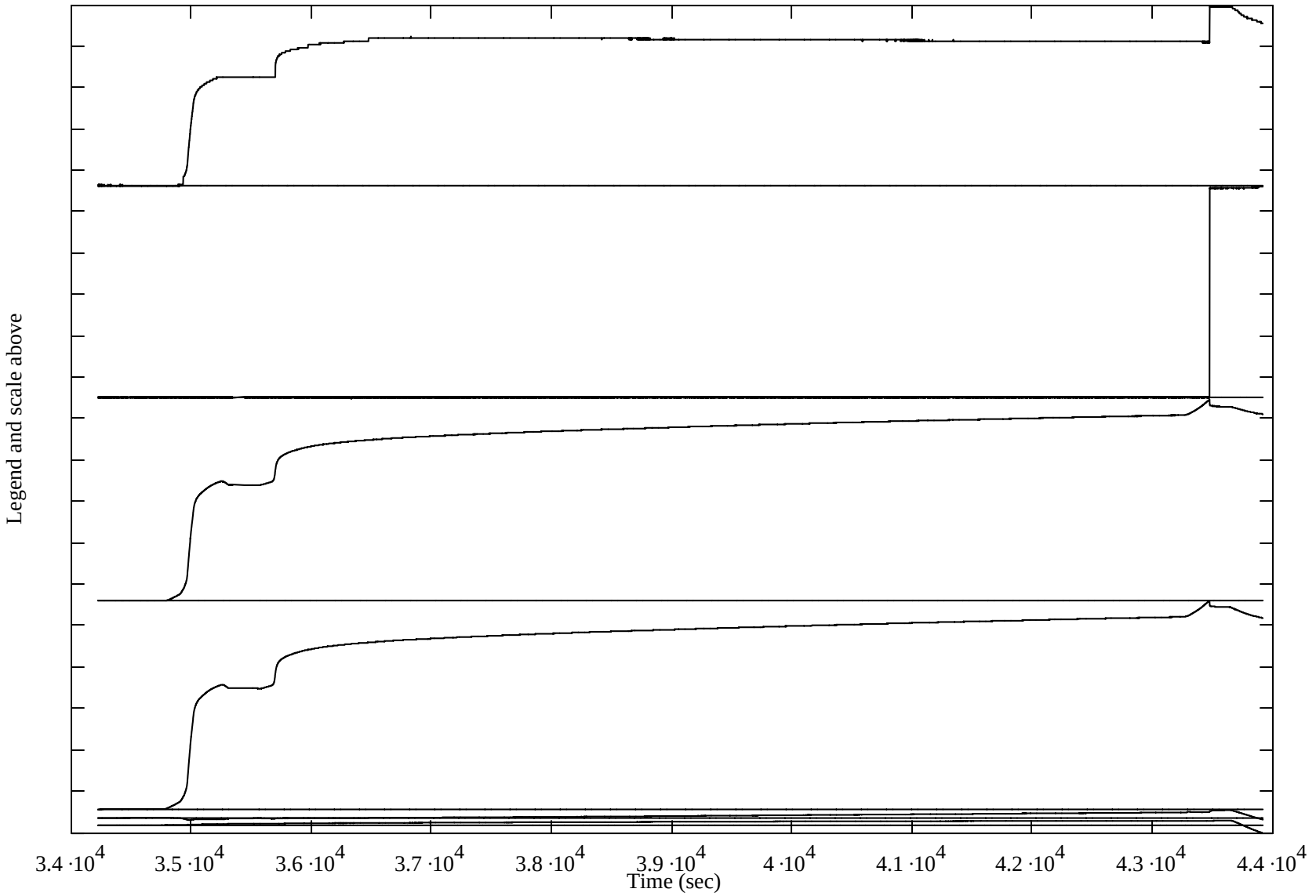

file = "CLM02_S2.txt" page = "4"

each_tick = 0.78
units

inst_from_top = ("P9" "P10" "P11" "P12" "P13" "P14" "P15" "P16" "P17")

pk_to_pk = (1.44 4.42 1.00 0.60 0.25 3.50 3.64 0.06 0.40)

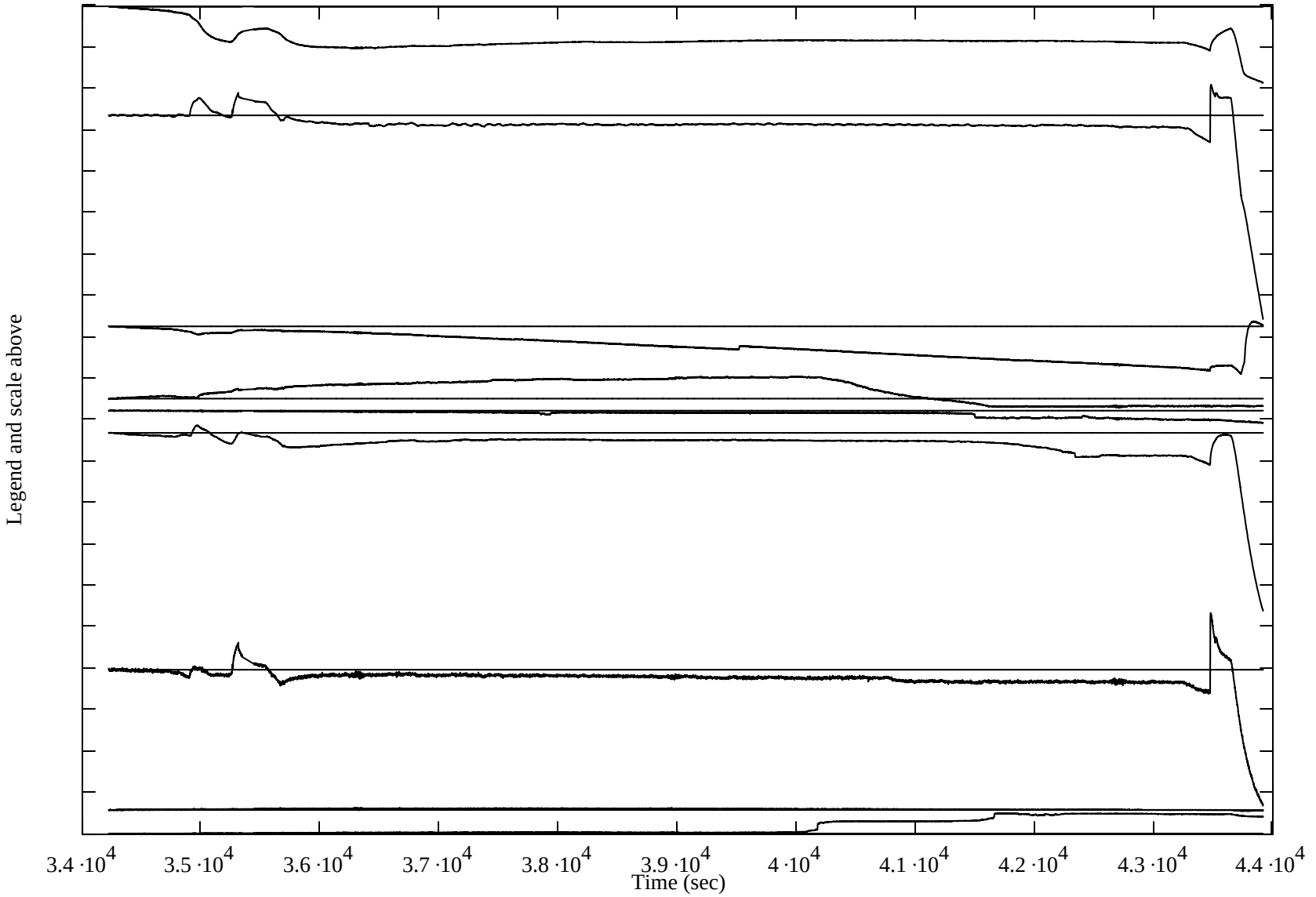

file = "CLM02_S2.txt" page = "5"